arXiv:cond-mat/0610241v3 [cond-mat.mtrl-sci] 12 Oct 2006

# The Symmetry of Multiferroics

A. B. Harris
*Department of Physics and Astronomy, University of Pennsylvania, Philadelphia, PA 19104*

(Dated: February 6, 2008)

This paper represents a detailed instruction manual for constructing the Landau expansion for magnetoelectric coupling in incommensurate ferroelectric magnets. The first step is to describe the magnetic ordering in terms of symmetry adapted coordinates which serve as complex valued magnetic order parameters whose transformation properties are displayed. In so doing we use the previously proposed technique to exploit inversion symmetry, since this symmetry had been universally overlooked. Having order parameters of known symmetry which describe the magnetic ordering, we are able to construct the trilinear interaction which couples incommensurate magnetic order to the uniform polarization in order to treat many of the multiferroic systems so far investigated. The role of this theory in comparison to microscopic models is discussed.

PACS numbers: 75.25.+z, 75.10.Jm, 75.40.Gb

## I. INTRODUCTION

Recently there has been increasing interest in the interaction between magnetic and electric degrees of freedom.[1] Much interest has centered on a family of multiferroics which display a phase transition in which uniform ferroelectric order appears simultaneously with incommensurate magnetic ordering. Early examples of such a system whose ferroelectric behavior and magnetic structure have been thoroughly studied are Terbium Manganate, $TbMnO_3$ (TMO).[2,3] and Nickel Vanadate, $Ni_3V_2O_8$ (NVO)[4,5,6,7]. A number of other systems have been shown to have combined magnetic and ferroelectric transitions,[8,9,10,11] but the investigation of their magnetic structure has been less comprehensive. Initially this combined transition was somewhat mysterious, but soon a Landau expansion was developed[4] to provide a phenomenological explanation of this phenomenon. An alternative picture, similar to an earlier result[12] based on the concept of a "spin-current," and which we refer to as the "spiral formulation,"[13] has gained popularity due to its simplicity, but as we will discuss, the Landau theory is more universally applicable and has a number of advantages. The purpose of the present paper is to describe the Landau formulation in the simplest possible terms and to apply it to a large number of currently studied multiferroics. In this way we hope to demystify this formulation.

It should be noted that this phenomenon (which we call "magnetically induced ferroelectricity") is closely related to the similar behavior of so-called "improper ferroelectrics," which are commonly understood to be the analogous systems in which uniform magnetic order (ferromagnetism or antiferromagnetism) drive ferroelectricity.[14] Several decades ago such systems were studied[15] and reviewed[14,16] and present many parallels with the recent developments.

One of the problems one encounters at the outset is how to properly describe the magnetic structure of systems with complicated unit cells. This, of course, is a very old subject, but surprisingly, as will be documented below, the full ramifications of symmetry are not widely known. Accordingly, we feel it necessary to repeat the description of the symmetry analysis of magnetic structures. While the first part of this symmetry analysis is well known to experts, we review it here, especially because our approach is often far simpler and less technical than the standard one. However, either approach lays the groundwork for incorporating the effects of inversion symmetry, which seem to have been overlooked until our analysis of NVO[3,4,5,6,7] and TMO.[3] Inversion symmetry was also addressed by Schweizer with a subsequent correction.[17] Very recently a more formal approach to this problem has been given by Radaelli and Chapon.[18] But, at least in the simplest cases, the approach initially proposed by us and used here seems easiest. We apply this formalism to a number of currently studied multiferroics, such as $MnWO_4$ (MWO), $TbMn_2O_5$ (TMO25), $YMn_2O_5$ (YMO25), and $CuFeO_2$ (CFO). As was the case for NVO[4,5,6,7] and TMO,[3] once one has in hand the symmetry properties of the magnetic order parameters, one is then able to construct the trilinear magnetoelectric coupling term in the free energy which provides a phenomenological explanation of the combined magnetic and ferroelectric phase transition.

This paper is organized in conformity with the above plan. In Sec. II we review a simplified version of the symmetry analysis known as *representation theory*, in which we directly analyze the symmetry of the inverse susceptibility matrix. Here we also review the technique we proposed some time ago[3,4,5,6,7] to incorporate the consequences of inversion symmetry. In Sec. III we apply this formalism to develop magnetic order parameters for a number of multiferroic systems and in Eq. (122) we give a simple example to show how inversion symmetry influences the symmetry of the allowed spin distribution. Then in Sec. IV, we use the symmetry of the order parameters to construct a magnetoelectric coupling free energy, whose symmetry properties are manifested. In Sec. V we summarize the results of these calculations and discuss their relation to calculations based on the spin current model[12] or the phenomenology of continuum theory.[13]

## II. REVIEW OF REPRESENTATION THEORY

As we shall see, to understand the phenomenology of the magnetoelectric coupling which gives rise to the combined magnetic and ferroelectric phase transition, it is essential to characterize and properly understand the symmetry of the magnetic ordering. In addition, as we shall see, to fully include symmetry restrictions on possible magnetic structures that can be accessed via a continuous phase transition is an extremely powerful aid in the magnetic structure analysis, Accordingly in this section we review how symmetry considerations restrict the possible magnetic structures which can appear at an ordering transition. The full symmetry analysis has previously been presented elsewhere,[3,4,5,6,7], but it is useful to repeat it here both to fix the notation and to give the reader convenient access to this analysis which is so essential to the present discussion. To avoid the complexities of the most general form of this analysis (called representation theory),[17,18,19] we will limit discussion to systems having some crucial simplifying features. First, we limit consideration to systems in which the magnetic ordering is incommensurate. In the examples we choose $k$ will usually lie along a symmetry direction of the crystal. Second, we only consider systems which have a center of inversion symmetry, because it is only such systems that have a sharp phase transition at which long-range ferroelectric order appears. Thirdly, we restrict attention to crystals having relatively simple symmetry. (What this means is that except for our discussion of $\mathrm{TbMn_2O_5}$ we will consider systems where we do not need the full apparatus of group theory, but can get away with simply labeling the spin functions which describe magnetic order by their eigenvalue under various symmetry operations.) By avoiding the complexities of the most general situations, it is hoped that this paper will be accessible to more readers. Finally, as we will see, it is crucial that the phase transitions we analyze are either continuous or very nearly so. In many of the examples we discuss, our simple approach[6] is vastly simpler than that of standard representation theory augmented by representation theory specialized techniques to explicitly include exploit inversion symmetry.

### A. Symmetry Analysis of the Magnetic Free Energy

In this subsection we give a review of the formalism used previously[3,4] and presented in detail in Refs. 6,7. Since we are mainly interested in symmetry properties, we will describe the magnetic ordering by a version of mean-field theory in which one writes the magnetic free energy $F_M$ as

$$\begin{aligned} F_M &= \frac{1}{2} \sum_{\mathbf{r},\alpha;\mathbf{r}'\beta} \chi^{-1}_{\alpha\beta}(\mathbf{r},\mathbf{r}') S_\alpha(\mathbf{r}) S_\beta(\mathbf{r}') \\ &\quad + \mathcal{O}\left(S^4\right) \ , \end{aligned} \tag{1}$$

where $S_\alpha(\mathbf{r})$ is the thermally averaged $\alpha$-component of the spin at position $\mathbf{r}$. In a moment, we will give an explicit approximation for the inverse susceptibility $\chi$. We now introduce Fourier transforms in either of two equivalent formulations. In the first (which we refer to as "actual position") one writes

$$S_\alpha(\mathbf{q},\tau) \ = \ N^{-1} \sum_{\mathbf{R}} S_\alpha(\mathbf{R}+\boldsymbol{\tau}) e^{i\mathbf{q}\cdot(\mathbf{R}+\boldsymbol{\tau})} \tag{2}$$

whereas in the second (which we refer to as "unit cell") one writes

$$S_\alpha(\mathbf{q},\tau) \ = \ N^{-1} \sum_{\mathbf{R}} S_\alpha(\mathbf{R}+\boldsymbol{\tau}) e^{i\mathbf{q}\cdot\mathbf{R}} \ , \tag{3}$$

where $N$ is the number of unit cells in the system, $\boldsymbol{\tau}$ is the location of the $\tau$th site within the unit cell, and $\mathbf{R}$ is a lattice vector. Note that in Eq. (2) the phase factor in the Fourier transform is defined in terms of the actual position of the spin rather than in terms of the origin of the unit cell, as is done in Eq. (3). In some case (viz. NVO) the results are simpler in the actual position formulation whereas for others (viz. MWO) the unit cell formulation is simpler. We will use whichever formulation is simpler. In either case the fact that $S_\alpha$ has to be real indicates that

$$S_\alpha(-\mathbf{q},\tau) \ = \ S_\alpha(\mathbf{q},\tau)^* \ . \tag{4}$$

We thus have

$$\begin{aligned} F_M &= \frac{1}{2} \sum_{\mathbf{q};\tau,\tau',\alpha,\beta} \chi^{-1}_{\alpha\beta}(\mathbf{q};\tau,\tau') S_\alpha(\mathbf{q},\tau)^* S_\beta(\mathbf{q},\tau') \\ &\quad + \mathcal{O}\left(S^4\right) \ , \end{aligned} \tag{5}$$

where (for the "actual position" formulation)

$$\chi^{-1}_{\alpha\beta}(\mathbf{q};\tau,\tau') \ = \ \sum_{\mathbf{R}} \chi^{-1}_{\alpha\beta}(\tau,\mathbf{R}+\tau') e^{i\mathbf{q}\cdot(\mathbf{R}+\boldsymbol{\tau}'-\boldsymbol{\tau})} \ . \tag{6}$$

To make our discussion more concrete we cite the simplest approximation for a system with general anisotropic exchange coupling, so that the Hamiltonian is

$$\mathcal{H} \ = \sum_{\alpha,\beta;\mathbf{r},\mathbf{r}'} J_{\alpha\beta}(\mathbf{r},\mathbf{r}') s_\alpha(\mathbf{r}) s_\beta(\mathbf{r}') + \sum_{\alpha\mathbf{r}} K_\alpha s_\alpha(\mathbf{r})^2 \ , \tag{7}$$

where $s_\alpha(\mathbf{r})$ is the $\alpha$-component of the spin operator at $\mathbf{r}$ and we have included a single ion anisotropy energy assuming three inequivalent axes, so that the $K_\alpha$ are all different. One has that

$$\chi^{-1}_{\alpha\beta}(\mathbf{r},\mathbf{r}') \ = \ J_{\alpha\beta}(\mathbf{r},\mathbf{r}') + [K_\alpha + ckT]\delta_{\alpha,\beta}\delta_{\mathbf{r},\mathbf{r}'} \ , \tag{8}$$

where $\delta_{a,b}$ is unity if $a = b$ and is zero otherwise and $c$ is a spin-dependent constant of order unity, so that $ckT$ is the entropy associated with a spin $S$. Then if we have one spin per unit cell, one has

$$\chi^{-1}_{\alpha\beta}(\mathbf{q}) \;=\; \delta_{\alpha\beta}\biggl(2J_1\left[\cos(a_\alpha q_x) + \cos(a_\alpha q_y) + \cos(a_\alpha q_z)\right] + akT + K_\alpha\biggr) \ , \qquad (9)$$

where $a_\alpha$ is the lattice constant in the $\alpha$-direction[20] and we assume that $K_x < K_y < K_z$. Graphs of $\chi^{-1}(\mathbf{q})$ are shown in Fig. 1 for both the ferromagnetic ($J_1 < 0$) and antiferromagnetic ($J_1 > 0$) cases. For the ferromagnetic case we now introduce a competing antiferromagnetic next-nearest neighbor (nnn) interaction $J_2 > 0$ along the $x$-axis, so that

$$\chi^{-1}_{\alpha\alpha}(q_x, q_y = 0, q_z = 0) = [4J_1 + 2J_1\cos(a_x q_x) + 2J_2\cos(2a_x q_x) + akT + K_\alpha] \ , \qquad (10)$$

and this is also shown in Fig. 1. As $T$ is lowered one reaches a critical temperature where one of the eigenvalues of the inverse susceptibility matrix becomes zero. This indicates that the paramagnetic phase is unstable with respect to order corresponding to the critical eigenvector associated with the zero eigenvalue. For the ferromagnet this happens for zero wavevector and for the antiferromagnet for a zone boundary wavevector in agreement with our obvious expectation. For competing interactions we see that the values of the $J$'s determine a wavevector at which an eigenvalue of $\chi^{-1}$ is minimal. This is the phenomenon called "wavevector selection," and in this case the selected value of $\mathbf{q}$ is determined by extremizing $\chi^{-1}$ to be[21]

$$\cos(a_x q) \;=\; -J_1/(4J_2) \ , \qquad (11)$$

providing $J_2 > -J_1/4$. (Otherwise the system is ferromagnetic.) Note also, that crystal symmetry may select a set of symmetry-related wavevectors, which comprise what is known as the *star* of $\mathbf{q}$. (For instance, if the system were tetragonal, then crystal symmetry would imply that one has the same nnn interactions along the $y$-axis, in which case the system selects a wavevector along the $x$-axis and one of equal magnitude along the $y$-axis.

From the above discussion it should be clear that if we assume a continuous transition so that the transition is associated with the instability in the terms in the free energy quadratic in the spin amplitudes, then the nature of the ordered phase is determined by the critical eigenvector of the inverse susceptibility, i. e. the eigenvector associated with the eigenvalue of inverse susceptibility which first goes to zero as the temperature is reduced. Accordingly, the aim of this paper analyze how crystal symmetry affects the possible forms of the critical eigenvector.

When the unit cell contains $n > 1$ spins, the inverse susceptibility for each wavevector $\mathbf{q}$ is a $3n \times 3n$ matrix. The ordering transition occurs when, for some selected wavevector(s), an eigenvalue first becomes zero as the temperature is reduced. In the above simple examples involving isotropic exchange interactions, the inverse susceptibility was $3 \times 3$ diagonal matrix, so that each eigenvector trivially has only one nonzero component. The critical eigenvector has spin oriented along the easiest axis, i. e. the one for which $K_\alpha$ is minimal. In the present more general case $n > 1$ and arbitrary interactions consistent with crystal symmetry are allowed. To avoid the technicalities of group theory, we use as our guiding principle the fact that the free energy, being an expansion in powers of the magnetizations relative to the the paramagnetic state, must be invariant under all the symmetry operations of the crystal.[22,23] This is the same principle that one uses in discussing the symmetry of the electrostatic potential in a crystal.[24] We now focus our attention on the critically selected wavevector $q$ which has an eigenvalue which first becomes zero as the temperature is lowered. This value of $\mathbf{q}$ is determined by the interactions and we will consider it to be an experimentally determined parameter. Operations which leave the quadratic free energy invariant must leave invariant the term in the free energy $F_2(\mathbf{q})$ which involves only the selected wavevector $\mathbf{q}$, namely

$$F_2(\mathbf{q}) \;\equiv\; \frac{1}{2}\sum_{\tau,\tau',\alpha,\beta} \chi^{-1}_{\alpha\beta}(\mathbf{q};\tau,\tau')S_\alpha(\mathbf{q},\tau)^* S_\beta(\mathbf{q},\tau') \qquad (12)$$

Any symmetry operation takes the original variables before transformation, $S_\alpha(\mathbf{q},\tau)$, into new ones indicated by primes. We write this transformation as

$$S'_\alpha(\mathbf{q},\boldsymbol{\tau}) = \sum_{\alpha'\boldsymbol{\tau}} U_{\alpha\boldsymbol{\tau};\alpha'\boldsymbol{\tau}'} S_{\alpha'}(\mathbf{q},\boldsymbol{\tau}') \ . \qquad (13)$$

According to a well known statement of elementary quantum mechanics, if an operator $T$ commutes with $\chi^{-1}(\mathbf{q})$, then the eigenvectors of $\chi^{-1}(\mathbf{q})$ are simultaneously eigenvectors of $T$. (This much involves a well known analysis.[25,26,27] We will later consider the effect of inversion, the analysis of which is universally overlooked). We will apply this simple condition to a number of multiferroic systems currently under investigation. (This approach can be much more straightforward than the standard one when the operations which conserve wavevector unavoidably involve translations.) As a first example we consider the case of NVO and use the "actual position" Fourier transforms. In Table I we give the general positions (this set of positions is the so-called Wyckoff orbit) for the space group Cmca (#64 in Ref. 28) of NVO and this table defines the operations of the space group of Cmca. In Table II we list the positions of the two types of sites occupied by the magnetic (Ni) ions, which are called "spine" and "cross-tie" sites in recognition of their distinctive coordination in the lattice, as can be seen from Fig. 2, where we show the conventional unit cell of NVO. Experiments[6,33] indicate that as the temperature is lowered, the system first develops in-

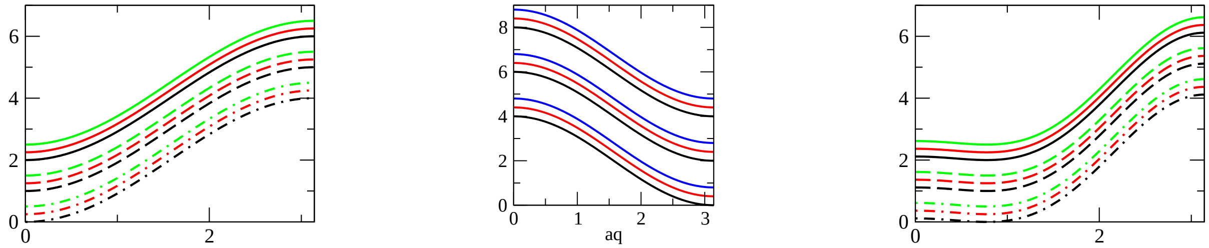

FIG. 1: Inverse susceptibility $\chi^{-1}(q,0,0)$. a) Ferromagnetic model ($J_1 < 0$), b) Antiferromagnetic model ($J_1 < 0$), and c) Model with competing interactions (the nn interaction is antiferromagnetic). In each panel one sees three groups of curves. Each group consists of the three curves for $\chi_{\alpha\alpha}(q)$ which depend on the component label $\alpha$ due to the anisotropy. The $x$ axis is the easiest axis and the $z$ axis is the hardest. (If the system is orthorhombic the three axes *must* all be inequivalent. The solid curves are for the highest temperature, the dashed curves are for an intermediate temperature, and the dash-dot curves are for $T = T_c$, the critical temperature for magnetic ordering. Panel c) illustrates the nontrivial wavevector selection which occurs when one has competing interactions.

| | |
|---|---|
| $\mathrm{E}\mathbf{r} = (x,y,z)$ | $2_c\mathbf{r} = (\overline{x},\overline{y}+1/2,z+1/2)$ |
| $2_b\mathbf{r} = (\overline{x},y+1/2,\overline{z}+1/2)$ | $2_a\mathbf{r} = (x,\overline{y},\overline{z})$ |
| $\mathcal{I}\mathbf{r} = (\overline{x},\overline{y},\overline{z})$ | $m_c\mathbf{r} = (x,y+1/2,\overline{z}+1/2)$ |
| $m_b\mathbf{r} = (x,\overline{y}+1/2,z+1/2)$ | $m_a\mathbf{r} = (\overline{x},y,z)$ |

TABLE I: General positions[28,29] within the primitive unit cell for Cmca which describe the symmetry operations[31] of this space group. $2_\alpha$ is a two-fold rotation (or screw) axis and $m_\alpha$ is a mirror (or glide) which takes $r_\alpha$ into $-r_\alpha$.

| | | |
|---|---|---|
| $\mathbf{r}_{s1}$ | $=$ | $(0.25,-0.13,0.25)$ |
| $\mathbf{r}_{s2}$ | $=$ | $(0.25,0.13,0.75)$ |
| $\mathbf{r}_{s3}$ | $=$ | $(0.75,0.13,0.75)$ |
| $\mathbf{r}_{s4}$ | $=$ | $(0.75,-0.13,0.25)$ |
| $\mathbf{r}_{c1}$ | $=$ | $(0,0,0)$ |
| $\mathbf{r}_{c2}$ | $=$ | $(0.5,0,0.5)$ |

TABLE II: Positions[29,30] of $\mathrm{Ni}^{2+}$ carrying $S$=1 within the primitive unit cell illustrated in Fig. 2. Here $\mathbf{r}_{sn}$ denotes the position of the $n$th spine site and $\mathbf{r}_{cn}$ that of the $n$th cross-tie site. NVO orders in space group Cmca, so there are six more atoms in the conventional orthorhombic unit cell which are obtained by a translation through $(0.5a, 0.5b, 0)$.

commensurate order with $\mathbf{q}$ along the $\mathbf{a}$-direction with $\hat{q} \approx 0.28$.[34]

The group of operations which conserve wavevector are generated by a) the two-fold rotation $2_x$ and b) the glide operation $m_z$, both of which are defined in Table I. We now discuss how the Fourier spin components transform under various symmetry operations. Here primed quantities denote the value of the quantity after transformation. Let $\mathcal{O} \equiv \mathcal{O}_s\mathcal{O}_r$ be a symmetry operation which we decompose into operations on the spin $\mathcal{O}_s$ and on the position $\mathcal{O}_r$. The effect of transforming a spin by such an operator is to replace the spin at the "final" position $\mathbf{R}_f$ by the transformed spin which initially was at the position $\mathcal{O}_r^{-1}\mathbf{R}_f$. So we write

$$\begin{aligned} S'_\alpha(\mathbf{R}_f,\boldsymbol{\tau}_f) &= \mathcal{O}_s S_\alpha(\mathcal{O}_r^{-1}[\mathbf{R}_f,\boldsymbol{\tau}_f]) \\ &= \xi_\alpha(\mathcal{O}_s) S_\alpha(\mathbf{R}_i,\boldsymbol{\tau}_i)\ , \end{aligned} \tag{14}$$

where the subscripts "i" and "f" denote initial and final values and $\xi_\alpha(\mathcal{O}_s)$ is the factor introduced by $\mathcal{O}_s$ for a pseudovector, namely

$$\begin{aligned} \xi_x(2_x) &= 1\ ,\quad \xi_y(2_x) = \xi_z(2_x) = -1\ , \\ \xi_x(m_z) &= \xi_y(m_z) = -1\ ,\quad \xi_z(m_z) = 1\ . \end{aligned} \tag{15}$$

Note that $\mathcal{O}S_\alpha(\mathbf{R},\boldsymbol{\tau})$ is not the result of applying $\mathcal{O}$ to move and reorient the spin at $\mathbf{R}+\boldsymbol{\tau}$, but instead is the value of the spin at $\mathbf{R}+\boldsymbol{\tau}$ after the spin distribution is acted upon by $\mathcal{O}$. Thus, for actual position Fourier transforms we have

$$\begin{aligned} S'_\alpha(\mathbf{q},\boldsymbol{\tau}_f) &= N^{-1}\sum_{\mathbf{R}} S'_\alpha(\mathbf{R}_f,\boldsymbol{\tau}_f) e^{i\mathbf{q}\cdot(\mathbf{R}_f+\boldsymbol{\tau}_f)} \\ &= \xi_\alpha(\mathcal{O}_s) N^{-1}\sum_{\mathbf{R}} S_\alpha(\mathbf{R}_i,\boldsymbol{\tau}_i) e^{i\mathbf{q}\cdot(\mathbf{R}_f+\boldsymbol{\tau}_f)} \\ &= \xi_\alpha(\mathcal{O}_s) S_\alpha(\mathbf{q},\boldsymbol{\tau}_i) e^{i\mathbf{q}\cdot[\mathbf{R}_f+\boldsymbol{\tau}_f-\mathbf{R}_i-\boldsymbol{\tau}_i]}\ . \end{aligned} \tag{16}$$

We may write this as

$$\mathcal{O}S_\alpha(\mathbf{q},\boldsymbol{\tau}_f) = \xi_\alpha(\mathcal{O}_s) S_\alpha(\mathbf{q},\boldsymbol{\tau}_i) e^{i\mathbf{q}\cdot[\mathbf{R}_f+\boldsymbol{\tau}_f-\mathbf{R}_i-\boldsymbol{\tau}_i]} \tag{17}$$

This formulation may not be totally intuitive, because one is tempted to regard the operation $\mathcal{O}$ acting on a spin at an initial location and taking it (and perhaps reorienting it) to another location. Here, instead, we consider the spin distribution. The transformed distribution at a location $\mathbf{r}$ is related to the distribution at the initial location $\mathcal{O}_r^{-1}\mathbf{r}$.

Similarly, the result for unit cell Fourier transforms is

$$S'_\alpha(\mathbf{q},\boldsymbol{\tau}_f) = \xi_\alpha(\mathcal{O}_s) S'_\alpha(\mathbf{q},\boldsymbol{\tau}_i) e^{i\mathbf{q}\cdot[\mathbf{R}_f-\mathbf{R}_i]}\ . \tag{18}$$

As before, we may write this as

$$\mathcal{O}S_\alpha(\mathbf{q},\boldsymbol{\tau}_f) \;=\; \xi_\alpha(\mathcal{O}_s)S_\alpha(\mathbf{q},\boldsymbol{\tau}_i)e^{i\mathbf{q}\cdot[\mathbf{R}_f-\mathbf{R}_i]} \ . \qquad (19)$$

Under transformation by inversion, $\xi_\alpha(\mathcal{I})=1$ and

$$\begin{aligned} S'_\alpha(\mathbf{q},\boldsymbol{\tau}_f)^* &= N^{-1}\sum_{\mathbf{R}} S_\alpha(\mathbf{R}_i,\boldsymbol{\tau}_i)e^{-i\mathbf{q}\cdot(\mathbf{R}_f+\boldsymbol{\tau}_f)} \\ &= S_\alpha(\mathbf{q},\boldsymbol{\tau}_i)e^{i\mathbf{q}\cdot[-\mathbf{R}_f-\boldsymbol{\tau}_f-\mathbf{R}_i-\boldsymbol{\tau}_i]} \\ &= S_\alpha(\mathbf{q},\boldsymbol{\tau}_i) \qquad (20) \end{aligned}$$

for actual position Fourier transforms. For unit cell transforms we get

$$\begin{aligned} S'_\alpha(\mathbf{q},\boldsymbol{\tau}_f)^* &= S_\alpha(\mathbf{q},\boldsymbol{\tau}_i)e^{i\mathbf{q}\cdot[-\mathbf{R}_f-\mathbf{R}_i]} \\ &= S_\alpha(\mathbf{q},\boldsymbol{\tau}_i)e^{i\mathbf{q}\cdot[\boldsymbol{\tau}_f+\boldsymbol{\tau}_i]} \ . \qquad (21) \end{aligned}$$

| Irrep | $\Gamma_1$ | $\Gamma_2$ | $\Gamma_3$ | $\Gamma_4$ |
|---|---|---|---|---|
| $\lambda(2_x)=$ | $+1$ | $+1$ | $-1$ | $-1$ |
| $\lambda(m_z)=$ | $+1$ | $-1$ | $-1$ | $+1$ |
| $\mathbf{S}(\mathbf{q},s1)$ | $n_s^a$<br>$n_s^b$<br>$n_s^c$ | $n_s^a$<br>$n_s^b$<br>$n_s^c$ | $n_s^a$<br>$n_s^b$<br>$n_s^c$ | $n_s^a$<br>$n_s^b$<br>${}^{c}_{s}$ |
| $\mathbf{S}(\mathbf{q},s2)$ | $n_s^a$<br>$-n_s^b$<br>$-n_s^c$ | $n_s^a$<br>$-n_s^b$<br>$-n_s^c$ | $-n_s^a$<br>$n_s^b$<br>$n_s^c$ | $-n_s^a$<br>$n_s^b$<br>$n_s^c$ |
| $\mathbf{S}(\mathbf{q},s3)$ | $-n_s^a$<br>$n_s^b$<br>$-n_s^c$ | $n_s^a$<br>$-n_s^b$<br>$n_s^c$ | $-n_s^a$<br>$n_s^b$<br>$-n_s^c$ | $n_s^a$<br>$-n_s^b$<br>$n_s^c$ |
| $\mathbf{S}(\mathbf{q},s4)$ | $-n_s^a$<br>$-n_s^b$<br>$n_s^c$ | $n_s^a$<br>$n_s^b$<br>$-n_s^c$ | $n_s^a$<br>$n_s^b$<br>$-n_s^c$ | $-n_s^a$<br>$-n_s^b$<br>$n_s^c$ |
| $\mathbf{S}(\mathbf{q},c1)$ | $n_c^a$<br>0<br>0 | $n_c^a$<br>0<br>0 | 0<br>$n_c^b$<br>$n_c^c$ | 0<br>$n_c^b$<br>$n_c^c$ |
| $\mathbf{S}(\mathbf{q},c2)$ | $-n_c^a$<br>0<br>0 | $n_c^a$<br>0<br>0 | 0<br>$n_c^b$<br>$-n_c^c$ | 0<br>$-n_c^b$<br>$n_c^c$ |

TABLE III: Allowed spin functions (i. e. actual position Fourier coefficients) within the unit cell of NVO for wavevector $(q,0,0)$ which are eigenvectors of $2_x$ and $m_z$ with the eigenvalues $\lambda$ listed. Irrep stands for the irreducible representation as labeled in Ref. 6. The labeling of the sites is as in Table II and Fig. 2. Here $n_p^\alpha$ ($p=$s or c, $\alpha=a,b,c$) denotes the complex quantity $n_p^\alpha(\mathbf{q})$.

Now we apply this formalism to find the actual position Fourier coefficients which are eigenfunctions of the two operators $2_x$ and $m_z$. In so doing note the simplicity of Eq. (16): since, for NVO, the operations $2_x$ and $m_z$ do not change the $x$ coordinate, we simply have

$$S'_\alpha(\mathbf{q},\boldsymbol{\tau}_f) \;=\; \xi_\alpha S'_\alpha(\mathbf{q},\boldsymbol{\tau}_i) \ . \qquad (22)$$

Thus the eigenvalue conditions for $2_x$ acting on the spine sites (#1-#4) are

$$\begin{aligned} S_\alpha(q,1)' &= \xi_\alpha(2_x)S_\alpha(q,2)=\lambda(2_x)S_\alpha(q,1) \\ S_\alpha(q,2)' &= \xi_\alpha(2_x)S_\alpha(q,1)=\lambda(2_x)S_\alpha(q,2) \\ S_\alpha(q,3)' &= \xi_\alpha(2_x)S_\alpha(q,4)=\lambda(2_x)S_\alpha(q,3) \\ S_\alpha(q,4)' &= \xi_\alpha(2_x)S_\alpha(q,3)=\lambda(2_x)S_\alpha(q,4) \ , \qquad (23) \end{aligned}$$

from which we see that $\lambda(2_x)=\pm1$ and

$$\begin{aligned} S_\alpha(q,2) &= [\xi_\alpha(2_x)/\lambda(2_x)]S_\alpha(q,1) \ , \\ S_\alpha(q,3) &= [\xi_\alpha(2_x)/\lambda(2_x)]S_\alpha(q,4) \ . \qquad (24) \end{aligned}$$

The eigenvalue conditions for $m_z$ acting on the spine sites are

$$\begin{aligned} S_\alpha(q,1)' &= \xi_\alpha(m_z)S_\alpha(q,4)=\lambda(m_z)S_\alpha(q,1) \\ S_\alpha(q,4)' &= \xi_\alpha(m_z)S_\alpha(q,1)=\lambda(m_z)S_\alpha(q,4) \\ S_\alpha(q,2)' &= \xi_\alpha(m_z)S_\alpha(q,3)=\lambda(m_z)S_\alpha(q,2) \\ S_\alpha(q,3)' &= \xi_\alpha(m_z)S_\alpha(q,2)=\lambda(m_z)S_\alpha(q,3) \ , \qquad (25) \end{aligned}$$

from which we see that $\lambda(m_z)=\pm1$ and

$$S_\alpha(q,4) \;=\; [\xi_\alpha(m_z)/\lambda(m_z)]S_\alpha(q,1) \ . \qquad (26)$$

We thereby construct the eigenvectors for the spine sites as given in Table III. The results for the cross-tie sites are obtained in the same way and are also given in the table. Each set of eigenvalues corresponds, in technical terms, to a single irreducible representation (irrep). Since each operator can have either of two eigenvalues, we have four irreps to consider. Note that these spin functions, since they are actually Fourier coefficients, are complex-valued quantities. [The spin itself is real because $F(-\mathbf{q})=F(\mathbf{q})^*$.] Note that each column of Table III gives the most general form of an allowed eigenvector for which one has 4 (or 5, depending on the irrep) independent complex constants. To further illustrate the meaning of this table we explicitly write, in Eq. (45), below, the spin distribution arising from one irrep, $\Gamma_4$.

So far, the present analysis reproduces the standard results and indeed computer programs exist to construct such tables. But for multiferroics it may be quicker to obtain and understand how to construct the possible spin functions by hand rather than to understand how to use the program! Usually these programs give the results in terms of unit cell Fourier transforms, which we claim are not as natural a representation in cases like NVO. In terms of unit cell Fourier transforms the eigenvalue conditions for $2_x$ acting on the spine sites (#1-#4) are the same as Eq. (23) for actual position Fourier transforms because the operation $2_x$ does not change the unit cell. However, for the glide operation $m_z$ this is not the case. If we start from site #1 or site #2 the translation along the $y$ axis takes the spin to a final unit cell displaced by $(-a/2)\hat{\imath}+(b/2)\hat{\jmath}$, whereas if we start from site #3 or site #4 the translation along the $y$ axis takes the spin to a final unit cell displaced by $(a/2)\hat{\imath}+(b/2)\hat{\jmath}$. Now the eigenvalue conditions for $m_z$ acting on the spine sites (#1-#4) are

$$\begin{aligned} S_\alpha(q,1)' &= \xi_\alpha(m_z)S_\alpha(q,4)\eta=\lambda(m_z)S_\alpha(q,1) \\ S_\alpha(q,4)' &= \xi_\alpha(m_z)S_\alpha(q,1)\eta^*=\lambda(m_z)S_\alpha(q,4) \\ S_\alpha(q,2)' &= \xi_\alpha(m_z)S_\alpha(q,3)\eta=\lambda(m_z)S_\alpha(q,2) \\ S_\alpha(q,3)' &= \xi_\alpha(m_z)S_\alpha(q,2)\eta^*=\lambda(m_z)S_\alpha(q,3) \ , \qquad (27) \end{aligned}$$

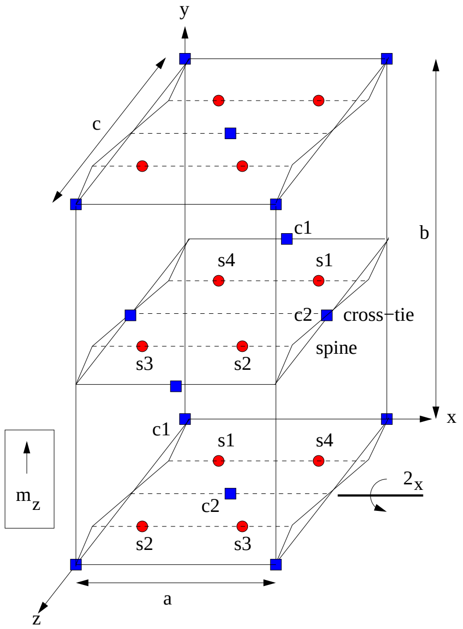

FIG. 2: (Color online). Ni sites in the conventional unit cell of NVO. The primitive translation vectors $\mathbf{v}_n$ are $\mathbf{v}_1 = (a/2)\hat{a} + (b/2)\hat{b}$, $\mathbf{v}_2 = (a/2)\hat{a} - (b/2)\hat{b}$, and $\mathbf{v}_3 = c\hat{c}$. The "cross-tie" sites (on-line=blue) c1 and c2 lie in a plane with $b = 0$. The "spine" sites (on-line=red) are labeled s1, s2, s3, and s4 and they may be visualized as forming chains parallel to the **a**-axis. These chains are in the buckled plane with $b = \pm\delta$, where $\delta = 0.13b$ as is indicated. Cross-tie sites in adjacent planes (displaced by $(\pm b/2)\hat{b}$) are indicated by open circles. Spine sites in adjacent planes are located directly above (or below) the sites in the plane shown. In the incommensurate phases the wavevector describing magnetic ordering lies along the **a** axis. The axis of the two-fold rotation about the $x$-axis is shown. The glide plane is indicated by the mirror plane at $z = \frac{3}{4}$ and the arrow above $m_z$ indicates that a translation of $b/2$ in the $y$-direction is involved.

where $\eta = \exp(i\pi q)$. One finds that all entries for $S(\mathbf{q}, s3)$, $S(\mathbf{q}, s4)$, and $S(\mathbf{q}, c2)$ now carry the phase factor $\eta^* = \exp(-i\pi\hat{q})$. But this is just the factor to make the unit cell result

$$\mathbf{S}(\mathbf{R}, \boldsymbol{\tau}) \;=\; \mathbf{S}(\mathbf{q}, \boldsymbol{\tau}) e^{-i\mathbf{q}\cdot\mathbf{R}} \tag{28}$$

be the same (to within an overall phase factor) as the actual position result

$$\mathbf{S}(\mathbf{R}, \boldsymbol{\tau}) \;=\; \mathbf{S}(\mathbf{q}, \boldsymbol{\tau}) e^{-i\mathbf{q}\cdot(\mathbf{R}+\boldsymbol{\tau})} \ . \tag{29}$$

We should emphasize that in such a simple case as NVO, it is actually not necessary to invoke any group theoretical concepts to arrive at the results of Table III for the most general spin distribution consistent with crystal symmetry.

More importantly, it is not commonly understood[25,26,27] that one can also extract information using the symmetry of an operation (inversion) which need *does not* conserve wavevector.[3,4,5,6,7,17,19] Since what we are about to say is unfamiliar, we start from first principles. The quadratic free energy may be written as

$$F_2 \;=\; \sum_{\mathbf{q}} \sum_{\tau,\tau';\alpha\beta} F_{\alpha\beta}^{\tau\tau'} S_\alpha(\mathbf{q}, \tau)^* S_\beta(\mathbf{q}, \tau') \ , \tag{30}$$

where we restrict the sum over wavevectors to the star of the wavevector of interest. One term of this sum is

$$F_2(\mathbf{q}_0) \;=\; \sum_{\tau,\tau';\alpha\beta} F_{\alpha\beta}^{\tau\tau'} S_\alpha(\mathbf{q}_0, \tau)^* S_\beta(\mathbf{q}_0, \tau') \ . \tag{31}$$

It should be clear that the quadratic free energy, $F_2$ is invariant under all the symmetry operations of the paramagnetic space group (i. e. what one calls the space group of the crystal).[22,23] For centrosymmetric crystals there are three classes of such symmetry operations. The first class consists of those operations which leave $q_0$ invariant and these are the symmetries taken into account in the usual formulation.[25,26,27] The second class consists of operations which take $q_0$ into another wavevector of the star (call it $\mathbf{q}_1$), where $\mathbf{q}_1 \neq -\mathbf{q}_0$. Use of these symmetries allows one to completely characterize the wavefunction at wavevector $\mathbf{q}_1$ in terms of the wavefunction for $\mathbf{q}_0$. These relations are needed if one is to discuss the possibility of simultaneously condensing more than one wavevector in the star of $\mathbf{q}$.[35] Finally, the third class consists of spatial inversion (unless the wavevector and its negative differ by a reciprocal lattice vector, in which case inversion belongs in class #1). The role of inversion symmetry is almost universally overlooked,[25,26,27] as is evident from examination of a number of recent papers. Unlike the operations of class #1 which takes $S_n(\mathbf{q})$ into an $S_{n'}(\mathbf{q})$ (for irreps of dimension one which is true for most cases considered in this paper), inversion takes $S_n(\mathbf{q})$ into an $S_{n'}(-\mathbf{q})$. Nevertheless it does take the form written in Eq. (31) into itself and restricts the possible form of the wavefunctions. So we now consider the consequences of invariance of $F_2$ under inversion.[3,4,5,6,7] For this purpose we write Eq. (12) in terms of the spin coordinates $m$ of Table III. (The result will, of course, depend on which irrep $\Gamma$ we consider.) In any case, the part of $F_2$ which depends on $\mathbf{q}_0$ can be written as

$$\begin{aligned} F_2(\mathbf{q}) \;&=\; \sum_{\tau,\tau';\alpha\beta} F_{\alpha\beta}^{\tau\tau'} S_\alpha(\mathbf{q}_0, \tau)^* S_\beta(\mathbf{q}_0, \tau') \\ &=\; \sum_{N,\alpha;N',\beta} G_{N,\alpha;N',\beta} [n_N^\alpha]^* [n_{N'}^\beta] \\ &=\; \sum_{N,\alpha;N',\beta} G_{N,\alpha;N',\beta} [\mathcal{I} n_N^\alpha]^* [\mathcal{I} n_{N'}^\beta] \ , \end{aligned} \tag{32}$$

where $N$ and $N'$ assume the values "s" for spin and "c" for cross-tie and $\alpha$ and $\beta$ label components. Now we need to understand the effect of $\mathcal{I}$ on the spin Fourier coefficients listed in Table III. Since we use actual position Fourier coefficients, we apply Eq. (20). For the cross-tie variables (which sit at a center of inversion symmetry) inversion takes the spin coordinates of one spine sublattice into the complex conjugate of itself:

$$\mathcal{I}\mathbf{S}(\mathbf{q},cn) = [\mathbf{S}(\mathbf{q},cn)]^* \ . \tag{33}$$

Thus in terms of the $n$'s this gives

$$\mathcal{I}n_c^\alpha = [n_c^\alpha]^* \ , \qquad\qquad \alpha = x,y,z \ . \tag{34}$$

The effect of inversion on the spine variables again follows from Eq. (20). Since inversion interchanges sublattice #1 and #3, we have

$$[\mathbf{S}(\mathbf{q},s3)]' = [\mathbf{S}(\mathbf{q},s1)]^* \ . \tag{35}$$

For $\lambda(2_x) = \lambda(m_z) = +1$ (i. e. for irrep $\Gamma_1$), we substitute the values of the spin vectors from the first column of Table III to get

$$\begin{aligned} \mathcal{I}[-n_s^a] &= [n_s^a]^* \ , \qquad \mathcal{I}[n_s^b] = [n_s^b]^* \ , \\ \mathcal{I}[-n_s^c] &= [n_s^c]^* \ . \end{aligned} \tag{36}$$

Note that some components introduce a factor $-1$ under inversion and others do not. (Which ones have the minus signs depends on which irrep we consider.) If we make a change of variable by replacing $n_s^\alpha$ in column #1 of Table III by $in_s^\alpha$ for those components for which $\mathcal{I}$ introduces a minus sign and leave the other components alone, then we may rewrite the first column of Table III in the form given in Table IV. In terms of these new variables one has

$$\mathcal{I}[n_s^\alpha] = [n_s^\alpha]^* \ . \tag{37}$$

(It is convenient to define the spin Fourier coefficients so that they all transform in the same way under inversion. Otherwise one would have to keep track of variables which transform with a plus sign and those which transform with a minus sign.) Repeating this process for all the other irreps we write the possible spin functions as those of Table IV. We give an explicit formula for the spin distribution for one irrep in Eq. (45) below.

Now we implement Eq. (32), where the spin functions are taken to be the variables listed in Table IV. First note that the matrix $\mathbf{G}$ in Eq. (32) has to be Hermitian to ensure that $F_2$ be real:

$$G_{M,\alpha;N,\beta} \ = \ [G_{N,\beta;M,\alpha}]^* \ . \tag{38}$$

| Irrep= | $\Gamma_1$ | $\Gamma_2$ | $\Gamma_3$ | $\Gamma_4$ |
|---|---|---|---|---|
| $\lambda(2_x) =$ | $+1$ | $+1$ | $-1$ | $-1$ |
| $\lambda(m_z) =$ | $+1$ | $-1$ | $-1$ | $+1$ |
| $\mathbf{S}(\mathbf{q},s1)$ | $in_s^a$<br>$n_s^b$<br>$in_s^c$ | $n_s^a$<br>$in_s^b$<br>$n_s^c$ | $in_s^a$<br>$n_s^b$<br>$in_s^c$ | $n_s^a$<br>$in_s^b$<br>$n_s^c$ |
| $\mathbf{S}(\mathbf{q},s2)$ | $in_s^a$<br>$-n_s^b$<br>$-in_s^c$ | $n_s^a$<br>$-in_s^b$<br>$-n_s^c$ | $-in_s^a$<br>$n_s^b$<br>$in_s^c$ | $-n_s^a$<br>$in_s^b$<br>$n_s^c$ |
| $\mathbf{S}(\mathbf{q},s3)$ | $-in_s^a$<br>$n_s^b$<br>$-in_s^c$ | $n_s^a$<br>$-in_s^b$<br>$n_s^c$ | $-in_s^a$<br>$n_s^b$<br>$-in_s^c$ | $n_s^a$<br>$-in_s^b$<br>$n_s^c$ |
| $\mathbf{S}(\mathbf{q},s4)$ | $-in_s^a$<br>$-n_s^b$<br>$in_s^c$ | $n_s^a$<br>$in_s^b$<br>$-n_s^c$ | $in_s^a$<br>$n_s^b$<br>$-in_s^c$ | $-n_s^a$<br>$-in_s^b$<br>$n_s^c$ |
| $\mathbf{S}(\mathbf{q},c1)$ | $n_c^a$<br>0<br>0 | $n_c^a$<br>0<br>0 | 0<br>$n_c^b$<br>$n_c^c$ | 0<br>$n_c^b$<br>$n_c^c$ |
| $\mathbf{S}(\mathbf{q},c2)$ | $-n_c^a$<br>0<br>0 | $n_c^a$<br>0<br>0 | 0<br>$n_c^b$<br>$-n_c^c$ | 0<br>$-n_c^b$<br>$n_c^c$ |

TABLE IV: As Table III except that now the effect of inversion symmetry is taken into account, as a result of which, apart from an overall phase factor all the $n$'s in this table can be taken to be real-valued.

Then, using Eq. (37), we find that Eq. (32) is

$$\begin{aligned} F_2(\mathbf{q}_0) \ &= \ \sum_{M,\alpha;N,\beta} [n_M^\alpha]^* G_{M,\alpha;N,\beta} n_N^\beta \\ &= \sum_{M,\alpha;N,\beta} [\mathcal{I}n_M^\alpha]^* G_{M,\alpha;N,\beta} [\mathcal{I}n_N^\beta] \\ &= \sum_{M,\alpha;N,\beta} n_M^\alpha G_{M,\alpha;N,\beta} [n_N^\beta]^* \\ &= \sum_{M,\alpha;N,\beta} [n_M^\alpha]^* G_{N,\beta;M,\alpha} [n_N^\beta] \ , \end{aligned} \tag{39}$$

where, in the last line, we interchanged the roles of the dummy indices $M,\alpha$ and $N,\beta$. By comparing the first and last lines, one sees that the matrix $G$ is symmetric. Since this matrix is also Hermitian, all its elements must be *real valued*. Thus all its eigenvectors can be taken to have only real-valued components. But the $m$'s are allowed to be complex valued. So, the conclusion is that for each irrep, we may write

$$n_N^\alpha(\Gamma) \ = \ e^{i\phi_\Gamma}[r_N^\alpha(\Gamma)] \ , \tag{40}$$

where the $r$'s are all real valued and $\phi_\Gamma$ is an overall phase which can be chosen arbitrarily for each $\Gamma$. It is likely that the phase will be fixed by high-order Umklapp terms in the free energy, but the effects of such phase locking may be beyond the range of experiments.

It is worth noting how these results should be (and in a few cases[3,4,6] have been) used in the structure determinations. One should choose the best fit to the diffraction data using, in turn, each irrep (i. e. each set of eigenvalues of $2_x$ and $m_z$). Within each representation one parametrizes the spin structure by choosing the Fourier coefficients as in the relevant column of Table IV. Note that instead of having 4 or 5 complex coefficients to describe the six sites within the unit cell (see Table III), one has only 4 or 5 (depending on the representation) *real-valued* coefficients to determine. The relative phases of the complex coefficients have all been fixed by invoking inversion symmetry. This is clearly a significant step in increasing the precision of the determination of the magnetic structure from experimental data.

## B. Order Parameters

We now review how the above symmetry classification influences the introduction of order parameters which allow the construction of Landau expansions.[4,6] The form of the order parameter should be such that it has the potential to describe all ordering which are allowed by the quadratic free energy $F_2$. Thus, for an isotropic Heisenberg model on a cubic lattice, the order parameter has three components (i. e. it involves a three dimensional irrep) because although the fourth order terms will restrict order to occur only along certain directions, as far as the quadratic terms are concerned, all directions are equivalent. The analogy here is that the overall phase of the spin function $\phi(\Gamma)$ is not fixed by the quadratic free energy and accordingly the order parameter must be a complex variable which includes such a phase. One also recognizes that although the amplitude of the critical eigenvector is not fixed by the quadratic terms in the free energy, the ratios of its components are fixed by the specific form of the inverse susceptibility matrix. Although we do not wish to discuss the explicit form of this matrix, what should be clear is that the components of the spins which order must be proportional to the components of the critical eigenvector. The actual amplitude of the spin ordering is determined by the competition between the quadratic and fourth order terms in the free energy. If $\Gamma_p$ is the irrep which is critical, then just below the ordering temperature we write

$$n_N^\alpha(\mathbf{q}) \ = \ \boldsymbol{\sigma}_p(\mathbf{q}) r_N^\alpha(\Gamma_p) \ , \tag{41}$$

where the $r$'s are real components of the critical eigenvector (coming from irrep $\Gamma_p$) of the matrix $\mathbf{G}$ of Eq. (32) and are now *normalized* by

$$\sum_{\alpha N} [r_N^\alpha]^2 = 1 \ . \tag{42}$$

Here the order parameter for irrep $\Gamma(\mathbf{q})$, $\boldsymbol{\sigma}_p(\mathbf{q})$ is a complex variable, since it has to incorporate the arbitrary complex phase $\phi_p$ associated with irrep $\Gamma_p$:

$$\boldsymbol{\sigma}_p(\pm|\mathbf{q}|) \ = \ \sigma_p e^{\pm i\phi_p} \ . \tag{43}$$

The order parameter transforms as indicated in the tables by its listed eigenvalues under the symmetry operations $2_x$ and $m_z$. Since the components of the critical eigenvector are dominantly determined by the quadratic terms,[36] one can say that just below the ordering temperature the description in terms of an order parameter continues to hold but

$$\sigma_p \sim |T_c - T|_p^\beta \ , \tag{44}$$

where mean-field theory gives $\beta = 1/2$ but corrections due to fluctuation are expected.[37]

To summarize and illustrate the use of Table IV we write an explicit expression for the magnetizations of the #1 spine sublattice and the #1 cross-tie sublattice for irrep $\Gamma_4$ [$\lambda(2_x) = -1$ and $\lambda(m_z) = +1$]. We use the definition of the order parameter and sum over both signs of the wavevector to get

$$\begin{aligned}
S_x(\mathbf{r}, s1) &= 2\sigma_4 r_s^x \cos(qx + \phi_4) \\
S_y(\mathbf{r}, s1) &= 2\sigma_4 r_s^y \sin(qx + \phi_4) \\
S_z(\mathbf{r}, s1) &= 2\sigma_4 r_s^z \cos(qx + \phi_4) \\
S_x(\mathbf{r}, s2) &= -2\sigma_4 r_s^x \cos(qx + \phi_4) \\
S_y(\mathbf{r}, s2) &= 2\sigma_4 r_s^y \sin(qx + \phi_4) \\
S_z(\mathbf{r}, s2) &= 2\sigma_4 r_s^z \cos(qx + \phi_4) \\
S_x(\mathbf{r}, s3) &= 2\sigma_4 r_s^x \cos(qx + \phi_4) \\
S_y(\mathbf{r}, s3) &= -2\sigma_4 r_s^y \sin(qx + \phi_4) \\
S_z(\mathbf{r}, s3) &= 2\sigma_4 r_s^z \cos(qx + \phi_4) \\
S_x(\mathbf{r}, s4) &= -2\sigma_4 r_s^x \cos(qx + \phi_4) \\
S_y(\mathbf{r}, s4) &= -2\sigma_4 r_s^y \sin(qx + \phi_4) \\
S_z(\mathbf{r}, s4) &= 2\sigma_4 r_s^z \cos(qx + \phi_4) \\
S_x(\mathbf{r}, c1) &= 0 \\
S_y(\mathbf{r}, c1) &= 2\sigma_4 r_c^y \cos(qx + \phi_4) \\
S_z(\mathbf{r}, c1) &= 2\sigma_4 r_c^z \cos(qx + \phi_4) \\
S_x(\mathbf{r}, c1) &= 0 \\
S_y(\mathbf{r}, c2) &= -2\sigma_4 r_c^y \cos(qx + \phi_4) \\
S_z(\mathbf{r}, c2) &= 2\sigma_4 r_c^z \cos(qx + \phi_4)
\end{aligned} \tag{45}$$

and similarly for the other irreps. Here $\mathbf{r} \equiv (x, y, z)$ is the actual location of the spin. Using explicit expressions like the above (or more directly from Table IV), one can verify that the order parameters have the transformation properties:

$$\begin{aligned}
2_x\boldsymbol{\sigma}_1(\mathbf{q}) &= +\boldsymbol{\sigma}_1(\mathbf{q}) \ , \qquad m_z\boldsymbol{\sigma}_1(\mathbf{q}) = +\boldsymbol{\sigma}_1(\mathbf{q}) \ , \\
2_x\boldsymbol{\sigma}_2(\mathbf{q}) &= +\boldsymbol{\sigma}_2(\mathbf{q}) \ , \qquad m_z\boldsymbol{\sigma}_2(\mathbf{q}) = -\boldsymbol{\sigma}_2(\mathbf{q}) \ , \\
2_x\boldsymbol{\sigma}_3(\mathbf{q}) &= -\boldsymbol{\sigma}_3(\mathbf{q}) \ , \qquad m_z\boldsymbol{\sigma}_3(\mathbf{q}) = -\boldsymbol{\sigma}_3(\mathbf{q}) \ , \\
2_x\boldsymbol{\sigma}_4(\mathbf{q}) &= -\boldsymbol{\sigma}_4(\mathbf{q}) \ , \qquad m_z\boldsymbol{\sigma}_4(\mathbf{q}) = +\boldsymbol{\sigma}_4(\mathbf{q})
\end{aligned} \tag{46}$$

and

$$\mathcal{I}\boldsymbol{\sigma}_n(\mathbf{q}) \ = \ [\boldsymbol{\sigma}_n(\mathbf{q})]^* . \tag{47}$$

Note that even when more than a single irrep is present, the introduction of order parameters, as done here, provides a framework within which one can represent the spin distribution as a linear combination of distributions each having a characteristic symmetry, as expressed by Eq. (46). When the structure of the unit cell is ignored[13] that information is not readily accessible. Also note that the phase of each irrep $\Gamma_n$ is defined so that when $\phi_n = 0$, the wave is inversion-symmetric about $\mathbf{r} = 0$. For a single irrep this specification is not important. However, when one has two irreps, then inversion symmetry is only maintained if their phases are equal.

In many systems, the initial incommensurate order that first occurs as the temperature is lowered becomes unstable as the temperature is further lowered.[21] Typically, the initial order involves spins oriented along their easy axis with sinusoidally varying magnitude. However, the fourth order terms in the Landau expansion favor fixed length spins. As the temperature is lowered the fixed length constraint becomes progressively more important and at a second, lower, critical temperature a transition occurs in which transverse components become nonzero. Although the situation is more complicated when there are several spins per unit cell, the result is similar: the fixed length constraint is best realized when more than a single irrep has condensed. So, for NVO and TMO as the temperature is lowered one encounters a second phase transition in which a second irrep appears. Within a low-order Landau expansion this phenomenon is described by a free energy of the form[6]

$$\begin{aligned} F &= \frac{1}{2}(T-T_>)\sigma_>^2 + \frac{1}{2}(T-T_<)\sigma_<^2 + u_>\sigma_>^4 \\ &\quad + u_<\sigma_<^4 + w\sigma_>^2\sigma_<^2 \ , \end{aligned} \tag{48}$$

where $T_> > T_<$. This system has been studied in detail by Bruce and Aharony.[38] For our purposes, the most important result is that for suitable values of the parameters ordering in $\sigma_>$ occurs at $T_>$ and at some lower temperature order in $\sigma_<$ may occur. The application of this theory to the present situation is simple: we can (and usually do) have two magnetic phase transitions in which first one irrep and then at a lower temperature a second irrep condense. A question arises as to whether the condensation of one irrep can induce the condensation of a second irrep. This is not possible because the two irreps have different symmetry. But could the presence of two irreps, $\Gamma_>$ and $\Gamma_<$ induce the appearance of a third irrep $\Gamma_3$ at the temperature at which $\Gamma_<$ first appears? For that to happen would require that $\Gamma_>^n \otimes \Gamma_<^m \otimes \Gamma_3$ contain the unit representation for some values of $n$ and $m$. This or any higher combination of representations is not allowed for the simple four irreps system like NVO. In more complex systems one might have to allow for such a phenomenon.

## III. APPLICATIONS

In this section we apply the above formalism to a number of multiferroics of current interest.

### A. MnWO$_4$

MnWO$_4$ (MWO) crystallizes in the space group P2/c (#14 in Ref. 28) whose general positions are given in Table V. The two magnetic Mn ions per unit cell are at positions

$$\boldsymbol{\tau}_1 = (\frac{1}{2}, y, \frac{1}{4}) \ , \quad \boldsymbol{\tau}_2 = (\frac{1}{2}, 1-y, \frac{3}{4}) \ . \tag{49}$$

The wavevector of incommensurate magnetic ordering is[34,39] $\mathbf{q} = (q_x, 1/2, q_z)$ with $q_x \approx -0.21$ and $q_z \approx 0.46$) and is left invariant by the identity and $m_y$. We start by constructing the eigenvectors of the quadratic free energy (i. e. the inverse susceptibility matrix). Here we use unit cell Fourier transforms to facilitate comparison with Ref. 39. Below $X$, $Y$, and $Z$ denote integers (in units of lattice constants). When

| | |
|---|---|
| $E\mathbf{r} = (x, y, z)$ | $m_y\mathbf{r} = (x, \overline{y}, z + \frac{1}{2})$ |
| $\mathcal{I}\mathbf{r} = (\overline{x}, \overline{y}, \overline{z})$ | $2_y\mathbf{r} = (\overline{x}, y, \overline{z} + \frac{1}{2})$ |

TABLE V: General Positions for space group P2/c.

$$\begin{aligned} \mathbf{R}_f + \boldsymbol{\tau}_f &= (X, Y, Z) + \boldsymbol{\tau}_1 \\ &= (X + \frac{1}{2}, Y + y, Z + \frac{1}{4}) \ , \end{aligned} \tag{50}$$

then

$$\begin{aligned} \mathbf{R}_i + \boldsymbol{\tau}_i &= [m_y]^{-1}(\mathbf{R}_f + \boldsymbol{\tau}_f) \\ &= (X + \frac{1}{2}, -Y - y, Z_{\frac{1}{4}}) \\ &= (X, -Y - 1, Z - 1) + \boldsymbol{\tau}_2 \ . \end{aligned} \tag{51}$$

Then Eq. (18) gives the eigenvalue condition to be

$$\begin{aligned} S'_\alpha(\mathbf{q}, \tau_1) &= \xi_\alpha(m_y) S_\alpha(\mathbf{q}, \boldsymbol{\tau}_2) e^{2\pi i \hat{\mathbf{q}} \cdot [(2Y+1)\hat{j} + \hat{k}]} \\ &= \xi_\alpha(m_y) S_\alpha(\mathbf{q}, \tau_2) e^{\pi i + 2\pi i \hat{q}_z} \\ &= \lambda S_\alpha(\mathbf{q}, \tau_1) \ , \end{aligned} \tag{52}$$

where $\xi_x(m_y) = -\xi_y(m_y) = \xi_z(m_y) = -1$. When

$$\begin{aligned} \mathbf{R}_f + \boldsymbol{\tau}_f &= (X, Y, Z) + \boldsymbol{\tau}_2 \\ &= (X + \frac{1}{2}, Y + 1 - y, Z + \frac{3}{4}) \ , \end{aligned} \tag{53}$$

then

$$\begin{aligned} \mathbf{R}_i + \boldsymbol{\tau}_i &= (X + \frac{1}{2}, -Y - 1 - y, Z + \frac{1}{4}) \\ &= (X, -Y - 1, Z) + \boldsymbol{\tau}_1 \ , \end{aligned} \tag{54}$$

and Eq. (18) gives the eigenvalue condition to be

$$\begin{aligned} S'_\alpha(\mathbf{q}, \tau_2) &= \xi_\alpha(m_y) S_\alpha(\mathbf{q}, \boldsymbol{\tau}_1) e^{2\pi i \hat{\mathbf{q}} \cdot (2Y+1)\hat{j}} \\ &= \xi_\alpha(m_y) S_\alpha(\mathbf{q}, \tau_1)[-1] = \lambda S_\alpha(\mathbf{q}, \tau_2) \ . \end{aligned} \tag{55}$$

From Eqs. (52) and (55) we get $\lambda = \pm e^{i\pi\hat{q}_z}$ and

$$S_\alpha(\mathbf{q}, \tau_2) = -[\xi_\alpha(m_y)/\lambda] S_\alpha(\mathbf{q}, \tau_1) \ . \tag{56}$$

So we get the results listed in Table VI.

So far the analysis is essentially the completely standard one. Now we use the fact that the free energy is invariant under spatial inversion, even though that operation does not conserve wavevector.[3,4,6,7] We now determine the effect of inversion on the $n$'s. As will become apparent use of unit cell Fourier transforms makes this

| Irrep | $\Gamma_1$ | $\Gamma_2$ |
|---|---|---|
| $\lambda(m_y) =$ | $e^{i\pi\hat{q}_z}$ | $-e^{i\pi\hat{q}_z}$ |
| $\mathbf{S}(\mathbf{q},1)$ | $a^*n_x$ | $a^*n_x$ |
|  | $a^*n_y$ | $a^*n_y$ |
|  | $a^*n_z$ | $a^*n_z$ |
| $\mathbf{S}(\mathbf{q},2)$ | $an_x$ | $-an_x$ |
|  | $-an_y$ | $an_y$ |
|  | $an_z$ | $-an_z$ |

TABLE VI: Allowed spin eigenfunctions for MWO (apart from an overall phase factor) before inversion symmetry is taken into account, where $a = \exp(-i\pi\hat{q}_z/2)$. Here the $n(\mathbf{q})$'s are complex and we have taken the liberty to adjust the overall phase to give a symmetrical looking result. But these results are equivalent to Table II of Ref. 39.

analysis more complicated than if we had used actual position transforms. We use Eq. (21) to write

$$\begin{aligned}\mathcal{I}S(\mathbf{q},\tau=1) &= S(\mathbf{q},\tau=2)^*e^{-2\pi i\hat{\mathbf{q}}\cdot(\hat{i}+\hat{j}+\hat{k})} \\ &\equiv bS(\mathbf{q},2)^* \ , \qquad (57)\end{aligned}$$

where $b = -\exp[-2\pi i(\hat{q}_x + \hat{q}_z)]$. For $\Gamma_2$ we get

$$\mathcal{I}[n_x, n_y, n_z] \ = \ [-n_x, n_y, -n_z]^*b \ , \qquad (58)$$

which we can write as

$$\mathcal{I}n_\alpha \ = \ b\xi_\alpha(m_y)n^*_\alpha \ . \qquad (59)$$

Now the free energy is quadratic in the Fourier spin coefficients, which are linearly related to the $n$'s. So the free energy can be written as

$$F_2 \ = \ \mathbf{n}^\dagger\mathbf{G}\mathbf{n} \ , \qquad (60)$$

where $\mathbf{n} = (n_x, n_y, n_z)$ is a column vector and $\mathbf{G}$ is a $3\times3$ matrix which we write as

$$\mathbf{G} \ = \ \begin{bmatrix} A & \alpha & \beta \\ \alpha^* & B & \gamma \\ \beta^* & \gamma^* & C \end{bmatrix} \ , \qquad (61)$$

where, for Hermiticity the Roman letters are real and the Greek ones complex. Now we use the fact that also we must have invariance with respect to inversion, which after all is a crystal symmetry. Thus

$$F_2 \ = \ [\mathcal{I}\mathbf{n}]^\dagger\mathbf{G}[\mathcal{I}\mathbf{n}] \ . \qquad (62)$$

This can be written as

$$\begin{aligned}F_2 &= \sum_{\alpha\beta} b\xi_\alpha(m_y)n_\alpha G_{\alpha\beta}b^*a^*\xi_\beta(m_y)n^*_\beta \\ &= \sum_{\alpha\beta}\xi_\alpha(m_y)n_\alpha G_{\alpha\beta}\xi_\beta(m_y)n^*_\beta \ . \qquad (63)\end{aligned}$$

| Irrep | $\Gamma_1$ | $\Gamma_2$ |
|---|---|---|
| $\lambda(m_y) =$ | $e^{i\pi\hat{q}_z}$ | $-e^{i\pi\hat{q}_z}$ |
| $\mathbf{S}(\mathbf{q},1)$ | $a^*r$ | $-ia^*r$ |
|  | $ia^*s$ | $a^*s$ |
|  | $a^*t$ | $-ia^*t$ |
| $\mathbf{S}(\mathbf{q},2)$ | $ar$ | $iar$ |
|  | $-ias$ | $as$ |
|  | $at$ | $iat$ |

TABLE VII: As Table VI, except that here inversion symmetry is taken into account. Here $r$, $s$, and $t$ are real. All six components can be multiplied by an overall phase factor which we have not explicitly written.

Thus we may write

$$\begin{aligned}F_2 &= \mathbf{n}^{\rm tr}\begin{bmatrix} A & -\alpha & \beta \\ -\alpha^* & B & -\gamma \\ \beta^* & -\gamma^* & C \end{bmatrix}\mathbf{n}^* \\ &= \mathbf{n}^\dagger\begin{bmatrix} A & -\alpha^* & \beta^* \\ -\alpha & B & -\gamma^* \\ \beta & -\gamma & C \end{bmatrix}\mathbf{n} \ , \qquad (64)\end{aligned}$$

where "tr" indicates transpose (so $\mathbf{n}^{\rm tr}$ is a row vector). Since the two expressions for $F_2$, Eqs. (60) and (64), must be equal we see that $\alpha = ia$, $\beta = b$, and $\gamma = ic$, where $a$, $b$, and $c$ must be real. Thus $\mathbf{G}$ is of the form

$$\mathbf{G} \ = \ \begin{bmatrix} A & ia & b \\ -ia & B & ic \\ b & -ic & C \end{bmatrix} \ , \qquad (65)$$

where all the letters are real. This means that the critical eigenvector describing the long range order has to be of the form

$$(n_x, n_y, n_z) \ = \ e^{i\phi}(r, is, t) \ , \qquad (66)$$

where $r$, $s$, and $t$ are real. For $\Gamma_2$ we set $e^{i\phi} = -i$. For $\Gamma_1$ a similar calculation again yields Eq. (66), but here we set $e^{i\phi} = 1$. (These choices are not essential. They just make the symmetry more obvious.) Thus we obtain the final results given in Table VII. Lautenschlager et al[39] say (just above Table II) "Depending on the choice of the amplitudes and phases ..." What we see here is that inversion symmetry fixes the phases without the possibility of a choice (just as it did for NVO). Note again that we have about half the variables to fix in a structure determination when we take advantage of inversion invariance to fix the phase of the complex structure constants.

### 1. *Order Parameter*

Now we discuss the definition of the order parameter for this system. For this purpose we replace $r$ by $\boldsymbol{\sigma}r$, $s$

by $\boldsymbol{\sigma}s$. etc., with the normalization that

$$r^2 + s^2 + t^2 = 1 \ . \tag{67}$$

Here the order parameter $\boldsymbol{\sigma}$ is complex because we always have the freedom to multiply the wavefunction by a phase factor. (This phase factor might be "locked" by higher order terms in the free energy, but we do not consider that phenomenon here.[43]) We record the symmetry properties of the order parameter. With our choice of phases we have

$$\begin{aligned} \mathcal{I}\boldsymbol{\sigma}_n(\mathbf{q}) &= [\boldsymbol{\sigma}_n(\mathbf{q})]^* \ , \\ m_y\boldsymbol{\sigma}_n(\mathbf{q}) &= \lambda(\Gamma_n)\boldsymbol{\sigma}_n(\mathbf{q}) \\ m_y\boldsymbol{\sigma}_n(-\mathbf{q}) &= \lambda(\Gamma_n)^*\boldsymbol{\sigma}_n(-\mathbf{q}) \ , \end{aligned} \tag{68}$$

where $\boldsymbol{\sigma}_n(\mathbf{q})$ is the complex-valued order parameter for ordering of irrep $\Gamma_n$ and $\lambda(\Gamma_n)$ is the eigenvalue of $m_y$ given in Table VII. Now we write an explicit formula for the spin distribution in terms of the order parameters of the two irreps:

$$\begin{aligned} \mathbf{S}(\mathbf{R}, \quad \tau = 1) &= 2\sigma_1 \Big[(r_1\hat{i} + t_1\hat{k})\cos(\mathbf{q}\cdot\mathbf{R} + \phi_1 - \pi q_z/2) \\ &\quad + s_1\hat{j}\sin(\mathbf{q}\cdot\mathbf{R} + \phi_1 - \pi q_z/2)\Big] \\ &\quad + 2\sigma_2\Big[(-r_2\hat{i} - t_2\hat{k})\sin(\mathbf{q}\cdot\mathbf{R} + \phi_2 - \pi q_z/2) \\ &\quad + s_2\hat{j}\cos(\mathbf{q}\cdot\mathbf{R} + \phi_2 - \pi q_z/2)\Big] \ , \end{aligned} \tag{69}$$

$$\begin{aligned} \mathbf{S}(\mathbf{R}, \quad \tau = 2) &= 2\sigma_1 \Big[(r_1\hat{i} + t_1\hat{k})\cos(\mathbf{q}\cdot\mathbf{R} + \phi_1 + \pi q_z/2) \\ &\quad - s_1\hat{j}\sin(\mathbf{q}\cdot\mathbf{R} + \phi_1 + \pi q_z/2)\Big] \\ &\quad + 2\sigma_2\Big[(r_2\hat{i} + t_2\hat{k})\sin(\mathbf{q}\cdot\mathbf{R} + \phi_2 + \pi q_z/2) \\ &\quad + s_2\hat{j}\cos(\mathbf{q}\cdot\mathbf{R} + \phi_2 + \pi q_z/2)\Big] \ . \end{aligned} \tag{70}$$

One can explicitly verify that these expressions are consistent with Eq. (68). Note that when only one of the order parameters (say $\sigma_n$) is nonzero, we have inversion symmetry with respect to a redefined origin where $\phi_n = 0$. For each irrep we have to specify three real parameters, $\sigma r_n$, $\sigma s_n$, and $\sigma t_n$ and one overall phase $\phi_n$ rather than three complex-valued parameters had we not invoked inversion symmetry.

### B. TbMnO$_3$

Here we give the full details of the calculations for TbMnO$_3$ described in Ref. 3. The presentation here differs cosmetically from that in Ref. 5. The space group of TbMnO$_3$ is Pbnm which is #62 in Ref. 28 (although the positions are listed there for the Pnma setting). The space group operations for a general Wyckoff orbit is given in Table VIII. In Table IX we list the positions of the Mn and Tb ions within the unit cell and these are also shown in Fig. 3.

| | |
|---|---|
| $E\mathbf{r} = (x, y, z)$ | $2_x\mathbf{r} = (x + \frac{1}{2}, \overline{y} + \frac{1}{2}, \overline{z})$ |
| $2_z = (\overline{x}, \overline{y}, z + \frac{1}{2})$ | $2_y = (\overline{x} + \frac{1}{2}, y + \frac{1}{2}, \overline{z} + \frac{1}{2})$ |
| $\mathcal{I}\mathbf{r} = (\overline{x}, \overline{y}, \overline{z})$ | $m_x\mathbf{r} = (\overline{x} + \frac{1}{2}, y + \frac{1}{2}, z)$ |
| $m_z\mathbf{r} = (x, y, \overline{z} + \frac{1}{2})$ | $m_y\mathbf{r} = (x + \frac{1}{2}, \overline{y} + \frac{1}{2}, z + \frac{1}{2})$ |

TABLE VIII: General Positions for Pbnm. Notation as in Table I.

| | | |
|---|---|---|
| Mn | $(1) = (0, \frac{1}{2}, 0)$ | $(2) = (\frac{1}{2}, 0, 0)$ |
| | $(3) = (0, \frac{1}{2}, \frac{1}{2})$ | $(4) = (\frac{1}{2}, 0, \frac{1}{2})$ |
| Tb | $(5) = (x, y, \frac{1}{4})$ | $(6) = (x + \frac{1}{2}, \overline{y} + \frac{1}{2}, \frac{3}{4})$ |
| | $(7) = (\overline{x}, \overline{y}, \frac{3}{4})$ | $(8) = (\overline{x} + \frac{1}{2}, y + \frac{1}{2}, \frac{1}{4})$ |

TABLE IX: Positions of the Magnetic Ions in the Pbnm Structure of TbMnO$_3$, with $x = 0.9836$ and $y = 0.0810$.[41]

To start we study the operations that leave invariant the wavevector of the incommensurate phase which first orders as the temperature is lowered. Experimentally[42] this wavevector is found to be $(0, q, 0)$, with[34] $q \approx 0.28(2\pi/b)$. These relevant operators (see Table VIII) $m_x$ and $m_z$. We follow the approach used for MWO, but use "actual location" Fourier transforms. We set $\mathbf{R}_f + \boldsymbol{\tau}_f \equiv \mathbf{r}$ in order to use Eq. (16) and we need to evaluate

$$\begin{aligned} \Lambda &\equiv \exp\Big(2\pi i(\mathbf{q}/b)\cdot[\mathbf{r} - [m_x]^{-1}\mathbf{r}\Big) \\ &= \exp\Big(2\pi(q/b)\hat{j}\cdot[y\hat{j} - [m_x]^{-1}y\hat{j}]\Big) = e^{i\pi\hat{q}} \end{aligned} \tag{71}$$

and

$$\begin{aligned} \Lambda' &\equiv \exp\Big(2\pi i(\mathbf{q}/b)\cdot[\mathbf{r} - [m_z]^{-1}\mathbf{r}\Big) \\ &= \exp\Big(2\pi i(q/b)\hat{j}\cdot[y\hat{j} - [m_x]^{-1}y\hat{j}]\Big) = 1 \ . \end{aligned} \tag{72}$$

We list, in Table X the transformation table of sublattice indices of TMO.

Therefore the eigenvalue conditions for transformation by $m_x$ are

$$S'_\alpha(\mathbf{q}, \tau_f) = \xi_\alpha(m_x)S_\alpha(\mathbf{q}, \tau_i)\Lambda = \lambda(m_x)S_\alpha(\mathbf{q}, \tau_f) \tag{73}$$

and

$$S'_\alpha(\mathbf{q}, \tau_f) = \xi_\alpha(m_z)S_\alpha(\mathbf{q}, \tau_i) = \lambda(m_z)S_\alpha(\mathbf{q}, \tau_f) \ , \tag{74}$$

where $\xi_x(m_x) = -\xi_y(m_x) = -\xi_z(m_x) = 1$ and $\xi_\alpha(m_z)$ was defined in Eq. (15). From these equations we see that $\lambda(m_x)$ assumes the values $\pm\Lambda$ and $\lambda(m_z)$ the values $\pm 1$. Then solving the above equations leads to the results

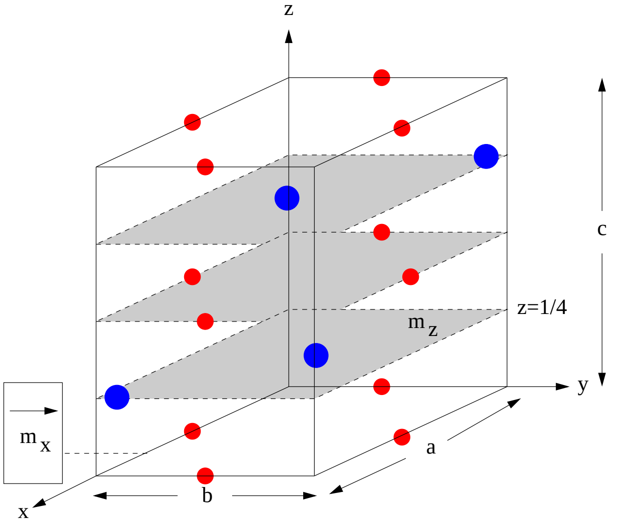

FIG. 3: (Color online). Mn sites (smaller circles, on-line red) and Tb sites (larger circles, on-line blue) in the primitive unit cell of TbMnO$_3$. The Tb sites are in the shaded planes at $z = n \pm \frac{1}{4}$ and the Mn sites are in planes $z = n$ or $z = n + \frac{1}{2}$, where $n$ is an integer. The incommensurate wavevector is along the **b** axis. The mirror plane at $z = 1/4$ is indicated and the glide plane $m_x$ is indicated by the mirror plane at $x = 3/4$ followed by a translation (indicated by the arrow) of $b/2$ along the $y$-axis.

| $\tau_i$ | $\tau_f(m_x)$ | $\tau_f(m_z)$ | $\tau_f(\mathcal{I})$ |
|---|---|---|---|
| 1 | 2 | 3 | 1 |
| 2 | 1 | 4 | 2 |
| 3 | 4 | 1 | 3 |
| 4 | 3 | 2 | 4 |
| 5 | 8 | 5 | 7 |
| 6 | 7 | 6 | 8 |
| 7 | 6 | 7 | 5 |
| 8 | 5 | 8 | 6 |

TABLE X: Transformation table for sublattice indices of TMO under various operations.

given in Table XI. (These results look different than those in Ref. 3 because here the Fourier transforms are defined relative to the actual positions, whereas there they are defined relative to the origin of the unit cell.)

Now, since the crystal is centrosymmetric, we take symmetry with respect to spatial inversion, $\mathcal{I}$, into account. As before, recall that $\mathcal{I}$ transports the spin to its spatially inverted position without changing the orientation of the spin (a pseudovector). The change of position is equivalent to changing the sign of the wavevector in the Fourier transform and this is accomplished by complex conjugation. Since the Mn ions sit at centers of inversion symmetry, one has, for the Mn sublattices,

$$\mathcal{I}\mathbf{S}(\mathbf{q}, n) \;=\; \mathbf{S}(\mathbf{q}, n)^* \ , \tag{75}$$

| Irrep | $\Gamma_1$ | $\Gamma_2$ | $\Gamma_3$ | $\Gamma_4$ |
|---|---|---|---|---|
| $\lambda(m_x) =$ | $+\Lambda$ | $-\Lambda$ | $-\Lambda$ | $+\Lambda$ |
| $\lambda(m_z) =$ | $+1$ | $-1$ | $+1$ | $-1$ |
| $\mathbf{S}(\mathbf{q}, M1)$ | $n_M^a$<br>$-n_M^b$<br>$-n_M^c$ | $-n_M^a$<br>$n_M^b$<br>$n_M^c$ | $-n_M^a$<br>$n_M^b$<br>$n_M^c$ | $n_M^a$<br>$-n_M^b$<br>$-n_M^c$ |
| $\mathbf{S}(\mathbf{q}, M2)$ | $n_M^a$<br>$n_M^b$<br>$n_M^c$ | $n_M^a$<br>$n_M^b$<br>$n_M^c$ | $n_M^a$<br>$n_M^b$<br>$n_M^c$ | $n_M^a$<br>$n_M^b$<br>$n_M^c$ |
| $\mathbf{S}(\mathbf{q}, M3)$ | $-n_M^a$<br>$n_M^b$<br>$-n_s^c$ | $-n_M^a$<br>$n_M^b$<br>$-n_M^c$ | $n_M^a$<br>$-n_M^b$<br>$n_M^c$ | $n_M^a$<br>$-n_M^b$<br>$n_M^c$ |
| $\mathbf{S}(\mathbf{q}, M4)$ | $-n_M^a$<br>$-n_M^b$<br>$n_M^c$ | $n_M^a$<br>$n_M^b$<br>$-n_M^c$ | $-n_M^a$<br>$-n_M^b$<br>$n_M^c$ | $n_M^a$<br>$n_M^b$<br>$-n_M^c$ |
| $\mathbf{S}(\mathbf{q}, T1)$ | $0$<br>$0$<br>$n_{T1}^c$ | $n_{T1}^a$<br>$n_{T1}^b$<br>$0$ | $0$<br>$0$<br>$n_{T1}^c$ | $n_{T1}^a$<br>$n_{T1}^b$<br>$0$ |
| $\mathbf{S}(\mathbf{q}, T2)$ | $0$<br>$0$<br>$-n_{T2}^c$ | $-n_{T2}^a$<br>$n_{T2}^b$<br>$0$ | $0$<br>$0$<br>$n_{T2}^c$ | $n_{T2}^a$<br>$-n_{T2}^b$<br>$0$ |
| $\mathbf{S}(\mathbf{q}, T3)$ | $0$<br>$0$<br>$n_{T2}^c$ | $n_{T2}^a$<br>$n_{T2}^b$<br>$0$ | $0$<br>$0$<br>$n_{T2}^c$ | $n_{T2}^a$<br>$n_{T2}^b$<br>$0$ |
| $\mathbf{S}(\mathbf{q}, T4)$ | $0$<br>$0$<br>$-n_{T1}^C$ | $-n_{T1}^a$<br>$n_{T1}^b$<br>$0$ | $0$<br>$0$<br>$n_{T1}^c$ | $n_{T1}^a$<br>$-n_{T1}^b$<br>$0$ |

TABLE XI: Spin functions (i. e. actual position Fourier coefficients) within the unit cell of TMO for wavevector $(0, q, 0)$ which are eigenvectors of $m_x$ and $m_z$ with the eigenvalues listed, with $\Lambda = \exp(-i\pi\hat{q})$. All the parameters are complex-valued. The irreducible representation (irrep) is labeled as in Ref. 3. Inversion symmetry is not yet taken into account. Note that the two Tb orbits have independent complex amplitudes.

where the second argument specifies the sublattice, as in Table IX. In order to discuss the symmetry of the coordinates we define $x_1 = n_M^a$, $x_2 = n_M^b$, $x_3 = n_M^c$ and for irreps $\Gamma_1$ and $\Gamma_3$, $x_4 = n_{T1}^c$ and $x_5 = n_{T2}^c$, whereas for irreps $\Gamma_2$ and $\Gamma_4$, $x_4 = n_{T1}^a$, $x_5 = n_{T2}^a$, $x_6 = n_{T1}^b$, and $x_7 = n_{T2}^b$. Thus Eq. (75) gives

$$\mathcal{I}x_n \;=\; x_n^* \ , \qquad\qquad n = 1,\ 2,\ 3\ . \tag{76}$$

For the Tb ions $\mathcal{I}$ interchanges sublattices #5 and #7 and interchanges sublattices #6 and #8. So we have

$$\begin{aligned} \mathcal{I}\mathbf{S}(\mathbf{q}, 5) &= \mathbf{S}(\mathbf{q}, 7)^* \\ \mathcal{I}\mathbf{S}(\mathbf{q}, 6) &= \mathbf{S}(\mathbf{q}, 8)^* \ . \end{aligned} \tag{77}$$

Therefore we have

$$\mathcal{I}x_4 = x_5^* \ , \qquad\qquad \mathcal{I}x_6 = x_7^* \ . \tag{78}$$

Now we use the invariance of the free energy under $\mathcal{I}$ to write

$$F_2 \;=\; \sum_{X,\alpha;Y,\beta} S_\alpha(\mathbf{q}, X)^* F_{nm} S_\beta(\mathbf{q}, Y)$$

$$
\begin{aligned}
&= \sum_{m,n} x_n^* G_{nm} x_m \\
&= \sum_{m,n} [\mathcal{I} x_n^*] G_{nm} [\mathcal{I} x_m] \ , \qquad (79)
\end{aligned}
$$

where the matrix **G** is Hermitian.

For irreps $\Gamma_1$ and $\Gamma_3$ the matrix **G** in Eq. (79) couples five variables. Equation (76) implies that the upper left $3 \times 3$ submatrix of **G** is real. Equations (76) and (78) imply that $G_{n,4} = G_{5,n}$ and for $n = 1, 2, 3$. We find that **G** assumes the form

$$
\mathbf{G} \ = \ \left[ \begin{array}{ccccc} a & b & c & \alpha & \alpha^* \\ b & d & e & \beta & \beta^* \\ c & e & f & \gamma & \gamma^* \\ \alpha^* & \beta^* & \gamma^* & g & \delta \\ \alpha & \beta & \gamma & \delta^* & g \end{array} \right] \ , \qquad (80)
$$

where the Roman letters are real valued and the Greek are complex valued. As shown in the appendix, the form of this matrix ensures that the critical eigenvector can be taken to be of the form

$$
\psi \ = \ (n_M^a, n_M^b, n_M^c, n_{T1}^c, n_{T1}^c{}^*) \equiv (r, s, t; \rho, \rho^*) \ , (81)
$$

where the Roman letters are real and the Greek ones complex. Of course, because the vector can be complex, we should include an overall phase factor (which amounts to arbitrarily placing the origin of the incommensurate structure), so that more generally

$$
\psi \ = \ e^{i\phi}(r, s, t; \rho, \rho^*) \ . \qquad (82)
$$

For irreps $\Gamma_2$ and $\Gamma_4$ the matrix **G** in Eq. (79) couples the seven variables listed just below Eq. (75). Equations (76) and (78) imply that $G_{n,4} = G_{5,n}$ and $G_{n,6} = G_{7,n}$ for $n = 1, 2, 3$. Therefore **G** assumes the form

$$
\mathbf{G} \ = \ \left[ \begin{array}{ccccccc} a & b & c & \alpha & \alpha^* & \xi & \xi^* \\ b & d & e & \beta & \beta^* & \eta & \eta^* \\ c & e & f & \gamma & \gamma^* & \kappa & \kappa^* \\ \alpha^* & \beta^* & \gamma^* & g & \delta & \mu & \nu \\ \alpha & \beta & \gamma & \delta^* & g & \nu^* & \mu^* \\ \xi^* & \eta^* & \kappa^* & \mu^* & \nu & h & \rho \\ \xi & \eta & \kappa & \nu^* & \mu & \rho^* & h \end{array} \right] \ , \qquad (83)
$$

where Roman letters are real and Greek are complex. As shown in the appendix, this form ensures that the eigenvectors are of the form

$$
\begin{aligned}
\psi \ &= \ (n_M^a, n_M^b, n_M^c, n_{T1}^a, n_{T2}^a, m_{T1}^b, n_{T2}^b) \\
&= \ e^{i\phi}(r, s, t; \tau, \tau^*, \sigma, \sigma^*) \ . \qquad (84)
\end{aligned}
$$

These results are summarized in Table XII. Note that the use of inversion symmetry fixes most of the phases and relates the amplitudes of the two Tb orbits, thereby eliminating almost half the fitting parameters.[3]

| Irrep | $\Gamma_1$ | $\Gamma_2$ | $\Gamma_3$ | $\Gamma_4$ |
|---|---|---|---|---|
| $\lambda(m_x) =$ | $+\Lambda$ | $-\Lambda$ | $-\Lambda$ | $+\Lambda$ |
| $\lambda(m_z) =$ | $+1$ | $-1$ | $+1$ | $-1$ |
| $\mathbf{S}(\mathbf{q}, M1)$ | $r$<br>$-s$<br>$-t$ | $-r$<br>$s$<br>$t$ | $-r$<br>$s$<br>$t$ | $r$<br>$-s$<br>$-t$ |
| $\mathbf{S}(\mathbf{q}, M2)$ | $r$<br>$s$<br>$t$ | $r$<br>$s$<br>$t$ | $r$<br>$s$<br>$t$ | $r$<br>$s$<br>$t$ |
| $\mathbf{S}(\mathbf{q}, M3)$ | $-r$<br>$s$<br>$-t$ | $-r$<br>$s$<br>$-t$ | $r$<br>$-s$<br>$t$ | $r$<br>$-s$<br>$t$ |
| $\mathbf{S}(\mathbf{q}, M4)$ | $-r$<br>$-s$<br>$t$ | $r$<br>$s$<br>$-t$ | $-r$<br>$-s$<br>$t$ | $r$<br>$s$<br>$-t$ |
| $\mathbf{S}(\mathbf{q}, T1)$ | $0$<br>$0$<br>$\rho$ | $\tau$<br>$\sigma$<br>$0$ | $0$<br>$0$<br>$\rho$ | $\tau$<br>$\sigma$<br>$0$ |
| $\mathbf{S}(\mathbf{q}, T2)$ | $0$<br>$0$<br>$-\rho^*$ | $-\tau^*$<br>$\sigma^*$<br>$0$ | $0$<br>$0$<br>$\rho^*$ | $\tau^*$<br>$-\sigma^*$<br>$0$ |
| $\mathbf{S}(\mathbf{q}, T3)$ | $0$<br>$0$<br>$\rho^*$ | $\tau^*$<br>$\sigma^*$<br>$0$ | $0$<br>$0$<br>$\rho^*$ | $\tau^*$<br>$\sigma^*$<br>$0$ |
| $\mathbf{S}(\mathbf{q}, T4)$ | $0$<br>$0$<br>$-\rho$ | $-\tau$<br>$\sigma$<br>$0$ | $0$<br>$0$<br>$\rho$ | $\tau$<br>$-\sigma$<br>$0$ |

TABLE XII: As Table XI. Apart from an overall phase $\phi_\Gamma$ for each irrep, inversion symmetry restricts all the manganese Fourier coefficients to be real and all the Tb coefficients to have the indicated phase relations.

### 1. *Order Parameters*

We now introduce order parameters $\boldsymbol{\sigma}_n(\mathbf{q}) \equiv \sigma_n e^{i\phi_n}$ for irrep $\Gamma_n$ in terms of which we can write the spin distribution. For instance under $\Gamma_3$ one has

$$
\begin{aligned}
S_x(\mathbf{r}, M1) \ &= \ -2r\sigma_3 \cos(qy + \phi_3) \\
S_y(\mathbf{r}, M1) \ &= \ 2s\sigma_3 \cos(qy + \phi_3) \\
S_z(\mathbf{r}, M1) \ &= \ 2t\sigma_3 \cos(qy + \phi_3) \\
S_x(\mathbf{r}, M2) \ &= \ 2r\sigma_3 \cos(qy + \phi_3) \\
S_y(\mathbf{r}, M2) \ &= \ 2s\sigma_3 \cos(qy + \phi_3) \\
S_z(\mathbf{r}, M2) \ &= \ 2t\sigma_3 \cos(qy + \phi_3) \\
S_x(\mathbf{r}, T1) \ &= \ S_y(\mathbf{r}, T1) = 0 \\
S_z(\mathbf{r}, T1) \ &= \ 2\rho\sigma_3 \cos(qy + \phi_3 + \phi_\rho) \\
S_x(\mathbf{r}, T2) \ &= \ S_y(\mathbf{r}, T2) = 0 \\
S_z(\mathbf{r}, T2) \ &= \ 2\rho\sigma_3 \cos(qy + \phi_3 - \phi_\rho) \ , \qquad (85)
\end{aligned}
$$

where we set $\boldsymbol{\rho} = \rho e^{i\phi_\rho}$ and the parameters are normalized by

$$
r^2 + s^2 + t^2 + |\rho|^2 \ = \ 1 \ . \qquad (86)
$$

In Eq. (85) $\mathbf{r} \equiv (x, y, z)$ is the actual position of the spin in question. From Table XI one can obtain the symmetry

| | |
|---|---|
| $E\mathbf{r} = (x, y, z)$ | $2_x\mathbf{r} = (x+\frac{1}{2}, \overline{y}+\frac{1}{2}, \overline{z})$ |
| $2_z = (\overline{x}, \overline{y}, z)$ | $2_y = (\overline{x}+\frac{1}{2}, y+\frac{1}{2}, \overline{z})$ |
| $\mathcal{I}\mathbf{r} = (\overline{x}, \overline{y}, \overline{z})$ | $m_x\mathbf{r} = (\overline{x}+\frac{1}{2}, y+\frac{1}{2}, z)$ |
| $m_z\mathbf{r} = (x, y, \overline{z})$ | $m_y\mathbf{r} = (x+\frac{1}{2}, \overline{y}+\frac{1}{2}, z)$ |

TABLE XIII: As Table XIII. General Positions for Pbam.

properties of the order parameters for each irrep. For instance

$$\begin{aligned} m_x\boldsymbol{\sigma}_1(\mathbf{q}) &= +\Lambda\boldsymbol{\sigma}_1(\mathbf{q}) \;, \qquad m_z\boldsymbol{\sigma}_1(\mathbf{q}) = +\boldsymbol{\sigma}_1(\mathbf{q}) \\ m_x\boldsymbol{\sigma}_2(\mathbf{q}) &= -\Lambda\boldsymbol{\sigma}_2(\mathbf{q}) \;, \qquad m_z\boldsymbol{\sigma}_2(\mathbf{q}) = -\boldsymbol{\sigma}_2(\mathbf{q}) \\ m_x\boldsymbol{\sigma}_3(\mathbf{q}) &= -\Lambda\boldsymbol{\sigma}_3(\mathbf{q}) \;, \qquad m_z\boldsymbol{\sigma}_3(\mathbf{q}) = \boldsymbol{\sigma}_3(\mathbf{q}) \\ m_x\boldsymbol{\sigma}_4(\mathbf{q}) &= +\Lambda\boldsymbol{\sigma}_4(\mathbf{q}) \;, \qquad m_z\boldsymbol{\sigma}_4(\mathbf{q}) = -\boldsymbol{\sigma}_4(\mathbf{q}) \end{aligned} \quad (87)$$

and

$$\mathcal{I}\boldsymbol{\sigma}_n(\mathbf{q}) \;=\; \boldsymbol{\sigma}_n^*(\mathbf{q}) \;. \qquad (88)$$

Note that in contrast to the case of NVO, inversion symmetry does not fix all the phases. However, it again drastically reduces the number of possible magnetic structure parameters which have to be determined. In particular, it is only by using inversion that one finds that the magnitudes of the Fourier coefficients of the two distinct Tb sites have to be the same. Note that if we choose the origin so that $\phi = 0$ (which amounts to renaming the origin so that that becomes true), then we recover inversion symmetry (taking account that inversion interchanges terbium sublattice #3 and #1). One can determine that the spin structure is inversion invariant when one condenses a single representation.

The result of Table 5 applies other manganates provided their wavevector is also of the form $(0, q_y, 0)$. This includes $\mathrm{YMnO_3}$[44] and $\mathrm{HoMnO_3}$.[45,46] Both these systems order into an incommensurate structure at about $T_c \approx 42$K. The Y compound has a second lower-temperature incommensurate phase, whereas the Ho compound has a lower-temperature commensurate phase.

## C. $\mathbf{TbMn_2O_5}$

The space group of $\mathrm{TbMn_2O_5}$ (TMO25) is Pbam (#55 in Ref. 28) and its general positions are listed in Table XIII. The positions of the magnetic ions are given in Table XIV and are shown in Fig. 4.

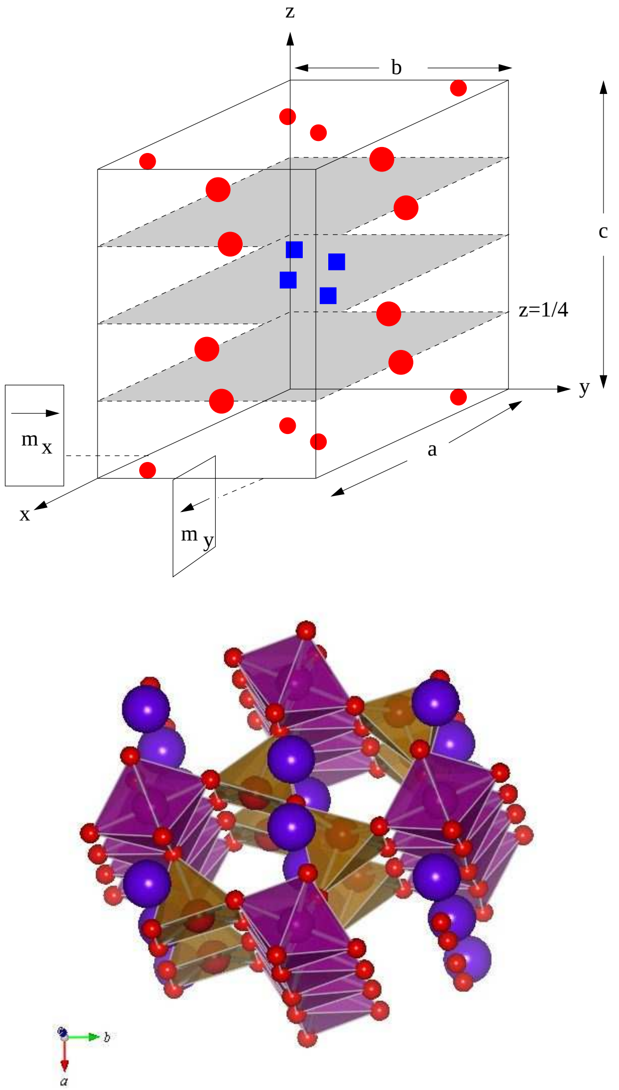

FIG. 4: (Color online). Two representations of $\mathrm{TbMn_2O_5}$. Top: Mn sites (on-line red) with smaller circles $\mathrm{Mn}^{3+}$ and larger circles $^{4+}$ and Tb sites (squares, on-line blue) in the primitive unit cell of $\mathrm{TbMn_2O_5}$. The $\mathrm{Mn}^{+4}$ sites are in the shaded planes at $z = n \pm \delta$ with $\delta \approx 0.25$ and the $\mathrm{Mn}^{+3}$ sites are in planes $z = n$, where $n$ is an integer. The Tb ions are in the planes $z = n + \frac{1}{2}$. The glide plane $m_x$ is indicated by the mirror plane at $x = 3/4$ followed by a translation (indicated by the arrow) of $b/2$ along the $y$-axis and similarly for the glide plane $m_y$. Bottom: Perspective view. Here the $\mathrm{Mn}^{3+}$ are inside oxygen pyramids of small balls and the $\mathrm{Mn}^{4+}$ are inside oxygen octahedra.

We will address the situation just below the ordering temperature of 43K.[10] We take the ordering wavevector to be[10] to be $(\frac{1}{2}, 0, q)$ with[34] $q \approx 0.306$. (This may be an approximate value.[49]) Initially we assume that the possible spin configurations consistent with a continuous transition at such a wavevector are eigenvectors of the operators $m_x$ and $m_y$ which leave the wavevector invariant. We proceed as for TMO. We use the unit cell Fourier transforms and write the eigenvector conditions for transformation by $m_x$ as

$$\begin{aligned} S_\alpha(\mathbf{q}, \tau_f)' &= \xi_\alpha(m_x) S_\alpha(\mathbf{q}, \tau_i) e^{i\mathbf{q}(\mathbf{r}_f - \mathbf{R}_i)} \\ &= \lambda_x S_\alpha(\mathbf{q}, \tau_f) \;, \end{aligned} \qquad (89)$$

where $\tau_i$ and $\mathbf{R}_i$ are respectively the sublattice indices and unit cell locations before transformation and $\tau_f$ and

| | | |
|---|---|---|
| $\mathrm{Mn}^{3+}$ | $(1) = (x, y, 0)$<br>$(3)(\overline{x} + \frac{1}{2}, y + \frac{1}{2}, 0)$ | $(2) = (\overline{x}, \overline{y}, 0)$<br>$(4) = (x + \frac{1}{2}, \overline{y} + \frac{1}{2}, 0)$ |
| $\mathrm{Mn}^{4+}$ | $(5) = (\frac{1}{2}, 0, z)$<br>$(7) = (\frac{1}{2}, 0, \overline{z})$ | $(6) = (0, \frac{1}{2}, z)$<br>$(8) = (0, \frac{1}{2}, \overline{z})$ |
| RE | $(9) = (X, Y, \frac{1}{2})$<br>$(11) = (\overline{X} + \frac{1}{2}, Y + \frac{1}{2}, \frac{1}{2})$ | $(10) = (\overline{X}, \overline{Y}, \frac{1}{2})$<br>$(12) = (X + \frac{1}{2}, \overline{Y} + \frac{1}{2}, \frac{1}{2})$ |

TABLE XIV: Positions of the magnetic ions of $\mathrm{TbMn_2O_5}$ in the Pbam structure. Here $x = 0.09$, $y = -0.15$, $z = 0.25$,[47] $X = 0.14$, and $Y = 0.17$.[48]. All these values are taken from the isostructural compound $\mathrm{HoMn_2O_5}$.

$\mathbf{R}_f$ are those after transformation. The eigenvalue equation for transformation by $m_y$ is

$$\begin{aligned} S_\alpha(\mathbf{q}, \tau_f)' &= \xi_\alpha(m_y) S_\alpha(\mathbf{q}, \tau_i) e^{i\mathbf{q}(\mathbf{r}_f - \mathbf{R}_i)} \\ &= \lambda_y S_\alpha(\mathbf{q}, \tau_f) \ . \end{aligned} \tag{90}$$

If one attempts to construct spin functions which are simultaneously eigenfunctions of $m_x$ and $m_y$ one finds that *these equations yield no solution.* While it is, of course, true that the operations $m_x$ and $m_y$ take an eigenfunction into an eigenfunction, it is only for irreps of dimension one that the initial and final eigenfunctions are the same, as we have assumed. The present case, when the wavevector is at the edge of the Brillouin zone is analogous to the phenomenon of "sticking" where, for nonsymmorphic space group (i. e. those having a screw axis or a glide plane) the energy bands (or phonon spectra) have an almost mysterious degeneracy at the zone boundary[50] and the only active irrep has dimension two. This means that the symmetry operations induce transformations within the subspace of pairs of eigenfunctions. We now determine such pairs of eigenfunctions by a straightforward approach which do not require any knowledge of group theory. Here we explicitly consider the symmetries of the matrix $\chi^{-1}$ for the quadratic terms in the free energy which here is a $36 \times 36$ dimensional matrix, which we write as

$$\boldsymbol{\chi}^{-1} = \begin{bmatrix} \mathbf{M}^{(xx)} & \mathbf{M}^{(xy)} & \mathbf{M}^{(xz)} \\ \mathbf{M}^{(xy)\dagger} & \mathbf{M}^{(yy)} & \mathbf{M}^{(yz)} \\ \mathbf{M}^{(zx)\dagger} & \mathbf{M}^{(yz)\dagger} & \mathbf{M}^{(zz)} \end{bmatrix} , \tag{91}$$

where $\mathbf{M}^{(ab)}$ is a 12 dimensional submatrix which describes coupling between $a$-component and $b$-component spins and is indexed by sublattice indices $\tau$ and $\tau'$ The symmetries we invoke are operations of the screw axes, $m_x$ and $m_y$ which conserve wavevector (to within a reciprocal lattice vector), and $\mathcal{I}$, whose effect is usually ignored. To guide the reader through the ensuing calculation we summarize the main steps. We first analyze separately the sectors involving the $x$, $y$, and $z$ spin components. We develop a unitary transformation which takes $\mathbf{M}^{(\alpha\alpha)}$ into a matrix all of whose elements are real. This fixes the phases within the 12 dimensional space of the $\alpha$ spin components within the unit cell (assuming these relations are not invalidated by the form of $\mathbf{M}^{(\alpha\beta)}$, with $\alpha \neq \beta$). The relative phases between different spin components is fixed by showing that the unitary transformation introduced above leads to $\mathbf{M}^{(xy)}$ having all real-valued matrix elements and $\mathbf{M}^{(xz)}$ and $\mathbf{M}^{(yz)}$ having all purely imaginary matrix elements. The conclusion, then, is that the phases in the sectors of $x$ and $y$ components are coupled in phase and the sector of $z$ components are out of phase with the $x$ and $y$ components.

| $n_i$ | $m_x$ | $m_y^{\mathrm{a}}$ | | $m_x m_y^{\mathrm{a}}$ | | $\mathcal{I}^{\mathrm{b}}$ | | $m_x m_y \mathcal{I}$ |
|---|---|---|---|---|---|---|---|---|
| | $n_f$ | $n_f$ | $e^{i\phi}$ | $n_f$ | $e^{i\phi}$ | $n_f$ | $e^{i\phi'}$ | $n_f$ |
| 1 | 3 | 4 | 1 | 2 | 1 | 2 | 1 | 1 |
| 2 | 4 | 3 | 1 | 1 | 1 | 1 | 1 | 2 |
| 3 | 1 | 2 | −1 | 4 | −1 | 4 | −1 | 3 |
| 4 | 2 | 1 | −1 | 3 | −1 | 3 | −1 | 4 |
| 5 | 6 | 6 | −1 | 5 | −1 | 7 | −1 | 7 |
| 6 | 5 | 5 | 1 | 6 | 1 | 8 | 1 | 8 |
| 7 | 8 | 8 | −1 | 7 | −1 | 5 | −1 | 8 |
| 8 | 7 | 7 | 1 | 8 | 1 | 6 | 1 | 7 |
| 9 | 11 | 12 | 1 | 10 | 1 | 10 | 1 | 9 |
| 10 | 12 | 11 | 1 | 9 | 1 | 9 | 1 | 10 |
| 11 | 9 | 10 | −1 | 12 | −1 | 12 | −1 | 11 |
| 12 | 10 | 9 | −1 | 11 | −1 | 11 | −1 | 12 |

TABLE XV: Transformation table for sublattice indices with associated factors for TMO25 under various operations. as defined by Eq. (19). For $m_x$, one has $\exp[i\mathbf{q} \cdot (\mathbf{R}_f - \mathbf{R}_i)] = 1$ for all cases and for $m_x m_y \mathcal{I}$ the analogous factor is $+1$ in all cases and this operator relates $S_\alpha(\mathbf{q}, \tau)$ and $S_\alpha(\mathbf{q}, \tau)^*$. NOTE: This table does not include the factor of $\xi_\alpha(\mathcal{O})$ which may be associated with an operation.

a) $\phi = \mathbf{q} \cdot (\mathbf{R}_f - \mathbf{R}_i)$, as required by Eq. (18).

b) $\phi' = \mathbf{q} \cdot (\boldsymbol{\tau}_i + \boldsymbol{\tau}_f)$, as required by Eq. (21).

### 1. *x Components*

As a preliminary, in Table XV we list the effect of the symmetry operations on the sublattice index. When these symmetries are used, one finds the $12 \times 12$ submatrix of $\mathbf{M}^{(xx)}$ which couples only the $x$-components of spins assumes the form

$$\left[\begin{array}{cccc|cc|cc|cccc} A & g & h & 0 & \alpha & \beta & \alpha^* & \beta^* & a & b & c & d \\ g & A & 0 & -h & -\alpha & \beta & -\alpha^* & \beta^* & b & a & -d & -c \\ h & 0 & A & g & \beta & \alpha & \beta^* & \alpha^* & c & d & a & b \\ 0 & -h & g & A & \beta & -\alpha & \beta^* & -\alpha^* & -d & -c & b & a \\ \hline \alpha^* & -\alpha^* & \beta^* & \beta^* & B & 0 & \epsilon & 0 & \gamma & -\gamma & \delta & \delta \\ \beta^* & \beta^* & \alpha^* & -\alpha^* & 0 & B & 0 & \epsilon & \delta & \delta & \gamma & -\gamma \\ \hline \alpha & -\alpha & \beta & \beta & \epsilon^* & 0 & B & 0 & \gamma^* & -\gamma^* & \delta^* & \delta^* \\ \beta & \beta & \alpha & -\alpha & 0 & \epsilon^* & 0 & B & \delta^* & \delta^* & \gamma^* & -\gamma^* \\ \hline a & b & c & -d & \gamma^* & \delta^* & \gamma & \delta & C & e & f & 0 \\ b & a & d & -c & -\gamma^* & \delta^* & -\gamma & \delta & e & C & 0 & -f \\ c & -d & a & b & \delta^* & \gamma^* & \delta & \gamma & f & 0 & C & e \\ d & -c & b & a & \delta^* & -\gamma^* & \delta & -\gamma & 0 & -f & e & C \end{array}\right] \tag{92}$$

where Roman letters are real quantities and Greek ones complex. (In this matrix the lines are used to separate different Wyckoff orbits.) The numbering of the rows and columns follows from Table XIV. I give a few examples of how symmetry is used to get this form. Consider the term $T_1$, where

$$T_1 \; = \; \chi_{1,5}^{-1} S_x(-\mathbf{q},1) S_x(\mathbf{q},5) \; . \tag{93}$$

Using Table XV we transform this by $m_x$ into

$$T_1' \; = \; \chi_{1,5}^{-1} S_x(-\mathbf{q},3) S_x(\mathbf{q},6) \; , \tag{94}$$

which says that the 1,5 matrix element is equal to the 3,6 matrix element. (Note that in writing down $T_1'$ we did not need to worry about $\xi_\alpha$, since this factor comes in squared as unity.) Likewise if we transform by $m_y$ we get

$$T_1' \; = \; \chi_{15}^{-1} [-S_x(-\mathbf{q},4)][S_x(\mathbf{q},6)] \; , \tag{95}$$

which says that the 1,5 matrix element is equal to the negative of the 4,6 matrix element. If we transform by $m_x m_y$ we get

$$T_1' \; = \; \chi_{1,5}^{-1} [S_x(-\mathbf{q},2)][-S_x(\mathbf{q},5)] \; , \tag{96}$$

which says that the 1,5 matrix element is equal to the negative of the 2,5 matrix element. To illustrate the effect of $\mathcal{I}$ on $T_1$ we write

$$T_1' \; = \; \chi_{1,5}^{-1} [S_x(\mathbf{q},2)][-S_x(-\mathbf{q},7)] \; , \tag{97}$$

so that the 1,5 element is the negative of the 7,2 element. From the form of the matrix in Eq. (92) (or equivalently referring to Table XX in Appendix B), we see that we bring this matrix into block diagonal form by introducing the wavefunctions for $S_x(\mathbf{q},\tau)$,

$$\begin{array}{||c||cccc|cc|cc|cccc||}
\hline
\tau = & 1 & 2 & 3 & 4 & 5 & 6 & 7 & 8 & 9 & 10 & 11 & 12 \\
\hline
\sqrt{2}O_{1,\tau}^{(x,1)} = & 1 & 0 & 1 & 0 & 0 & 0 & 0 & 0 & 0 & 0 & 0 & 0 \\
\sqrt{2}O_{2,\tau}^{(x,1)} = & 0 & 1 & 0 & 1 & 0 & 0 & 0 & 0 & 0 & 0 & 0 & 0 \\
2O_{3,\tau}^{(x,1)} = & 0 & 0 & 0 & 0 & 1 & 1 & 1 & 1 & 0 & 0 & 0 & 0 \\
2O_{4,\tau}^{(x,1)} = & 0 & 0 & 0 & 0 & i & i & -i & -i & 0 & 0 & 0 & 0 \\
\sqrt{2}O_{5,\tau}^{(x,1)} = & 0 & 0 & 0 & 0 & 0 & 0 & 0 & 0 & 1 & 0 & 1 & 0 \\
\sqrt{2}O_{6,\tau}^{(x,1)} = & 0 & 0 & 0 & 0 & 0 & 0 & 0 & 0 & 0 & 1 & 0 & 1 \\
\hline
\end{array} \; . \tag{98}$$

The superscripts $\alpha, n$ on $\mathbf{O}$ label, respectively, the Cartesian component and the column of the irrep according to which the wavefunction transforms. The subscripts $m, \tau$ label, respectively, the index number of the wavefunction and the sublattice label. In this subspace $\langle \mathbf{O}_n^{(x,1)} | M^{(xx)} | \mathbf{O}_m^{(x,1)} \rangle \equiv \langle n | M^{(xx)} | m \rangle$ is

$$\left[ \begin{array}{c|c|c|c|c|c}
\hline
A+h & g & \alpha'+\beta' & -\alpha''-\beta'' & a+c & b+d \\
g & A-h & \beta'-\alpha' & \alpha''-\beta'' & b-d & a-c \\
\alpha'+\beta' & \beta'-\alpha' & B+\epsilon' & \epsilon" & \delta'+\gamma' & \delta'-\gamma' \\
-\alpha''-\beta'' & \alpha''-\beta'' & \epsilon'' & B-\epsilon' & \delta''+\gamma'' & \delta''-\gamma'' \\
a+c & b-d & \delta'+\gamma' & \delta''+\gamma'' & C+f & e \\
b+d & a-c & \delta'-\gamma' & \delta''-\gamma'' & e & C-f \\
\hline
\end{array} \right] , \tag{99}$$

where the coefficients are separated into real and imaginary parts as $\sqrt{2}\alpha \; = \; \alpha' + i\alpha''$, $\sqrt{2}\beta \; = \; \beta' + i\beta''$ $\sqrt{2}\gamma \; = \; \gamma' + i\gamma''$, and $\sqrt{2}\delta \; = \; \delta' + i\delta''$. There are no nonzero matrix elements between wavefunctions which transform according to different columns of the irrep.

The partners of these functions can be found from

$$\mathbf{O}_n^{(x,2)} \; = \; m_y \mathbf{O}_n^{(x,1)} \; , \tag{100}$$

so that, using Table XV and including the factor $\xi_\alpha$, we get

$$\begin{array}{||c||cccc|cc|cc|cccc||}
\hline
\tau = & 1 & 2 & 3 & 4 & 5 & 6 & 7 & 8 & 9 & 10 & 11 & 12 \\
\hline
\sqrt{2}O_{1,\tau}^{(x,2)} = & 0 & 1 & 0 & -1 & 0 & 0 & 0 & 0 & 0 & 0 & 0 & 0 \\
\sqrt{2}O_{2,\tau}^{(x,2)} = & 1 & 0 & -1 & 0 & 0 & 0 & 0 & 0 & 0 & 0 & 0 & 0 \\
2O_{3,\tau}^{(x,2)} = & 0 & 0 & 0 & 0 & -1 & 1 & -1 & 1 & 0 & 0 & 0 & 0 \\
2O_{4,\tau}^{(x,2)} = & 0 & 0 & 0 & 0 & -i & i & i & -i & 0 & 0 & 0 & 0 \\
\sqrt{2}O_{5,\tau}^{(x,2)} = & 0 & 0 & 0 & 0 & 0 & 0 & 0 & 0 & 0 & 1 & 0 & -1 \\
\sqrt{2}O_{6,\tau}^{(x,2)} = & 0 & 0 & 0 & 0 & 0 & 0 & 0 & 0 & 1 & 0 & -1 & 0 \\
\hline
\end{array} . \tag{101}$$

Within this subspace the matrix $\langle n | M^{(xx)} | m \rangle$ is the same as in Eq. (99) because

$$\langle n | m_y^{-1} M^{(xx)} m_y | m \rangle \; = \; \langle n | M^{(xx)} | m \rangle \; . \tag{102}$$

These functions transform as expected for a two dimensional irrep, namely,

$$\begin{aligned}
m_x \begin{bmatrix} O_n^{(x,1)} \\ O_n^{(x,2)} \end{bmatrix} \; &= \; \begin{bmatrix} O_n^{(x,1)} \\ -O_n^{(x,2)} \end{bmatrix} \\
m_y \begin{bmatrix} O_n^{(x,1)} \\ O_n^{(x,2)} \end{bmatrix} \; &= \; \begin{bmatrix} O_n^{(x,2)} \\ -O_n^{(x,1)} \end{bmatrix} \; .
\end{aligned} \tag{103}$$

We will refer to the transformed coordinates of Eqs. (98) and (101) as "symmetry adapted coordinates." The fact that the model-specific matrix that couples them is real, means that the critical eigenvector is a linear combination of symmetry adapted coordinates with *real* coefficients.

### 2. *y Components*

The $12 \times 12$ matrix $M^{(yy)}$ coupling $y$ components of spin has exactly the same form as that given in Eq. (92), although the values of the constants are unrelated. This is because here one has $\xi_y^2 = 1$ in place of $\xi_x^2 = 1$. Therefore the associated wavefunctions can be expressed just as in Eqs. (98) and (101) except that all the superscripts are changed from $x$ to $y$ and $\tau$ now labels $S_y(\mathbf{q},\tau)$. However, the transformation of the $y$ components rather than the $x$ components, requires replacing $\xi_x$ by $\xi_y$ which induces sign changes, so that

$$\begin{aligned}
m_x \begin{bmatrix} O_n^{(y,1)} \\ O_n^{(y,2)} \end{bmatrix} \; &= \; \begin{bmatrix} -O_n^{(y,1)} \\ O_n^{(y,2)} \end{bmatrix} \\
m_y \begin{bmatrix} O_n^{(y,1)} \\ O_n^{(y,2)} \end{bmatrix} \; &= \; \begin{bmatrix} -O_n^{(y,2)} \\ O_n^{(y,1)} \end{bmatrix} \; .
\end{aligned} \tag{104}$$

We want to construct wavefunctions in this sector which transform just like the $x$ components, so that they can be appropriately combined with the wavefunctions for the $x$-components. In view of Eq. (103) we set

$$O^{(y,1)}_{n,\tau} \;=\; O^{(x,2)}_{n,\tau} \ , \quad O^{(y,2)}_{n,\tau} = O^{(x,1)}_{n,\tau} \ . \qquad (105)$$

So the coefficients for $\mathbf{O}^{(y,1)}_n$ are given by Eq. (101) and those for $\mathbf{O}^{(y,2)}_n$ by Eq. (98). These wavefunctions are constructed to transform exactly as those for the $x$ components.

### 3. *z Components*

Similarly, we consider the effect of the transformations of the $z$ components. In this case we take account of the factor $\xi_z$ to get

$$\begin{aligned} m_x \begin{bmatrix} O^{(z,1)}_n \\ O^{(z,2)}_n \end{bmatrix} &= \begin{bmatrix} -O^{(z,1)}_n \\ O^{(z,2)}_n \end{bmatrix} \\ m_y \begin{bmatrix} O^{(z,1)}_n \\ O^{(z,2)}_n \end{bmatrix} &= \begin{bmatrix} O^{(z,2)}_n \\ -O^{(z,1)}_n \end{bmatrix} \ . \qquad (106) \end{aligned}$$

We now construct wavefunctions in this sector which transform just like the $x$ components. In view of Eq. (103) we set

$$O^{(z,1)}_{n,\tau} \;=\; O^{(x,2)}_{n,\tau} \ , \quad O^{(z,2)}_{n,\tau} = -O^{(x,1)}_{n,\tau} \ , \qquad (107)$$

So the coefficients for $\mathbf{O}^{(z,1)}_n$ are given by Eq. (101) and those for $\mathbf{O}^{(z,2)}_n$ are the negatives of those of Eq. (98). These wavefunctions are constructed to transform exactly as those for the $x$ components.

### 4. *The Total Wavefunction and Order Parameters*

Now we analyze the form of $\mathbf{M}^{(ab)}$ of Eq. (91) for $a \neq b$, using inversion symmetry. To do this it is convenient to invoke invariance under the symmetry operation $m_x m_y \mathcal{I}$ whose effect is given in Table XV. We write

$$\begin{aligned} m_x m_y \mathcal{I} S_a(\mathbf{q}, \tau) \;&=\; \xi_a(m_x)\xi_a(m_y) \\ &\quad \times S_a(\mathbf{q}, \mathcal{R}\tau)^* \ , \qquad (108) \end{aligned}$$

where $\mathcal{R}\tau = \tau$ for $\tau \neq 5, 6, 7, 8$, otherwise $\mathcal{R}\tau = \tau \pm 2$ within the remaining sector of $\tau$'s and $a$ (and later $b$) denotes one of $x$, $y$, and $z$. Thus

$$\begin{aligned} T \;&\equiv\; S_a(\mathbf{q}, \tau)^* M^{(ab)}_{\tau\tau'} S_b(\mathbf{q}, \tau') \\ &=\; [m_x m_y \mathcal{I} S_a(\mathbf{q}, \tau)]^* M^{(ab)}_{\tau\tau'} [m_x m_y \mathcal{I} S_b(\mathbf{q}, \tau')] \\ &=\; C_{ab} S_a(\mathbf{q}, \mathcal{R}\tau) M^{(ab)}_{\tau\tau'} S_b(\mathbf{q}, \mathcal{R}\tau')^* \ , \qquad (109) \end{aligned}$$

where

$$C_{ab} \;=\; \xi_a(m_x)\xi_a(m_y)\xi_b(m_x)\xi_b(m_y) \ . \qquad (110)$$

From this we deduce that

$$M^{(ba)}_{\mathcal{R}\tau', \mathcal{R}\tau} \;=\; C_{ab} M^{(ab)}_{\tau\tau'} \ , \qquad (111)$$

or, since $\mathbf{M}$ is Hermitian that

$$M^{(ab)}_{\tau\tau'} \;=\; C_{ab} \left[ M^{(ab)}_{\mathcal{R}^{-1}\tau, \mathcal{R}^{-1}\tau'} \right]^* \ . \qquad (112)$$

Now we consider the matrices $\mathbf{M}^{(ab)}$, in the symmetry adapted representation where

$$\begin{aligned} M^{(ab)}_{n,m} \;&=\; \sum_{\tau\tau'} [O^{ap}_{n\tau}]^* M^{(ab)}_{\tau\tau'} O^{bp}_{m\tau'} \\ &=\; \sum_{\tau\tau'} C_{ab} [O^{ap}_{n\tau}]^* \left[ M^{(ab)}_{\mathcal{R}^{-1}\tau, \mathcal{R}^{-1}\tau'} \right]^* O^{bp}_{m\tau'} \\ &=\; C_{ab} \sum_{\tau\tau'} [O^{ap}_{n\mathcal{R}\tau}]^* \left[ M^{(ab)}_{\tau,\tau'} \right]^* O^{bp}_{m\mathcal{R}\tau'} \ . \qquad (113) \end{aligned}$$

There are no matrix elements connecting $p$ and $p' \neq p$ and the result is independent of $p$. One can verify from Eqs. (98) and (101) that

$$O^{ap}_{n,\mathcal{R}\tau} \;=\; \left[ O^{ap}_{n,\tau} \right]^* \ , \qquad (114)$$

so that

$$\begin{aligned} M^{(ab)}_{n,m} \;&=\; C_{ab} \Big( [O^{\alpha p}_{n\tau}]^* \, M^{(ab)}_{\tau,\tau'} O^{bp}_{m\tau'} \Big)^* \\ &=\; C_{ab} \left[ M^{\alpha\beta}_{nm} \right]^* \ . \qquad (115) \end{aligned}$$

We have that $C_{xy} = -C_{xz} = -C_{yz} = 1$, so that all the elements of $\mathbf{M}^{(xy)}$ are real and all the elements of $\mathbf{M}^{(xz)}$ and $\mathbf{M}^{(yz)}$ are imaginary. Thus apart from an over all phase for the eigenfunction of each column, the phases of all the Fourier coefficients are fixed. What this means is that the critical eigenvector can be written as

$$\begin{aligned} \psi \;&=\; \sum_{p=1}^{2} \boldsymbol{\sigma}_p \sum_{n=1}^{6} \bigg( r_{nx} \mathbf{O}^{(x,p)}_n + r_{ny} \mathbf{O}^{(y,p)}_n \\ &\qquad + i r_{nz} \mathbf{O}^{(z,p)}_n \bigg) \ , \qquad (116) \end{aligned}$$

where the $r$'s are all real-valued and are normalized by

$$\sum_{n=1}^{6} \sum_{\alpha} [r_{n\alpha}]^2 \;=\; 1 \ , \qquad (117)$$

and $\boldsymbol{\sigma}_p$ are arbitrary complex numbers. Thus we have the result of Table XVI.

The order parameters are

$$\boldsymbol{\sigma}_1 \;\equiv\; \sigma_1 e^{i\phi_1} \ , \quad \boldsymbol{\sigma}_2 \equiv \sigma_2 e^{i\phi_2} \ . \qquad (118)$$

Neither the relative magnitudes of $\boldsymbol{\sigma}_1$ and $\boldsymbol{\sigma}_2$ nor their phases are fixed by the quadratic terms within the Landau expansion. Note that the structure parameters of Table XVI are determined by the microscopic interactions

| Spin | $\boldsymbol{\sigma}_1$ | $\boldsymbol{\sigma}_2$ | Spin | $\boldsymbol{\sigma}_1$ | $\boldsymbol{\sigma}_2$ |
|---|---|---|---|---|---|
| $\mathbf{S}(\mathbf{q},1)$ | $r_{1x}$<br>$r_{1y}$<br>$ir_{1z}$ | $r_{2x}$<br>$r_{2y}$<br>$ir_{2z}$ | $\mathbf{S}(\mathbf{q},7)$ | $z_x^*$<br>$-z_y^*$<br>$iz_z^*$ | $-z_x^*$<br>$z_y^*$<br>$iz_z^*$ |
| $\mathbf{S}(\mathbf{q},2)$ | $r_{2x}$<br>$r_{2y}$<br>$-ir_{2z}$ | $r_{1x}$<br>$r_{1y}$<br>$-ir_{1z}$ | $\mathbf{S}(\mathbf{q},8)$ | $z_x^*$<br>$z_y^*$<br>$-iz_z^*$ | $z_x^*$<br>$z_y^*$<br>$iz_z^*$ |
| $\mathbf{S}(\mathbf{q},3)$ | $r_{1x}$<br>$-r_{1y}$<br>$-ir_{1z}$ | $-r_{2x}$<br>$r_{2y}$<br>$ir_{2z}$ | $\mathbf{S}(\mathbf{q},9)$ | $r_{5x}$<br>$r_{5y}$<br>$ir_{5z}$ | $r_{6x}$<br>$r_{6y}$<br>$ir_{6z}$ |
| $\mathbf{S}(\mathbf{q},4)$ | $r_{2x}$<br>$-r_{2y}$<br>$ir_{2z}$ | $-r_{1x}$<br>$r_{1y}$<br>$-ir_{1z}$ | $\mathbf{S}(\mathbf{q},10)$ | $r_{6x}$<br>$r_{6y}$<br>$-ir_{6z}$ | $r_{5x}$<br>$r_{5y}$<br>$-ir_{5z}$ |
| $\mathbf{S}(\mathbf{q},5)$ | $z_x$<br>$-z_y$<br>$iz_z$ | $-z_x$<br>$z_y$<br>$iz_z$ | $\mathbf{S}(\mathbf{q},11)$ | $r_{5x}$<br>$-r_{5y}$<br>$-ir_{5z}$ | $-r_{6x}$<br>$r_{6y}$<br>$ir_{6z}$ |
| $\mathbf{S}(\mathbf{q},6)$ | $z_x$<br>$z_y$<br>$-iz_z$ | $z_x$<br>$z_y$<br>$iz_z$ | $\mathbf{S}(\mathbf{q},12)$ | $r_{6x}$<br>$-r_{6y}$<br>$ir_{6z}$ | $-r_{5x}$<br>$r_{5y}$<br>$-ir_{5z}$ |

TABLE XVI: Normalized spin functions (i. e. Fourier coefficients) within the unit cell of $\mathrm{TbMn_2O_5}$ for wavevector $(\frac{1}{2},0,q)$. Here $z_\alpha = (r_{3\alpha} + ir_{4\alpha})/\sqrt{2}$. All the $r$'s are real variables. The wavefunction listed under $\sigma_1$ ($\sigma_2$) transforms according to the first (second) column of the irrep. The actual spin structure is a linear combination of the two columns with arbitrary complex coefficients.

which determine the matrix elements in the quadratic free energy. (Since these are usually not well known, one has recourse to a symmetry analysis.) The direction in $\boldsymbol{\sigma}_1$-$\boldsymbol{\sigma}_2$ space which the system assumes, is determined by fourth or higher-order terms in the Landau expansion. Since not much is known about these terms, this direction is reaosonably treated as a parameter to be extracted from the experimental data. We use Table XVI to write the most general spin functions consistent with crystal symmetry as

$$\begin{aligned}
\mathbf{S}(\mathbf{R},1) &= \sigma_1 \Big[ (r_{1x}\hat{\imath} + r_{1y}\hat{\jmath}) \cos(\mathbf{q}\cdot\mathbf{R} + \phi_1) \\
&\quad + r_{1z}\hat{k} \sin(\mathbf{q}\cdot\mathbf{R} + \phi_1) \Big] \\
&\quad + \sigma_2 \Big[ (r_{2x}\hat{\imath} + r_{2y}\hat{\jmath}] \cos(\mathbf{q}\cdot\mathbf{R} + \phi_2) \\
&\quad + r_{2z}\hat{k} \sin(\mathbf{q}\cdot\mathbf{R} + \phi_2) \Big]
\end{aligned}$$

$$\begin{aligned}
\mathbf{S}(\mathbf{R},2) &= \sigma_1 \Big[ (r_{2x}\hat{\imath} + r_{2y}\hat{\jmath}) \cos(\mathbf{q}\cdot\mathbf{R} + \phi_1) \\
&\quad - r_{2z}\hat{k} \sin(\mathbf{q}\cdot\mathbf{R} + \phi_1) \Big] \\
&\quad + \sigma_2 \Big[ (r_{1x}\hat{\imath} + r_{1y}\hat{\jmath}] \cos(\mathbf{q}\cdot\mathbf{R} + \phi_2) \\
&\quad - r_{1z}\hat{k} \sin(\mathbf{q}\cdot\mathbf{R} + \phi_2) \Big]
\end{aligned}$$

$$\begin{aligned}
\mathbf{S}(\mathbf{R},3) &= \sigma_1 \Big[ (r_{1x}\hat{\imath} - r_{1y}\hat{\jmath}) \cos(\mathbf{q}\cdot\mathbf{R} + \phi_1) \\
&\quad - r_{1z}\hat{k} \sin(\mathbf{q}\cdot\mathbf{R} + \phi_1) \Big] \\
&\quad + \sigma_2 \Big[ (-r_{2x}\hat{\imath} + r_{2y}\hat{\jmath}] \cos(\mathbf{q}\cdot\mathbf{R} + \phi_2) \\
&\quad + r_{2z}\hat{k} \sin(\mathbf{q}\cdot\mathbf{R} + \phi_2) \Big]
\end{aligned}$$

$$\begin{aligned}
\mathbf{S}(\mathbf{R},4) &= \sigma_1 \Big[ (r_{2x}\hat{\imath} - r_{2y}\hat{\jmath}) \cos(\mathbf{q}\cdot\mathbf{R} + \phi_1) \\
&\quad + r_{2z}\hat{k} \sin(\mathbf{q}\cdot\mathbf{R} + \phi_1) \Big] \\
&\quad + \sigma_2 \Big[ (-r_{1x}\hat{\imath} + r_{1y}\hat{\jmath}] \cos(\mathbf{q}\cdot\mathbf{R} + \phi_2) \\
&\quad - r_{1z}\hat{k} \sin(\mathbf{q}\cdot\mathbf{R} + \phi_2) \Big]
\end{aligned}$$

$$\begin{aligned}
\mathbf{S}(\mathbf{R},5) &= \sigma_1 \Big[ (z_x'\hat{\imath} - z_y'\hat{\jmath} - z_z''\hat{k}) \cos(\mathbf{q}\cdot\mathbf{R} + \phi_1) \\
&\quad + (z_x''\hat{\imath} - z_y''\hat{\jmath} + z_z'\hat{k}) \sin(\mathbf{q}\cdot\mathbf{R} + \phi_1) \Big] \\
&\quad + \sigma_2 \Big[ (-z_x'\hat{\imath} + z_y'\hat{\jmath} - z_z''\hat{k}] \cos(\mathbf{q}\cdot\mathbf{R} + \phi_2) \\
&\quad + (-z_x''\hat{\imath} + z_y''\hat{\jmath} + z_z'\hat{k}) \sin(\mathbf{q}\cdot\mathbf{R} + \phi_2) \Big]
\end{aligned}$$

$$\begin{aligned}
\mathbf{S}(\mathbf{R}_6) &= \sigma_1 \Big[ (z_x'\hat{\imath} + z_y'\hat{\jmath} + z_z''\hat{k}) \cos(\mathbf{q}\cdot\mathbf{R} + \phi_1) \\
&\quad + (z_x''\hat{\imath} + z_y''\hat{\jmath} i - z_z'\hat{k}) \sin(\mathbf{q}\cdot\mathbf{R} + \phi_1) \Big] \\
&\quad + \sigma_2 \Big[ (z_x'\hat{\imath} + z_y'\hat{\jmath} - z_z''\hat{k}] \cos(\mathbf{q}\cdot\mathbf{R} + \phi_2) \\
&\quad + (z_x''\hat{\imath} + z_y''\hat{\jmath} + z_z'\hat{k}) \sin(\mathbf{q}\cdot\mathbf{R} + \phi_2) \Big]
\end{aligned}$$

$$\begin{aligned}
\mathbf{S}(\mathbf{R},7) &= \sigma_1 \Big[ (z_x'\hat{\imath} - z_y'\hat{\jmath} + z_z''\hat{k}) \cos(\mathbf{q}\cdot\mathbf{R} + \phi_1) \\
&\quad + (-z_x''\hat{\imath} + z_y''\hat{\jmath} + z_z'\hat{k}) \sin(\mathbf{q}\cdot\mathbf{R} + \phi_1) \Big] \\
&\quad + \sigma_2 \Big[ (-z_x'\hat{\imath} + z_y\hat{\jmath} + z_z''\hat{k}] \cos(\mathbf{q}\cdot\mathbf{R} + \phi_2) \\
&\quad + (z_x''\hat{\imath} - z_y''\hat{\jmath} + z_z'\hat{k}) \sin(\mathbf{q}\cdot\mathbf{R} + \phi_2) \Big]
\end{aligned}$$

$$\begin{aligned}
\mathbf{S}(\mathbf{R}_8) &= \sigma_1 \Big[ (z_x'\hat{\imath} + z_y'\hat{\jmath} - z_z''\hat{k}) \cos(\mathbf{q}\cdot\mathbf{R} + \phi_1) \\
&\quad + (-z_x''\hat{\imath} - z_y''\hat{\jmath} - z_z'\hat{k}) \sin(\mathbf{q}\cdot\mathbf{R} + \phi_1) \Big] \\
&\quad + \sigma_2 \Big[ (z_x'\hat{\imath} + z_y\hat{\jmath} + z_z''\hat{k}] \cos(\mathbf{q}\cdot\mathbf{R} + \phi_2) \\
&\quad + (-z_x''\hat{\imath} - z_y''\hat{\jmath} + z_z'\hat{k}) \sin(\mathbf{q}\cdot\mathbf{R} + \phi_2) \Big]
\end{aligned}$$

$$\begin{aligned}
\mathbf{S}(\mathbf{R},9) &= \sigma_1 \Big[ (r_{5x}\hat{\imath} + r_{5y}\hat{\jmath}) \cos(\mathbf{q}\cdot\mathbf{R} + \phi_1) \\
&\quad + r_{5z}\hat{k} \sin(\mathbf{q}\cdot\mathbf{R} + \phi_1) \Big] \\
&\quad + \sigma_2 \Big[ (r_{6x}\hat{\imath} + r_{6y}\hat{\jmath}] \cos(\mathbf{q}\cdot\mathbf{R} + \phi_2) \\
&\quad + r_{6z}\hat{k} \sin(\mathbf{q}\cdot\mathbf{R} + \phi_2) \Big]
\end{aligned}$$

$$\begin{aligned}
\mathbf{S}(\mathbf{R},10) &= \sigma_1 \Big[ (r_{6x}\hat{\imath} + r_{6y}\hat{\jmath}) \cos(\mathbf{q}\cdot\mathbf{R} + \phi_1) \\
&\quad - r_{6z}\hat{k} \sin(\mathbf{q}\cdot\mathbf{R} + \phi_1) \Big]
\end{aligned}$$

$$
\begin{aligned}
&\quad +\sigma_2 \Big[(r_{5x}\hat{i} + r_{5y}\hat{j}] \cos(\mathbf{q}\cdot\mathbf{R} + \phi_2) \\
&\quad -r_{5z}\hat{k} \sin(\mathbf{q}\cdot\mathbf{R} + \phi_2)\Big] \\
\mathbf{S}(\mathbf{R}, 11) \ &= \ \sigma_1 \Big[(r_{5x}\hat{i} - r_{5y}\hat{j}) \cos(\mathbf{q}\cdot\mathbf{R} + \phi_1) \\
&\quad -r_{5z}\hat{k} \sin(\mathbf{q}\cdot\mathbf{R} + \phi_1)\Big] \\
&\quad +\sigma_2 \Big[(-r_{6x}\hat{i} + r_{6y}\hat{j}] \cos(\mathbf{q}\cdot\mathbf{R} + \phi_2) \\
&\quad +r_{6z}\hat{k} \sin(\mathbf{q}\cdot\mathbf{R} + \phi_2)\Big] \\
\mathbf{S}(\mathbf{R}, 12) \ &= \ \sigma_1 \Big[(r_{6x}\hat{i} - r_{6y}\hat{j}) \cos(\mathbf{q}\cdot\mathbf{R} + \phi_1) \\
&\quad +r_{6z}\hat{k} \sin(\mathbf{q}\cdot\mathbf{R} + \phi_1)\Big] \\
&\quad +\sigma_2 \Big[(-r_{5x}\hat{i} + r_{5y}\hat{j}] \cos(\mathbf{q}\cdot\mathbf{R} + \phi_2) \\
&\quad -r_{5z}\hat{k} \sin(\mathbf{q}\cdot\mathbf{R} + \phi_2)\Big]
\end{aligned}
\tag{119}
$$

In Table XVI the position of each spin is $\mathbf{R} + \boldsymbol{\tau}_n$, where the $\boldsymbol{\tau}$ are listed in Table XIV and $\mathbf{R}$ is a Bravais lattice vector. The symmetry properties of the order parameters are

$$
\begin{aligned}
m_x \begin{bmatrix} \boldsymbol{\sigma}_1 \\ \boldsymbol{\sigma}_2 \end{bmatrix} &= \begin{bmatrix} \boldsymbol{\sigma}_1 \\ -\boldsymbol{\sigma}_2 \end{bmatrix} \\
m_y \begin{bmatrix} \boldsymbol{\sigma}_1 \\ \boldsymbol{\sigma}_2 \end{bmatrix} &= \begin{bmatrix} \boldsymbol{\sigma}_2 \\ -\boldsymbol{\sigma}_1 \end{bmatrix} \\
\mathcal{I} \begin{bmatrix} \boldsymbol{\sigma}_1 \\ \boldsymbol{\sigma}_2 \end{bmatrix} &= \begin{bmatrix} \boldsymbol{\sigma}_2^* \\ \boldsymbol{\sigma}_1^* \end{bmatrix} .
\end{aligned}
\tag{120}
$$

We now check a few representative cases of the above transformation. If we apply $m_x$ to $S(\mathbf{q}, 1)$ we do not change the signs of the $x$ component but do change the signs of the $y$ and $z$ components. As a result we get $S(\mathbf{q}, 3)$ except that $\sigma_y$ has changed sign, in agreement with the first line of Eq. (120). If we apply $m_y$ to $S(\mathbf{q}, 1)$ we do not change the sign of the $y$ component but do change the signs of the $x$ and $z$ components. As a result we get $S(\mathbf{q}, 4)$ except that now $\boldsymbol{\sigma}_1$ is replaced by $\boldsymbol{\sigma}_2$ and $\boldsymbol{\sigma}_2$ is replaced by $\boldsymbol{\sigma}_1$, in agreement with the second line of Eq. (120). When inversion is applied to $S(\mathbf{q}, 1)$ we change the sign of $\mathbf{R}$ but not the orientation of the spins which are pseudovectors. We then obtain $S(\mathbf{q}, 2)$ providing we replace $\boldsymbol{\sigma}_1$ by $\boldsymbol{\sigma}_2^*$ and $\boldsymbol{\sigma}_2$ by $\boldsymbol{\sigma}_1^*$, in agreement with the last line of Eq. (120).

### 5. *Comparison to Group Theory*

Here I briefly compare the above calculation to the one using the simplest formulation of representation theory. The first step in the standard formulation is to find the irreps of the group of the wavevector. The easiest way to do this is to introduce a double group having eight elements (see Appendix B) since we need to take account of the operator $m_y^2 \equiv -E$. (This is done in Appendix B.) From this one finds that each Wyckoff orbit and each spin component can be considered separately (since they do not transform into one another under the operations we consider). Then, in every case the only irrep that appears is the two dimensional one for which we set

$$
m_x \ = \ \begin{bmatrix} 1 & 0 \\ 0 & \text{-1} \end{bmatrix} \ m_y = \begin{bmatrix} 0 & 1 \\ \text{-1} & 0 \end{bmatrix} \ m_x m_y = \begin{bmatrix} 0 & 1 \\ 1 & 0 \end{bmatrix}
\tag{121}
$$

Indeed, one can verify that the functions in the second (third) column of Table XVI comprise a basis vector for column one (two) of this two dimensional irrep. One might ask: "Why have we undertaken the ugly detailed consideration of the matrix for $F_2$?" The point is that within standard representation theory all the variables in Table XVI would be independently assigned *arbitrary* phases. In addition, the amplitudes for the Tb orbits (sublattices #5, #6 and sublattices #7, #8) would have independent amplitudes. To get the results actually shown in Table XVI one would have to do the equivalent of analyzing the effect of inversion invariance of the free energy. This task would be a very technical exercise in the arcane aspects of group theory which here we avoid by an exercise in algebra, which though messy, is basically high school math. I also warn the reader that canned programs to perform the standard representation analysis can not always be relied upon to be correct. It is worth noting that published papers dealing with TMO25 have not invoked inversion symmetry. For instance in Ref. 10 one sees the statement "As in the incommensurate case[3], each of the magnetic atoms in the unit cell is allowed to have an independent SDW, i. e., its own amplitude and phase," and later on in Ref. 49 "all phases were subsequently fixed ... to be rational fractions of $\pi$." Use of the present theory would eliminate most of the phases and would relate the two distinct $\mathrm{Mn}^{4+}$ Wyckoff orbits (just as happened for TMO).

Finally, to see the effect of inversion on a concrete level I analyze the situation within the $\mathrm{Mn}^{3+}$ orbit and consider only the $x$ components of spin. The inverse susceptibility would then be the upper left $4 \times 4$ submatrix shown in Eq. (92). Had we not used inversion symmetry this submatrix would be the same except that one would have had

$$
M_{14} = -M_{23} = M_{32} = -M_{41} = ir \ ,
\tag{122}
$$

where $r$ is real. One can verify that when $r = 0$ the eigenvectors can be taken to have only real components, whereas when $r \neq 0$, the eigenvectors are complex with relative phases dependent on the value of $r$,

### 6. *Comparison to $YMn_2O_5$*

$\mathrm{YMn_2O_5}$ (YMO25) is isostructural to TM025, so its magnetic structure is relevant to the present discussion.

I will consider the highest temperature magnetically ordered phase, which appears between about 20K and 45K. In this compound Y is nonmagnetic and in the higher-temperature ordered phase $q_z = 1/4$, so the system is commensurate. But since the value of $q_z$ is not special, the symmetry of this state is essentially the same as that of TMO25. Throughout this subsection the structural information is taken from Fig. 2 of Ref. 11. (The uppermost panel is mislabeled and is obviously the one we want for the highest temperature ordered phase.)

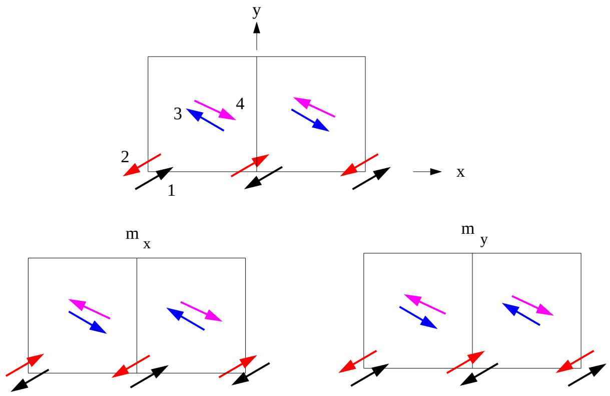

FIG. 5: (Color online). Top: The spin structure of the $Mn^{3+}$ ions in $YMn_2O_5$ (limited to one **a-b** pane), taken from Fig. 2 of Ref. 11. The sublattices are labeled in our convention. Bottom left: the spin structure of after transformation by $m_x$. Bottom right: spin structure of $TbMn_2O_5$ after transformation by $m_y$.

From Fig. 5 we see that the spin wavefunction is an eigenvector of $m_x$ with eigenvalue $-1$. So this structure must be that of the second column of the irrep. In accordance with this identification one sees that the initial wavefunction is orthogonal to the wavefunction transformed by $m_y$ (since this transformation will produce a wavefunction associated with the first column). Referring to Eq. (119), one sees that to describe the pattern of $Mn^{3+}$ spins one chooses

$$\begin{aligned} \boldsymbol{\sigma}_1 &= 0 \ , \quad r_{2x} = -r_{1x} \approx 0.95 \ , \\ & r_{1y} = -r_{2y} \approx 0.3 \ . \end{aligned} \tag{123}$$

The point we make here is that $\boldsymbol{\sigma}_1 = 0$. Although the values of these order parameters were not given in Ref. 11, it seems clear that in the lower temperature phase the order parameters must be comparable in magnitude.

### D. $CuFeO_2$

The space group of $CuFeO_2$ (CFO) is[53] R$\overline{3}$m (#166 in Ref. 28) and its general positions are given in Table XVII.

| | | |
|---|---|---|
| $E\mathbf{r} = (x,y,z)$<br>$m_3\mathbf{r} = (y,x,z)$ | $3\mathbf{r} = (z,x,y)$<br>$m_2\mathbf{r} = (z,y,x)$ | $3^2\mathbf{r} = (y,z,x)$<br>$m_1\mathbf{r} = (x,z,y)$ |
| $\mathcal{I}\mathbf{r} = (\overline{x},\overline{y},\overline{z})$<br>$\mathcal{I}m_3\mathbf{r} = (\overline{y},\overline{x},\overline{z})$ | $\mathcal{I}3\mathbf{r} = (\overline{z},\overline{x},\overline{y})$<br>$\mathcal{I}m_2\mathbf{r} = (\overline{z},\overline{y},\overline{x})$ | $\mathcal{I}3^2\mathbf{r} = (\overline{y},\overline{z},\overline{x})$<br>$\mathcal{I}m_1\mathbf{r} = (\overline{x},\overline{z},\overline{y})$ |

TABLE XVII: General Positions for R$\overline{3}$m, with respect to rhombohedral axes. Here "3" denotes a three-fold rotation and $m_n$ labels the three mirror planes which contain the three-fold axis.

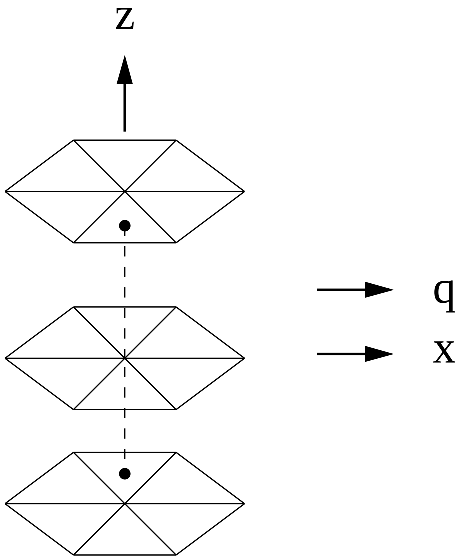

FIG. 6: The lattice of magnetic Fe ions in CFO. Here I show sections of three adjacent triangular lattice layers. The wavevector lies along the $x$-axis. The dashed line indicates that the central site lies directly above (below) the center of gravity, indicated by a dot, of a triangle of the layer below (above) it.

We are interested in structures that can appear for general wavevectors of the type $\mathbf{q} \equiv (q,q,0)$ (in crystallographic notation), in other words for wavevectors parallel to a nearest neighbor vector of the triangular plane of Fe ions. The only operation (other than the identity) that conserves wavevector is $2_x$ a two-fold rotation about the axis of the wavevector. Clearly, the Fourier component $m_z(\mathbf{q})$ obeys

$$2_x m_x(\mathbf{q}) = m_x(\mathbf{q}) \tag{124}$$

and we call this irrep #1. For irrep #2 we have

$$\begin{aligned} 2_x m_y(\mathbf{q}) &= -m_y(\mathbf{q}) \\ 2_x m_z(\mathbf{q}) &= -m_z(\mathbf{q}) \ . \end{aligned} \tag{125}$$

As before inversion fixes the phase of these coefficients to be the same (within a given irrep), so one has

$$m_x = \boldsymbol{\sigma}_1 \tag{126}$$

and

$$m_y = \boldsymbol{\sigma}_2 r \ , m_z = \boldsymbol{\sigma}_2 s \ , \tag{127}$$

where $r^2 + s^2 = 1$ and $\boldsymbol{\sigma}_n(\pm|\mathbf{q}|) = \sigma_n e^{\pm i\phi_n}$. Thus, if both irreps are present, we would have

$$\begin{aligned} m_x(\mathbf{r}) &= 2\sigma_1 \cos(qx + \phi_1) \\ m_y(\mathbf{r}) &= 2\sigma_2 r \cos(qx + \phi_2) \\ m_z(\mathbf{r}) &= 2\sigma_2 s \cos(qx + \phi_2) \ . \end{aligned} \tag{128}$$

We have the transformation properties

$$\begin{aligned} 2_x\boldsymbol{\sigma}_1 &= \boldsymbol{\sigma}_1 \ , \ \ 2_x\boldsymbol{\sigma}_2 = -\boldsymbol{\sigma}_2 \\ \mathcal{I}\boldsymbol{\sigma}_1 &= [\boldsymbol{\sigma}_1]^* \ , \ \ \mathcal{I}\boldsymbol{\sigma}_2 = [\boldsymbol{\sigma}_2]^* \ . \end{aligned} \tag{129}$$

For future reference it is interesting to note that at zero applied electric and magnetic fields the free energy must be invariant under taking either $\boldsymbol{\sigma}_1$ or $\boldsymbol{\sigma}_2$ into its negative. To see this write the free energy as an expansion in powers of the order parameters:

$$F = \sum_{k,l,m,n} a_{klmn} \boldsymbol{\sigma}_1^k \boldsymbol{\sigma}_1^{*l} \boldsymbol{\sigma}_2^m \boldsymbol{\sigma}_2^{*n} \ . \tag{130}$$

To be time reversal invariant, the total number of powers $(k+l+m+n)$ must be even. Also, to be invariant under $2_x$ the total number of powers of $\boldsymbol{\sigma}_2$ $(m+n)$ has to be even. So both $k+l$ and $m+n$ are even. But wavevector conservation implies that $l+n = k+m$ (assuming we have a truly incommensurate phase). Thus $l = k + 2\sigma$ and $n = m - 2\sigma$. Then

$$F = \sum_{k,l,m,n} a_{klmn} \sigma_1^{2k+2\sigma} \sigma_2^{2m-2\sigma} e^{2i\sigma(\phi_2 - \phi_1)} \ . \tag{131}$$

## E. Discussion

### 1. *Summary of Results*

In Table XVIII we collect the results for various multiferroics.

### 2. *Effect of Quartic Terms*

As we now discuss, the quartic terms in the Landau expansion can have significant qualitative effects.[6] In general, the quartic terms are the lowest order ones which favor the fixed length spin constraint, a constraint which is known to be dominant at low temperature.[54] How this constraint comes into play depends on what state is selected by the quadratic terms. For instance, in the simplest scenario when one has a ferromagnet or an antiferromagnet, the instability is such (see Fig. 1) that ordering with uniform spin length takes place. Thus, as the temperature is lowered within the ordered phase, the ordering of wavevectors near $q = 0$ for the ferromagnet (near $q = \pi$ for the antiferromagnet) which would have become unstable if only the quadratic terms were relevant, is strongly disfavored by the quartic terms. In the systems considered here the situation is quite different. For instance, in NVO,[33] TMO,[3] and MWO[39] the quadratic terms select an incommensurate structure in which the spins are aligned along an easy axis and their magnitudes are sinusoidally modulated. As the temperature is lowered the quartic terms lead to an instability in which transverse spin component break the symmetry of the longitudinal incommensurate phase. This scenario explains why the highest-temperature incommensurate longitudinal phase becomes unstable to a lower-temperature incommensurate phase which has both longitudinal and transverse components which more nearly conserve spin length.

To see this result formally for NVO, TMO, or MWO, let $\boldsymbol{\sigma}_>$ $(\boldsymbol{\sigma}_<)$ be the complex valued order parameter for the higher-temperature longitudinal (lower-temperature transverse) ordering. The fourth order terms then lead to the free energy as

$$\begin{aligned} F &= a(T - T_>)|\boldsymbol{\sigma}_>|^2 + b(T - T_<)|\boldsymbol{\sigma}_<|^2 \\ &\quad + A(|\boldsymbol{\sigma}_>|^2 + |\boldsymbol{\sigma}_<|^2)^2 + B|\boldsymbol{\sigma}_>\boldsymbol{\sigma}_<|^2 \\ &\quad + C[(\boldsymbol{\sigma}_<\boldsymbol{\sigma}_>^*)^2 + (\boldsymbol{\sigma}_<^*\boldsymbol{\sigma}_>)^2] \ , \end{aligned} \tag{132}$$

where $A$, $B$, and $C$ are real. That $C$ is real is a result of inversion symmetry, which, for these systems leads to $\mathcal{I}\boldsymbol{\sigma}_n = \boldsymbol{\sigma}_n^*$. The high-temperature representation does allow transverse components and could, in principle, satisfy the fixed length constraint. In the usual situation, however, the exchange couplings are nearly isotropic and this state is not energetically favored. If the higher temperature structure is longitudinal, then $B$ will surely be negative, whereas if the higher temperature structure conserves spin length $B$ will probably be positive. By properly choosing the relative phases of the two order parameters the term in $C$ always favors having two irreps. So the usual scenario in which the longitudinal phase becomes unstable relative to transverse ordering is explained (in this phenomenology) by having $B$ be negative, so that the discussion after Eq. (48) applies.

To finish the argument it remains to consider the term in $C$, which can be written as

$$\delta F_4 = 2C\sigma_<^2\sigma_>^2 \cos(2\phi_< - 2\phi_>) \ , \tag{133}$$

where again we expressed the order parameters as in Eq. (43). Normally, if two irreps are favored, it is because together they better satisfy the fixed length constraint. What that means is that when spins have substantial length in one irrep, the contribution to their spin length from the second irrep is small. In other words, the two irreps are out of phase and we therefore expect that to minimize $\delta F_4$ we do not set $\phi_< = \phi_>$, but rather

$$\phi_< = \phi_> \pm \pi/2 \ . \tag{134}$$

In other words, we expect $C$ in Eq. (133) to be positive. The same reasoning indicates that the fourth order terms will favor $\phi_2 - \phi_1 = \pi/2$ in Eq. (128) for CFO.

For all of these systems which have two consecutive continuous transitions one has a family of broken symmetry states. At the highest temperature transition one

| Phase | $T_<$(K) | $T_>$(K) | $\mathbf{q}$ | Irreps | Refs. | FE? | Refs. |
|---|---|---|---|---|---|---|---|
| NVO (HTI) | 6.3 | 9.1 | (q,0,0) | $\Gamma_4$ | 6,33 | No | 4,6 |
| NVO (LTI) | 3.9 | 6.3 | (q,0,0) | $\Gamma_4 + \Gamma_1$ | 6,33 | $\parallel b$ | 4,6 |
| TMO (HTI) | 28 | 41 | $(0,q,0)$ | $\Gamma_3$ | 3,42 | No | 2 |
| TMO (LTI) |  | 28 | $(0,q,0)$ | $\Gamma_3 + \Gamma_2$ | 3 | $\parallel c$ | 2 |
| $TbMn_2O_5$ (HTI) | 38 | 43 | $(\frac{1}{2},0,q)^{(a)}$ | $\Gamma^{(b)}$ | 10,49 | No | 58 |
| $TbMn_2O_5$ (LTI) | 33 | 38 | $(\frac{1}{2},0,q)$ | $\Gamma^{(c)}$ | 10,49 | $\parallel b$ | 58 |
| $YMn_2O_5$ (C)$^{(d)}$ | 23 | 45 | $(\frac{1}{2},0,\frac{1}{4})$ | $\Gamma^{(b)}$ | 11 | $\parallel b$ | 58 |
| $YMn_2O_5$ (IC) |  | 23 | $(\approx \frac{1}{2},0,q)$ |  | 11 | $\parallel b$ | 58 |
| CFO$^{(e)}$ (HTI) | 10 | 14 | $(q,q,0)$ | $\Gamma_1$ | 51 | No | 9 |
| CFO (LTI) | 0? | 10 | $(q,q,0)$ | $\Gamma_1 + \Gamma_2$ | $9^{(f)}$ | $\perp c$ | 9 |
| MWO | 12.7 | 13.2 | $(q_x,\frac{1}{2},q_z)$ | $\Gamma_2$ | 39 | No | 40 |
| MWO | 7.6 | 12.7 | $(q_x,\frac{1}{2},q_z)$ | $\Gamma_2 + \Gamma_1$ | 39 | $\parallel b$ | 40 |

TABLE XVIII: Incommensurate Phases of various multiferroics. Except for CFO each phase is stable for zero applied magnetic field for $T_< < T < T_>$. When $T_< = 0$ it means that the phase is stable down to the lowest temperature investigated. We give the incommensurate wavevector and the associated irreducible representations in the notation of our tables. In the column labeled "FE?" if the system is ferroelectric we give the direction of the spontaneous polarization, otherwise the entry is "No."

a) At the highest temperature the value of $q_x$ might not be exactly 1/2.
b) The irrep is the two dimensional one (see Appendix B). In the HTI phase only one basis vector is active.
c) The irrep is the two dimensional one (see Appendix B). In the LTI phase both basis vectors are active.
d) This phase commensurate.
e) Data for $CuFeO_2$ is for $H \approx 8$T.
f) The magnetic structure was inferred from the existence of ferroelectricity.

has spontaneously broken symmetry which arbitrarily selects between $\sigma_>$ and $-\sigma_>$. (This is the simplest scenario when the wavevector is not truly incommensurate.) Independently of which sign is selected for the order parameter $\boldsymbol{\sigma}_>$, one similarly has a further spontaneous breaking of symmetry to obtain arbitrarily either $i\sigma_<$ or $-i\sigma_<$. (Here, as mentioned, we assume a relative phase $\pi/2$ for $\boldsymbol{\sigma}_<$. In this scenario, then, there are four equivalent low temperature phases corresponding to the choice of signs of the two order parameters.

The cases of TMO25 and YMO25 are different from the above because they have two order parameters from the same two-dimensional irrep and which therefore are simultaneously critical. At quadratic order one has $SU_2$ symmetry, but this is broken by quartic terms in the free energy. The symmetry of these is such that in the representation of Eq. (120) one has

$$\begin{aligned} F &= a(T-T_c)\left[|\boldsymbol{\sigma}_1|^2 + |\boldsymbol{\sigma}_2|^2\right] \\ &\quad + A(|\boldsymbol{\sigma}_1|^2 + |\boldsymbol{\sigma}_2|^2)^2 + B|\boldsymbol{\sigma}_1\boldsymbol{\sigma}_2|^2 \\ &\quad + C\left[(\boldsymbol{\sigma}_1\boldsymbol{\sigma}_2^*)^2 + (\boldsymbol{\sigma}_1^*\boldsymbol{\sigma}_2)^2\right] \ . \end{aligned} \tag{135}$$

Terms odd in $\boldsymbol{\sigma}_2$ are not allowed according to Eq. (120). Also wavevector conservation indicates that two variables must be at wavevector $\mathbf{q}$ and two at wavwevector $-\mathbf{q}$. Also $A$, $B$, and $C$ are real. That $C$ is real is a result of symmetry under $m_y$, as in Eq. (120). Here the fourth order anisotropy makes itself felt as soon as the ordered phase is entered. One can see that the phase difference between $\boldsymbol{\sigma}_1$ and $\boldsymbol{\sigma}_2$ depends on the term proportional to $C$. Since the fixed spin length constraint favors this phase difference to be $\pi/2$, we intuit that $C$ is positive, so that $\boldsymbol{\sigma}_2 = \pm i\boldsymbol{\sigma}_1$. In any case, after minimizing with respect to the relative phase of the two order parameters, one gets the sum of the $B$ and $C$ terms as

$$\delta F_4 = (B - |C|)|\boldsymbol{\sigma}_1\boldsymbol{\sigma}_2|^2 \ . \tag{136}$$

If $B - |C|$ is positive, then either $\boldsymbol{\sigma}_1 = 0$ or $\boldsymbol{\sigma}_2 = 0$. In the former case the state is odd under $m_x$ and in the latter case even under $m_x$. If $B - |C|$ is negative, then the quartic terms favor

$$|\boldsymbol{\sigma}_1| = |\boldsymbol{\sigma}_2| \ . \tag{137}$$

It is amusing that the quartic terms in the Landau expansion dictate that these are the two allowable scenarios unless one admits to having a multicritical point where $B - |C| = 0$.

Now we first consider YMO25 in its higher temperature commensurate (HTC) ordered phase. For it additional fourth order terms occur because $4\mathbf{q}$ is a reciprocal lattice vector, but these are not important for the present discussion. Here the analysis of Ref. 11 indicates (see the discussion of our Fig. 5) that only a single order parameter condenses in the HTC phase. This indicates that energetics must favor positive $B-|C|$ in this case. The question is whether $B - |C|$ is also positive for TMO25. As we will see in the next section one has ferroelectricity unless the magnitudes of the two order parameters are the same. For YMO25 the HTC phase is ferroelectric and the conclusion that only one order parameter is active comports with this. However, for TMO25 the situation is not completely clear. Apparently there is a region such that one has magnetic ordering without ferroelectricity.[10,58] If this is so, then TMO25 differs from YMO25 in that its high temperature incommensurate phase has two equal magnitude order parameters.

## IV. MAGNETOELECTRIC COUPLING

Ferroelectricity is induced in these incommensurate magnets by a coupling which is somewhat similar to that for the so-called "improper ferroelectrics."[14] To see how such a coupling arises within a phenomenological picture, we imagine expanding the free energy in powers of the magnetic order parameters which we have studied in detail in the previous section and also the vector order parameter for ferroelectricity which is the spontaneous polarization $\mathbf{P}$, which, of course, is a zero wavevector quantity. If we had noninteracting magnetic and electric systems, then we would write the noninteracting free energy, $F_{\rm non}$ as

$$\begin{aligned} F_{\rm non} &= \frac{1}{2}\sum_\alpha \chi_{E,\alpha}^{-1} P_\alpha^2 \\ &\quad + \frac{1}{2}\sum_\Gamma a_\Gamma (T-T_\Gamma)|\sigma_\Gamma(\mathbf{q})|^2 + \mathcal{O}(\sigma^4) \,. \end{aligned} \tag{138}$$

The first term describes a system which is not close to being unstable relative to developing a spontaneous polarization (since in the systems we consider ferroelectricity is *induced* by magnetic ordering). The magnetic terms describe the possibility of having one or more phase transitions at which successively more magnetic order parameters become nonzero. As we have mentioned, the scenario of having two phase transitions in incommensurate magnets is a very common one,[21] and such a scenario is well documented for both NVO[6,33] and TMO.[2,3] A similar phenomenological description of second harmonic generation has invoked the necessity of having simultaneously two irreps.[55] Below we will indicate the existence of a term linear in $P$, schematically of the form $-\lambda M^2 P$, where $\lambda$ is a coupling constant about which not much beyond its symmetry is known. One sees that when the free energy, including this term, is minimized with respect to $P$ one obtains the equilibrium value of $P$ as

$$\langle P \rangle \;=\; \chi_E \lambda M^2 \,. \tag{139}$$

### A. Symmetry of Magnetoelectric Interaction

We now consider the free energy of the combined magnetic and electric degrees of freedom which we write as

$$F \;=\; F_{\rm non} + F_{\rm int} \,. \tag{140}$$

In view of time reversal invariance and wavevector conservation, the lowest combination of $M(q)$'s that can appear is proportional to $M_\alpha(-\mathbf{q})M_\beta(\mathbf{q})$. So generically the term we focus on will be of the form

$$F_{\rm int} \;=\; \sum_{\alpha\beta\gamma} c_{\alpha\beta\gamma} M_\alpha(\mathbf{q}) M_\beta(-\mathbf{q}) P_\gamma \,, \tag{141}$$

where $\alpha$, $\beta$, and $\gamma$ label Cartesian components. But, as we have seen in detail, the quantities $M_\alpha(\mathbf{q})$ are linearly related to the order parameter $\sigma_\Gamma(\mathbf{q})$, associated with the irrep $\Gamma$. Thus instead of Eq. (141) we write

$$F_{\rm int} \;=\; \sum_{\Gamma,\Gamma',\gamma} A_{\Gamma\Gamma'\gamma} \sigma_\Gamma(\mathbf{q}) \sigma_{\Gamma'}(\mathbf{q})^* P_\gamma \,. \tag{142}$$

The advantage of this writing the interaction in this form is that it is expressed in terms of quantities whose symmetry is manifest. In particular, the order parameters we have introduced have well specified symmetries. For instance it is easy to see that for most of the systems studied here, magnetism can not induce ferroelectricity when there is only a single representation present.[3,4] This follows from the fact that for NVO and TMO, for instance,

$$\mathcal{I}|\sigma_n|^2 = |\sigma_n|^2 \,, \tag{143}$$

as is evident from Eq. (47). The interpretation of this is simple: when one has one representation, it is essentially the same as having a single incommensurate wave. But such a single wave will have inversion symmetry (to as close a tolerance as we wish) with respect to some lattice point. This is enough to exclude ferroelectricity. So the canonical scenario[3,4] is that ferroelectricity appears, not when the first incommensurate magnetic order parameter condenses, but rather when a second such order parameter condenses. Unless the two waves have the same origin, their centers of inversion symmetry do not coincide and there is no inversion symmetry and hence ferroelectricity will occur. One might ask whether or not the two waves (i. e. two irreps) will be in phase. The effect, discussed above, of quartic terms is crucial here. The quartic terms typically favors the fixed length spin constraint. To approximately satisfy this constraint, one needs to superpose two waves which are out of phase. Indeed the formal result, obtained below, shows that the spontaneous polarization is proportional to the sine of the phase difference between the two irreps.[4] We now consider the various systems in turn.

### B. NVO, TMO, and MWO

We now analyze the canonical magneto-electric interaction in the cases of NVO, TMO, ad MWO. These cases are all similar to one another and in each case the order parameters have been defined so as to obey Eq. (47). This relation indicates that if we may choose the origin of the incommensurate system so that the phase of the order parameter *at the origin of a unit cell* is arbitrarily close to zero. When this phase is zero, the spin distribution of this irrep has inversion symmetry relative to this origin. In the case when only a single irrep is active, this symmetry then indicates that the magnetic structure can not induce a spontaneous polarization.[4] As mentioned, in the high temperature incommensurate phases of NVO, TMO, and MWO only one irrep is present, and this argument indicates that the magneto-electric interaction vanishes in agreement with the experimental observation[2,4,40] that this phase is not ferroelectric.

We now turn to the general case when one or more irreps are present.[4,5,6,7] We write the magneto-electric interaction as

$$F_{\rm int} = \frac{1}{2}\sum_{\gamma\Gamma\Gamma'} P_\gamma \left[A_{\Gamma\Gamma'\gamma}\boldsymbol{\sigma}_\Gamma(\mathbf{q})\boldsymbol{\sigma}_{\Gamma'}(\mathbf{q})^* + A_{\Gamma'\Gamma\gamma}\boldsymbol{\sigma}_{\Gamma'}(\mathbf{q})\boldsymbol{\sigma}_\Gamma(\mathbf{q})^*\right] . \qquad (144)$$

For this to yield a real value of $F$ we must have Hermiticity: $A_{\Gamma\Gamma'\gamma} = A^*_{\Gamma'\Gamma\gamma}$. In addition, because this is an expansion relative to the state in which all order parameters are zero, this interaction has to be inversion under all operations which leave this "vacuum" state invariant.[22,23] In other words this interaction has to be invariant under inversion (which takes $P_\gamma$ into $-P_\gamma$). This condition, together with Eq. (47) indicates that $A_{\Gamma\Gamma'\gamma} = -A_{\Gamma'\Gamma\gamma}$. This condition taken in conjunction with Hermiticity indicates that $A_{\Gamma\Gamma'\gamma}$ is pure imaginary. Thus

$$F_{\rm int} = \frac{i}{2}\sum_{\gamma\Gamma\Gamma'} P_\gamma r_{\Gamma\Gamma'\gamma}\left[\boldsymbol{\sigma}_\Gamma(\mathbf{q})\boldsymbol{\sigma}_{\Gamma'}(\mathbf{q})^* - \boldsymbol{\sigma}_\Gamma(\mathbf{q})^*\boldsymbol{\sigma}_{\Gamma'}(\mathbf{q})\right] . \qquad (145)$$

Since usually we have only two differenet irreps, we write this as

$$F_{\rm int} = \sum_\gamma r_\gamma P_\gamma \sigma_> \sigma_< \sin(\phi_> - \phi_<) . \qquad (146)$$

where $r_\gamma$ is real. The fact that the result vanishes when the two waves are in phase is clear because in that case one can find a common origin for both irreps about which one has inversion symmetry. In that special case one has inversion symmetry and no spontaneous polarization can be induced by magnetism. The above argument applies to all three systems, NVO,[4] TMO,[3] and MWO. As we will see in a moment, it is still possible for inversion symmetry to be broken and yet induced ferroelectricity not be allowed.

We can also deduce the direction of the spontaneous polarization by using the transformation properties of the order parameters. given in Eq. (46). We start by analyzing the experimentally relevant cases at low or zero applied magnetic field. For NVO the magnetism in the lower temperature incommensurate phase is described[6,33] by the two irreps $\Gamma_4$ and $\Gamma_1$. One sees from Eq. (46) that the product $\sigma_1^*\sigma_4$ is even under $m_z$ and odd under $2_x$. For the interaction to be an invariant, $P_\gamma$ has to transform this way also. This implies that only the **b**-component of the spontaneous polarization can be nonzero, as observed.[4] For TMO the lower temperature incommensurate phase at low magnetic field is described[3] by irreps $\Gamma_3$ and $\Gamma_2$. From Table XII we see that $\sigma_3^*\sigma_2$ is even under $m_x$ and odd under $m_z$, which indicates that $\mathbf{P}$ has to be even under $m_x$ and odd under $m_z$. This can only happen if $\mathbf{P}$ lies along the **c** direction, as observed.[2]

Finally, for MWO, we see that $\boldsymbol{\sigma}_1\boldsymbol{\sigma}_2^*$ is odd under $m_y$. This indicates that $P_\gamma$ also has to be odd under $m_y$. In other words $\mathbf{P}$ can only be oriented along the **b** direction, again as observed.[40] In this connection one should note that this conclusion is a result of crystal symmetry, assuming that the magnetic structure results from two continuous transitions, so that representation theory is relevant. This conclusion is at variance with the argument given by Heyer *et al.*[56] who "expect a polarization in the plane spanned by the easy axis and the **b** axis ...," which they justify on the basis of the spiral model.[12,13] It should be noted that their observation that the spontaneous polarization has a nonzero component along the **a**-axis at zero applied magnetic field contradicts the symmetry analysis given here. The authors mention that some of the unexpected behavior they observe might possibly be attributed to a small content of impurities.

It is important to realize that the above results are a consequence of crystal symmetry. In view of that, it is not sensible to claim that the fact that a theory gives the result that the polarization lies along **b** makes it more plausible than some competing theory. The point is that any model, if analyzed correctly, must give the correct orientation for **P**.

It is also worth noting that this phenomenology has some semiquantitative predictions. To see this, we minimize $F_{\rm non} + F_{\rm int}$ with respect to $\mathbf{P}$ to get

$$P_\gamma = -\chi_{E,\gamma} r_\gamma \sigma_> \sigma_< \sin(\phi_> - \phi_<) . \qquad (147)$$

This result indicates that near the magneto-ferroelectric phase transition of NVO one has $P \propto \sigma_4\sigma_1$,[57] or since the high-temperature order parameter $\sigma_4$ is more or less saturated when the ferroelectric phase is entered, one has $P \propto \sigma_1$, where $\boldsymbol{\sigma}_1$ is the order parameter of the lower temperature incommensurate phase.

As we discussed, in the low temperature incommensurate phase one will have arbitrary signs of the two order parameters. However, the presence of a smll electric field will favor one particular sign of the polarization and hence, by Eq. (147) one particular sign for the product $\sigma_>\sigma_<$. Presumably this could be tested by a neutron diffraction experiment.

### C. TMO25

The case of TMO25 is somewhat different. Here we have only a single irrep. One expects that as the temperature is lowered, ordering into an incommensurate state will take place, but the quadratic terms in the free energy do not select a direction in $\boldsymbol{\sigma}_1$-$\boldsymbol{\sigma}_2$ space. At present the data has not been analyzed to say which direction is favored at temperature just below the highest ordering temperature. (For YMO25, as mentioned above, the direction $\boldsymbol{\sigma}_1 = 0$ is favored.) As the temperature is reduced, it is not possible for another representation to appear because only one irrep is involved. However, ordering according to a second eigenvalue could occur. We first analyze the situation assuming that we have only a single doubly degenerate eigenvalue. In this case we can have a spin distribution [as given in Eq. (119)] involving the two order parameters $\boldsymbol{\sigma}_1$ and $\boldsymbol{\sigma}_2$ which measure the amplitude and phase of the ordering of the eigenvector of the second and third columns of Table XVI, respectively. In terms of these order parameters, the magneto-electric coupling can be written as

$$F_{\rm int} \;=\; \sum_{nm\gamma} a_{nm\gamma} \sigma_n^* \sigma_m P\gamma \ , \qquad (148)$$

where $\gamma = x, y, z$ and $n, m = 1, 2$ label the columns of the irrep labeled $\boldsymbol{\sigma}_1$ and $\boldsymbol{\sigma}_2$, respectively, in Table XVI. Since reality requires that $a_{nm\gamma} = a^*_{mn\gamma}$, this interaction is of the form

$$F_{\rm int} \;=\; \sum_\gamma P_\gamma \Bigg[ a_{1\gamma} |\boldsymbol{\sigma}_1|^2 + a_{2\gamma} |\boldsymbol{\sigma}_2|^2 + b_\gamma \boldsymbol{\sigma}_1 \boldsymbol{\sigma}_2^* + b_\gamma^* \boldsymbol{\sigma}_1^* \boldsymbol{\sigma}_2 \Bigg] \ . \qquad (149)$$

Now use invariance under inversion, taking note of Eq. (120). One sees that under inversion $\boldsymbol{\sigma}_1 \boldsymbol{\sigma}_2^* P_\gamma$ changes sign, so the only terms which survive lead to the result

$$F_{\rm int} \;=\; \sum_\gamma r_\gamma P_\gamma [ |\boldsymbol{\sigma}_1|^2 - |\boldsymbol{\sigma}_2|^2 ] \ . \qquad (150)$$

As we discussed in connection with Eq. (137) we have two scenarios depending on whether $B - |C|$ in Eq. (136) is positive or negative. If it is positive, then only one order parameter is nonzero and we have a nonzero spontaneous polarization according to Eq. (150). In that case, using Eq. (120) we see that $[|\boldsymbol{\sigma}_1|^2 - |\boldsymbol{\sigma}_2|^2]$ is even under $m_x$ and odd under $m_y$. For $F_{\rm int}$ to be invariant under inversion therefore requires that $P_\gamma$ be odd under $m_y$ and even under $m_x$, so $\mathbf{P}$ has to be along $\mathbf{b}$ as is found.[58] In the other scenario, when $B - |C|$ is negative, then the right-hand side of Eq. (150) is zero and the state is not ferroelectric. For TMO25 we are probably in the ferroelectric scenario. Our analysis therefore suggests that the spin structure of TMO25 should be given by Eq. (119) with only one of the order parameters nonzero. It would be interesting to analyze the diffraction data to test this assertion.

### D. CFO

Again we start with the familiar magneto-electric interaction

$$F_{\rm int} \;=\; \sum_{nm\gamma} A_{nm\gamma} \boldsymbol{\sigma}_n \boldsymbol{\sigma}_m^* P_\gamma \ , \qquad (151)$$

where reality implies that $A_{nm\gamma} = A^*_{mn\gamma}$. Since we have $\mathcal{I} \boldsymbol{\sigma}_n = \boldsymbol{\sigma}_n^*$, we eliminate terms with $n = m$: we need two irreps for ferroelectricity. Indeed, the higher temperature phase with a single order parameter $\boldsymbol{\sigma}_1$ is not ferroelectric.[9] Thus the magnetoelectric interaction must be of the form

$$F_{\rm int} \;=\; \sum_\gamma \left[ a_\gamma \boldsymbol{\sigma}_1 \boldsymbol{\sigma}_2^* + a_\gamma^* \boldsymbol{\sigma}_1^* \boldsymbol{\sigma}_2 \right] P_\gamma \ . \qquad (152)$$

Inversion symmetry indicates that $a_\gamma = -a_\gamma^*$, so we write

$$\begin{aligned} F_{\rm int} \;&=\; i \sum_\gamma r_\gamma \left[ \boldsymbol{\sigma}_1 \boldsymbol{\sigma}_2^* - \boldsymbol{\sigma}_1^* \boldsymbol{\sigma}_2 \right] P_\gamma \\ &=\; 2 \sum_\gamma r_\gamma \sigma_1 \sigma_2 \sin(\phi_2 - \phi_1) P_\gamma \ , \end{aligned} \qquad (153)$$

where $r_\gamma$ is real. Now use Eq. (129) which gives that $\boldsymbol{\sigma}_1 \boldsymbol{\sigma}_2^*$ changes sign under $2_x$. So for the interaction to be invariant under $2_x$ (as it must be), $P_\gamma$ has to be odd under $2_x$. This means that $\mathbf{P}$ has to be perpendicular to the $x$ axis. Note that symmetry does not force $\mathbf{P}$ to lie along the three-fold axis because the orientation of the incommensurate wavevector has broken the three-fold symmetry.

In the above analysis we did not mention the fact that the existence of the ferroelectric phase rquires a magnetic field of about 8-10T oriented along the three-fold axis. In principle one should expand the free energy in powers of $H$. Then presumably as a function of $H$ one reaches a regime where first one incommensurate phase orders and then at a lower temperature the second incommensurate order parameter appears. Then the phenomenology of the trilinear magnetoelectric interaction would come into play as analyzed above. There is one additional point which merits attention. Namely, $\mathbf{q}$ could assume a symmetry-related value obtained by one or two three-fold rotations about the $\mathbf{c}$ axis. In the absence of any external perturbation to break the three-fold symmetry, the system would spontaneously break symmetry by arbitrarily selecting one of the wavevectors in the star. However, it is interesting to speculate whether the application of a weak in-plane magnetic (or electric) field would be enough to enforce the selection of one of the wavevectors in the star. If this were so, then the transverse component of the polarization (which, however, might be small) would be rotated by the application of such a small external field.

### E. High Magnetic Field

We can also say a word or two about what happens when a magnetic field is applied. In TMO, for instance, one finds[2] that for applied magnetic fields above about 10T in either the **a** or **b** directions, the lower temperature incommensurate phase has a spontaneous polarization along the **a** axis. Keep in mind that we want to identify this phase with two irreps and from the phase diagram we know that the higher temperature incommensurate phase is maintained into this high field regime. So the higher temperature phase is still that of $\Gamma_3$ at these high fields. Referring to Table XII we see that to get $\sigma_m \sigma_n^*$ to be odd under $m_x$ and even under $m_z$ (in order to get a polarization along the **a** axis) we can only combine irrep $\Gamma_1$ with the assumed preexisting $\Gamma_3$. Therefore it is clear that the magnetic structure has to change at the same time that direction of spontaneous polarization changes as a function of applied magnetic field.[7,13] It is also interesting, in this connection to speculate on what happens if the lower additional irrep had been $\Gamma_4$ so that $\Gamma_4$ and $\Gamma_3$ would coexist. In that case $\sigma_4 \sigma_3^*$ is odd under *both* $m_x$ and $m_z$. These conditions are not consistent with any direction of polarization, so in this hypothetical case, even though we have two irreps and break inversion symmetry, a polar vector (such as the spontaneous polarization) is not allowed.[63]

For MWO a magnetic field along the **b** axis of about 10T causes the spontaneous polarization to switch its direction from along the **b**-axis to along the **a** axis.[40] We have no phenomenological explanation of this behavior at present. This behavior seems to imply that the wavevector for $H > 10\mathrm{T}$ is no longer of the form $\mathbf{q} = (q_x, \frac{1}{2}, q_z)$.

### F. Discussion

What is to be learned from the symmetry analysis of the magnetoelectric interactions? Perhaps the most important point to keep in mind is to recognize which results are purely a result of crystal symmetry and which are model dependent. For instance, as we have seen, the direction of the spontaneous polarization is usually a result of crystal symmetry. So the fact that a microscopic theory leads to the observed direction of the polarization does not lend credence to one model as opposed to another. In a semiquantitative vein, one can say that symmetry alone predicts that near the combined magnetoelectric phase transition $P$ will be approximately proportional to the order parameter raised to the $n$th power, where the value of $n$ is a result of symmetry. ($n = 1$ for NVO or TMO, whereas $n = 2$ for TMO25).

It also goes without saying that our phenomenological results are supposed to apply generally, independently of what microscopic mechanism might be operative for the system in question. (A number of such microscopic calculations have appeared recently.[12,59,60,61,62]) Therefore, we treat YMO25 and NVO with the same methodology although these systems are said[10] to have different microscopic mechanisms. A popular phenomenological description is that given by Mostovoy[13] based on a continuum formulation. However, this development, although appealing in its simplicity, does not correctly capture the symmetry of several systems because it completely ignores the effect of the different possible symmetries within the magnetic unit cell.[63] Furthermore, it does not apply to multiferroic systems, such as TMO25 or YMO25, in which the plane of rotation of the spins is perpendicular to the wavevector.[11] (The spin-current model[12] also does not explain ferroelectricity in these systems.) In addition, a big advantage of the symmetry analysis presented here concerns small perturbations. While the structure of NVO and TMO is predominantly a spiral in the ferroelectric phase, one can speculate on whether there are small spiral-like components in the nonferroelectric phase. In other words, could small transverse components lead to a small (maybe too small for current experiments to see) spontaneous polarization? If we take into account the small magnetic moments induced on the oxygen ions, could these lead to a small spontaneous polarization in an otherwise nonferroelectric phase? The answer to these questions is obvious within a symmetry analysis like that we have given: these induced effects still are governed by the symmetry of the phase which can only be lowered by a spontaneous symmetry breaking (which we only expect if we cross a phase boundary). Therefore all such possible induced effects are taken into account by our symmetry analysis.

Finally, we note that the form of the magneto-electric interaction $\sim M^2 P$ suggests a microscopic mechanism that has general validity, although it is not necessarily the dominant mechanism. This observation stimulated an investigation of the spin phonon interaction one obtains by considering the exchange Hamilton

$$\mathcal{H} = \sum_{ij\alpha\beta} J_{\alpha\beta}(i,j) S_\alpha(i) S_\beta(j) \tag{154}$$

when $J_{\alpha\beta}(i,j)$ is expanded to linear order in phonon displacements.[59] After some algebra it was shown that the results for the direction of the induced spontaneous polarization (when the spins are ordered appropriately) agrees with the results of the symmetry arguments used here. In addition a first-principles calculation of the phonon modes led to plausible guesses as to which phonon modes play the key role in the magneto-electric coupling. But whatever the microscopic model, the phenomenology presented here should apply.

## V. CONCLUSION

In this paper we have shown in detail how one can describe the symmetry of magnetic and magneto-electric phenomena and have illustrated the technique by discussing several examples recently considered in the literature.

The principal results of this work are

- We discussed a method alternative to the traditional one (called representation analysis) for constructing allowed spin functions which describe incommensurate magnetic ordering. In many cases this technique can be especially simple and does not require an understanding of group theory.

- For systems with a center of inversion symmetry, whether the simple method mentioned above or the more traditional traditional representation formalism is used, it is essential to further include the restrictions imposed by inversion symmetry, as we pointed out previously.[3,4,5,6,7]

- We have illustrated this technique by applying it to systematize the magnetic structure analysis of several multiferroics many of which had not been analyzed using inversion symmetry.

- By considering several examples of multiferroics we further illustrated the general applicability of the trilinear magneto-electric coupling of the form $M(\mathbf{q})M(-\mathbf{q})P$, where $M(\mathbf{q})$ is the magnetization at wavevector $\mathbf{q}$ and $P$ is the uniform spontaneous polarization. Usually, when expressed in terms of order parameters, this interaction requires two active irreducible representations.

- For $\mathrm{TbMn_2O_5}$ we analyzed the fourth order terms in the Landau expansion and predict that the fact that the system magnetically orders into a ferroelectric phase indicates that the spin state is described by a single order parameter according to Eq. (119). The analysis of the diffraction data to test this assertion has not yet been done.

- We briefly discussed the implications of symmetry in assessing the role of various models proposed for multiferroics.

## ACKNOWLEDGEMENTS

I acknowledge inspiration and advice from M. Kenzelmann who carried out several of the group theoretical calculations presented here. It should be obvious that this paper owes much to my other collaborators, especially G. Lawes, T. Yildirim, A. Aharony, O. Entin-Wohlman, C. Broholm, and A. Ramirez. I thank S.-H. Lee for providing me with the figure of $\mathrm{TbMn_2O_5}$ and for insisting that I clarify various arguments. I thank J. Villain for calling my attention to some of the history of representation theory.

## APPENDIX A: FORM OF EIGENVECTOR

In this appendix we show that the matrix $\mathbf{G}$ of the form of Eq. (83) [and this includes as a subcase the form of Eq. (80)] has eigenvectors of the form given in Eq. (84). Define $\mathbf{G}' \equiv \mathbf{U}^{-1}\mathbf{G}\mathbf{U}$, where

$$\mathbf{U} \ = \ \left[\begin{array}{ccccccc} 1 & 0 & 0 & 0 & 0 & 0 & 0 \\ 0 & 1 & 0 & 0 & 0 & 0 & 0 \\ 0 & 0 & 1 & 0 & 0 & 0 & 0 \\ 0 & 0 & 0 & 1/\sqrt{2} & i/\sqrt{2} & 0 & 0 \\ 0 & 0 & 0 & 1/\sqrt{2} & -i/\sqrt{2} & 0 & 0 \\ 0 & 0 & 0 & 0 & 0 & 1/\sqrt{2} & i/\sqrt{2} \\ 0 & 0 & 0 & 0 & 0 & 1/\sqrt{2} & -i/\sqrt{2} \end{array}\right] \tag{A1}$$

We find that

$$\mathbf{U}^{-1}\mathbf{G}\mathbf{U} = \left[\begin{array}{ccccccc} a & b & c & \sqrt{2}\alpha' & \sqrt{2}\alpha'' & \sqrt{2}\xi' & \sqrt{2}\xi'' \\ b & d & e & \sqrt{2}\beta' & \sqrt{2}\beta'' & \sqrt{2}\eta' & \sqrt{2}\eta'' \\ c & e & f & \sqrt{2}\gamma' & \sqrt{2}\gamma'' & \sqrt{2}\kappa' & \sqrt{2}\kappa'' \\ \sqrt{2}\alpha' & \sqrt{2}\beta' & \sqrt{2}\gamma' & g+\delta' & \delta'' & \mu'+\nu' & -\mu''-\nu'' \\ \sqrt{2}\alpha'' & \sqrt{2}\beta'' & \sqrt{2}\gamma'' & \delta'' & g-\delta' & \mu''-\nu'' & \mu'-\nu' \\ \sqrt{2}\xi' & \sqrt{2}\eta' & \sqrt{2}\kappa' & \mu'+\nu' & \mu''-\nu'' & h+\rho' & \rho'' \\ \sqrt{2}\xi'' & \sqrt{2}\eta'' & \sqrt{2}\kappa'' & -\mu''-\nu'' & \mu'-\nu' & \rho'' & h-\rho' \end{array}\right] \tag{A2}$$

where $\alpha'$ and $\alpha''$ are the real and imaginary parts, respectively of $\alpha$ and similarly for the other complex variables. Note that we have transformed the original matrix into a real symmetric matrix. Any eigenvector (which we denote $|R\rangle$) of the transformed matrix has real-valued components and thus satisfies the equation

$$\mathbf{U}^{-1}\mathbf{G}\mathbf{U}|R\rangle \ = \ \lambda_R|R\rangle, \tag{A3}$$

from which it follows that

$$[\mathbf{G}]\mathbf{U}|R\rangle \ = \ \lambda_R\mathbf{U}|R\rangle, \tag{A4}$$

so that any eigenvector of $\mathbf{G}$ is of the form $\mathbf{U}|R\rangle$, where all components of $|R\rangle$ are real. If $|R\rangle$ has components $r1, r2, \ldots r7$, then

$$\begin{aligned} \mathbf{U}|R\rangle \ = \ & [r1, r2, r3, (r_4+ir_5)/\sqrt{2}, (r_4-ir_5)/\sqrt{2}, \\ & (r_6+ir_7)/\sqrt{2}, (r_6-ir_7)/\sqrt{2}] \ , \end{aligned} \tag{A5}$$

which has the form asserted.

## APPENDIX B: IRREPS FOR TMO25

In this appendix we give the representation analysis for $\mathrm{TbMn_2O_5}$ for wavevectors of the form $(\frac{1}{2}, 0, q)$, where $q$ has a nonspecial value. The operators we consider are $E$, $m_x$, $m_y$ and $m_x m_y$, as defined in Table XIII. Note that $m_y^2(x,y,z) = (x+1,y,z)$, so that $m_y^2 = -1$ for this wavevector. Thus, the above set of four operators do not actually form a group. Accordingly we consider the double group which follows by introducing $-E$ defined by $m_y^2 = -E$, $(-E)^2 = E$, and $(-E)\mathcal{O}(-E) = \mathcal{O}$. Since addition has no meaning within a group we do not discuss additive properties such as $(E) + (-E) = 0$. Then, if we define $-\mathcal{O} \equiv (-E)\mathcal{O}$, we have the character table given in Table XIX.

| Irrep | $E$ | $\pm m_x$ | $\pm m_y$ | $\pm m_x m_y$ | $-E$ |
|---|---|---|---|---|---|
| $\Gamma_a$ | 1 | 1 | 1 | 1 | 1 |
| $\Gamma_b$ | 1 | -1 | 1 | -1 | 1 |
| $\Gamma_c$ | 1 | 1 | -1 | -1 | 1 |
| $\Gamma_d$ | 1 | -1 | -1 | 1 | 1 |
| $\Gamma_2$ | 2 | 0 | 0 | 0 | -2 |
| $G$ | $n$ | 0 | 0 | 0 | $-n$ |

TABLE XIX: Character table for the double group of the wavevector. In the first line we list the five classes of operators for this group. In the last line we indicate the characters for the group $G$ which is induced by the $n$-dimensional reducible representation in the space of the $\alpha$ spin component of spins in a given Wyckoff orbit.

| Spin | $\boldsymbol{\sigma}_1$ | $\boldsymbol{\sigma}_2$ | Spin | $\boldsymbol{\sigma}_1$ | $\boldsymbol{\sigma}_2$ |
|---|---|---|---|---|---|
| $\mathbf{S}(\mathbf{q},1)$ | $r_{1x}$<br>$r_{1y}$<br>$r_{1z}$ | $r_{2x}$<br>$r_{2y}$<br>$r_{2z}$ | $\mathbf{S}(\mathbf{q},7)$ | $r_{6x}$<br>$r_{6y}$<br>$r_{6z}$ | $-r_{6x}$<br>$-r_{6y}$<br>$r_{6z}$ |
| $\mathbf{S}(\mathbf{q},2)$ | $r_{2x}$<br>$r_{2y}$<br>$-r_{2z}$ | $r_{1x}$<br>$r_{1y}$<br>$-r_{1z}$ | $\mathbf{S}(\mathbf{q},8)$ | $r_{6x}$<br>$-r_{6y}$<br>$-r_{6z}$ | $r_{6x}$<br>$-r_{6y}$<br>$r_{6z}$ |
| $\mathbf{S}(\mathbf{q},3)$ | $r_{1x}$<br>$-r_{1y}$<br>$-r_{1z}$ | $-r_{2x}$<br>$r_{2y}$<br>$r_{2z}$ | $\mathbf{S}(\mathbf{q},9)$ | $r_{3x}$<br>$r_{3y}$<br>$r_{3z}$ | $r_{4x}$<br>$r_{4y}$<br>$r_{4z}$ |
| $\mathbf{S}(\mathbf{q},4)$ | $r_{2x}$<br>$-r_{2y}$<br>$r_{2z}$ | $-r_{1x}$<br>$r_{1y}$<br>$-r_{1z}$ | $\mathbf{S}(\mathbf{q},10)$ | $r_{4x}$<br>$r_{4y}$<br>$-r_{4z}$ | $r_{3x}$<br>$r_{3y}$<br>$-r_{3z}$ |
| $\mathbf{S}(\mathbf{q},5)$ | $r_{5x}$<br>$r_{5y}$<br>$r_{5z}$ | $-r_{5x}$<br>$-r_{5y}$<br>$r_{5z}$ | $\mathbf{S}(\mathbf{q},11)$ | $r_{3x}$<br>$-r_{3y}$<br>$-r_{3z}$ | $-r_{4x}$<br>$r_{4y}$<br>$r_{4z}$ |
| $\mathbf{S}(\mathbf{q},6)$ | $r_{5x}$<br>$-r_{5y}$<br>$-r_{5z}$ | $r_{5x}$<br>$-r_{5y}$<br>$r_{5z}$ | $\mathbf{S}(\mathbf{q},12)$ | $r_{4x}$<br>$-r_{4y}$<br>$r_{4z}$ | $-r_{3x}$<br>$r_{3y}$<br>$-r_{3z}$ |

TABLE XX: Spin functions (i. e. unit cell Fourier coefficients) determined by standard representation analysis without invoking symmetry operations that relate **q** and −**q**. The second and third columns give the functions which transform according to the first and second column of the two dimensional irrep. These coefficients are all complex parameters.

The $\mathrm{Mn}^{4+}$ Wyckoff orbits contain two atoms and all the other orbits contain four atoms. In either case we may consider separately an orbit and a single component, $x$, $y$, or $z$ of spin. So the corresponding spin functions form a basis set of $n$ vectors, where $n = 2$ for the single spin components of $\mathrm{Mn}^{4+}$ and $n = 4$, otherwise. In each case, the operations involving $m_x$ and/or $m_y$ interchange sites and therefore have zero diagonal elements. Their character, which is their trace within this space of $n$ vectors is therefore zero. On the other hand $E$ and $-E$ give diagonal elements of $+1$ and $-1$, respectively. So their character (or trace) is $\pm n$ and we have the last line of the table for this reducible representation $G$.

In this character table we also list (in the last line) the characters of these operations within the vector space of wavefunctions of a given spin component over a Wyckoff orbit of $n$ sites. Comparing this last line of the table to the character of the irreps we see that $\mathbf{G}$ contains only the irrep $\Gamma_2$ and it contains this irrep $n/2$ times. This means that for the system of three spin components over 12 sites, we have 36 complex components and these function generate a reducible representation which contains $\Gamma_2$ 18 times. If there were no other symmetries to consider, this result would imply that to determine the structure one would have to fix the 18 complex-valued parameters. The two dimensional representation can be realized by Eq. (121). The basis vectors which transform as the first and second columns, respectively of the two dimensional representation are given in Table XX. One can check the entries of this table by verifying that the effect of $m_x$ and $m_y$ on the vectors of this table are in conformity with Eq. (121).

However, after taking account of inversion symmetry we have only 18 real-valued structural parameters of Table XVI to determine.

---

[1] M. Fiebig, J. Phys. D: Appl. Phys. **38**, R123 (2005).

[2] T. Kimura, T. Goto, H. Shintani, K. Ishizka, T. Arima, and Y. Tokura, Nature **426**, 55 (2003).

[3] M. Kenzelmann, A. B. Harris, S. Jonas, C. Broholm, J. Schafer, S. B. Kim, C. L. Zhang, S.-W. Cheong, O. Vajk, and J. W. Lynn, Phys. Rev. Lett. **95**, 087206 (2005).

[4] G. Lawes, A. B. Harris, T. Kimura, N. Rogado, R. J. Cava, A. Aharony, O. Entin-Wohlman, T. Yildirim, M. Kenzelmann, C. Broholm, and A. P. Ramirez, Phys. Rev. Lett. **95**, 087205 (2005)

[5] A. B. Harris, J. Appl. Phys. **99**, 08E303 (2006).

[6] M. Kenzelmann, A. B. Harris, A. Aharony, O. Entin-Wohlman, T. Yildirim, Q. Huang, S. Park, G. Lawes, C. Broholm, N. Rogado, R. J. Cava, K. H. Kim, G. Jorge, and A. P. Ramirez, Phys. Rev. B **74**, 014429 (2006).

[7] A. B. Harris and G. Lawes, "Ferroelectricity in Incommensurate Magnets," in "The Handbook of Magnetism and Advanced Magnetic Materials," Ed. H. Kronmuller and S. Parkin, Wiley 2006. cond-mat/0508617.

[8] T. Goto, T. Kimura, G. Lawes, A. P. Ramirez, and Y.

Tokura, Phys. Rev. Lett. **92**, 257201 (2004).

[9] T. Kimura, J. C. Lashley, and A. P. Ramirez, Phys. Rev. B **73**, 220401(R) (2006).

[10] L. C. Chapon, G. R. Blake, M. J. Guttmann, S. Park, N. Hur, P. G. Radaelli, and S.-W. Cheong, Phys. Rev. Lett. **93**, 177402 (2004).

[11] L. C. Chapon, P. G. Radaelli, G. R. Blake, S. Park, and S.-W. Cheong, Phys. Rev. Lett. **96**, 097601 (2006).

[12] H. Katsura, N. Nagaosa, and A. V. Balatsky, Phys. Rev. Lett. **95** 057205 (2005).

[13] M. Mostovoy, Phys. Rev. Lett. **96**, 067601 (2006).

[14] G. A. Smolenskii and I. E. Chupis, Sov. Phys. Usp. **25**, 475 (1982).

[15] B. Dorner, J. Axe, and G. Shirane, Phys. Rev. B **6**, 1950 (1972).

[16] R. A. Cowley, Advances in Physics **29**, 1 (1980).

[17] J. Schweizer, C. R. Physique **6**, 375 (2005). Erratum, to be published in C. R. Physique.

[18] P. G. Radaelli and L. C. Chapon, cond-mat 0609087.

[19] J. Villain, J. Schweizer, and A. B. Harris, to be published.

[20] For orthorhombic crystals we will interchangeably refer to axes as either $x$, $y$, $z$, or **a**, **b**. **c**.

[21] T. Nagamiya, in *Solid State Physics*, ed. F. Seitz and D. Turnbull (Academic, New York, 1967), Vol. 20, p346.

[22] I. E. Dzialoshinskii, Sov. Phys. JETP **5**, 1259 (1957).

[23] L. D. Landau and E. M. Lifshitz, *Statistical Physics* (Pergamon, London, 1958).

[24] K. D. Bowers and J. Owen, Rep. Prg. Phys. **1**, 304 (1955).

[25] E. F. Bertaut, Journal de Physique, Collloque C1, **32** 462 (1971).

[26] J. Schweizer, J. Phys. **IV**, 11 (2001) Pr9.

[27] J. Rossat-Mignod, in *Methods of Experimental Physics*, Chap. 20: *Magnetic Structures*, ed. K. Skold and D. L. Price, Vol. **23**, p69 (Academic Press, 1987).

[28] A. J. C. Wilson, *International Tables for Crystallography* (Kluwer Academic, Dordrecht, 1995) Vol. A.

[29] Coordinates of positions within the unit cell are given as fractions of the appropriate lattice constants.

[30] E. E. Sauerbrei, F. Faggiani, and C. Calvo, Acta Crystallogr. B **29** 2304 (1973).

[31] Often these symmetry operations are labeled $h_n$, referring Refs. 28 or 32. Rather than use these symbols with no mnemonic value, we introduce the notation $m_\alpha$ for a mirror (or glide) plane which changes the sign of the $\alpha$ coordinate and $2_\alpha$ for a two-fold rotation (or screw) axis parallel to the $\alpha$ direction.

[32] O. V. Kovalev, *Representations of Crystallographic Space Groups: Irreducible Representations, Induced representations and Corepresentations* (Gordon and Breahc, Amsterdam, 1993).

[33] G.Lawes, M. Kenzelmann, N. Rogado, K. H. Kim, G. Jorge, R. J. Cava, A. Aharony, O. Entin-Wohlman, A. B. Harris, T. Yildirim, Q. Z. Huang, S. Park, C. Broholm, and A. P. Ramirez, Phys. Rev. Lett. **93**, 247201 (2004).

[34] We use the convention that $\hat{q}$ denotes a wavevector in reciprocal lattice units (rlu) so that $q_x$ in real units is $2\pi\hat{q}_x/a$. When $q$ is multiplied by a distance obviously one has to either take $q$ in real units or take distances in inverse rlu's.

[35] A. B. Harris and J. Schweizer, Phys. Rev. B **74** ppp (2006).

[36] The fourth order terms can also renormalize the quadratic terms, especially if one is far from the critical point. But asymptotically close to the transition this effect is negligible.

[37] H. Kawamura, Phys. Rev. B **38**, 4916 (1988).

[38] A. D. Bruce and A. Aharony, Phys. Rev. B **11**, 478 (1975).

[39] G. Lautenschlager, H. Weitzel, T. Vogt, R. Hock,A. Böhm, M. Bonnet, and H. Fuess, Phys. Rev. B **48**, 6087 (1993).

[40] K. Taniguchi, N. Abe, T. Takenobu, Y. Iwasa, and T. Arima, Phys. Rev. Lett. **97**, 097203 (2006).

[41] J. Blasco, C. Ritter, J. Garcia, J. M. de Teresa, J. Pérez-Cacho, and M. R. Ibarra, Phys. Rev. B **62**, 5609 (2000).

[42] R. Kajimoto, H. Yoshizawa, H. Shintani, T. Kimura, and Y. Tokura, Phys. Rev. B **70** 012401 (2004); **70**, 219904(E) (2004).

[43] Symmetry constraints on lock-in is discussed by Y. Park, K. Cho, and H.-G. Kim, J. Appl. Phys. **83**, 4628 (1998).

[44] A. Munoz, J. A. Alonso, M. T. Casais, M. J. Martinez-Lope, J. L. Martinez, and M. T. Fernandez-Diaz, J. Phys. Condens. Matter **14**, 3285 (2002).

[45] A. Munoz, M. T. Casais, J. A. Alonso, M. J. Martinez-Lope, J. L. Martinez, and M. T. Fernandez-Diaz, Inorg. Chem. **40**, 1020 (2001).

[46] H. W. Brinks, J. Rodriguez-Carvajal, H. Fjellvag, A. Kjekshus, and B. C. Hauback, Phys. Rev. B **63**, 094411 (2001).

[47] G. Buisson, Phys. Stat. Sol. **16**, 533 (1973).

[48] G. Buisson, Phys. Stat. Sol. **17**, 191 (1973).

[49] G. R. Blake, L. C. Chapon, P. G. Radaelli, S. Park N. Hur, S.-W. Cheong, and J. Rodriguez-Carvajal, Phys. Rev. B **71**, 214402 (2005).

[50] V. Heine, *Group Theory in Quantum Mechanics*, (Pergamon, New York, 1960) p284. For an example, see A. J. Berlinsky and C. F. Coll, III, Phys. Rev. B **5**, 1587 (1972).

[51] S. Mitsuda, H. Yoshizawa, N. Yamaguchi, and M. Mekata, J. Phys. Soc. Jpn. **60**, 1885 (1991).

[52] When we "fix" the phase $\phi$ of a variable, it means that the variable is of the form $re^{i\phi}$, where $r$ is real, but not necessarily positive.

[53] C. T. Prewitt, R. D. Shannon, and D. B. Rogers, Inorg. Chem. **10**, 791 (1971).

[54] T. Kaplan, Phil. Mag., in press.

[55] D. Frohlich, St Leute, V. V. Pavlov, and R. V. Pisarev, Phys. Rev. Lett. **81**, 3239 (1998).

[56] O. Heyer, N. Hollmann, I. Klassen, S. Jodlauk, L. Bohatý, P. Becker, J. A. Mydosh, T. Lorenz, and D. Khomskii, cond-mat/0608498.

[57] It is true that the coefficient $r_\gamma$ can depend on temperature and it would be of the form $r_\gamma(T) \approx r_\gamma(T_c) + r_1(T - T_c)$. There is no reason to think that $r_\gamma(T_c)$ would be unusually small, and we therefore have the desired result as long as we are not far from the critical temperature, $T_c$.

[58] I. Kagomiya, S. Matsumoto, K. Kohn, Y. Fukuda, T. Shoubu, H. Kimura, Y. Noda, and N. Ikeda, Ferroelectrics **286**, 167 (2003.

[59] A. B, Harris, T. Yildirim, A. Aharony, and O. Entin-Wohlman, Phys. Rev. B **73** 184433 (2006).

[60] I. A. Sergienko and E. Dagotto, Phys. Rev. B **73**, 094434 (2006).

[61] I. A. Sergienko, C. Sen, and E. Dagotto, cond-mat/0608075.

[62] D. I. Khomskii, J. Magn. Magn. Mat. (2004).

[63] M. Kenzelmann and A. B. Harris, to be published.